

Postglacial Relative Sea-Level History of the Prince Rupert Area, British Columbia, Canada

Bryn Letham^a (corresponding author; bryn.letham@gmail.com)

Andrew Martindale^a (andrew.martindale@ubc.ca)

Rebecca Macdonald^a (rebamacdonald@gmail.com)

Eric Guiry^a (eguiry@mun.ca)

Jacob Jones^a (jacobj16.ubc@gmail.com)

Kenneth M. Ames^b (amesk@pdx.edu)

^aDepartment of Anthropology, University of British Columbia, 6303 NW Marine Drive, Vancouver, Canada, V6K 1Z1

^bDepartment of Anthropology, Portland State University, P.O. Box 751, Portland, Oregon 97207, USA

Abstract:

This paper presents a history of relative sea level (RSL) change for the last 15,000 years in the Prince Rupert region on the northern coast of British Columbia, Canada. One hundred twenty-three radiocarbon ages of organic material from isolation basin cores, sediment sequence exposures, and archaeological sites having a recognized relation to past sea levels constrain postglacial RSL. The large number of new measurements relating to past sea-level provides a well constrained RSL curve that differs in significant ways from previously published results. After deglaciation following the Last Glacial Maximum, the region experienced an isostatically-induced rapid RSL drop from as much 50 m asl to as low as -6.3 m asl in as little as a few centuries between 14,500 BP and 13,500 BP. After a lowstand below current sea level for about 2000 years during the terminal Pleistocene, RSL rose again to a highstand at least 6 m asl after the end of the Younger Dryas. RSL slowly dropped through the Holocene to close to its current position by 2000-1500 BP, with some potential fluctuations between 3500 and 1500 BP. This study highlights variation in RSL histories across relatively short distances, which must be accounted for by local RSL reconstructions such as this one. This RSL curve aided in the identification of an 8000-9000 year old archaeological site on a 10-12 m asl terrace, currently the earliest dated archaeological site in the area, and it provides guidance for searching for even older archaeological remains. We highlight the utility and potential of this refined RSL history for developing surveys for other archaeological sites associated with paleoshorelines.

Key words: relative sea level change, paleoshorelines, Northwest Coast, archaeology, Prince Rupert, diatoms

1. Introduction

Several decades ago, pioneering regional compilations of radiocarbon dated relative sea level (RSL) data by Mathews et al. (1970) and Clague et al. (1982) demonstrated the variability of RSL histories on the west coast of North America since the end of the Fraser Glaciation, largely related to the location and thickness of ice sheets, the timing of their retreat, and the net result of subsequent isostatic adjustments, eustatic sea level change, neotectonic movements, and sedimentation processes. New compilations have highlighted and re-emphasized this variability (Engelhart et al. 2015; Shugar et al. 2014). RSL histories are key components of paleoenvironmental and landscape reconstructions, and are intimately tied to understanding geomorphological and biological (both human and non-human) change on coastal landscapes through the Holocene. Knowing how RSL changes transform coastal landscapes is a key component for identifying and interpreting the archaeological record along coasts, particularly for the terminal Pleistocene and early Holocene. To date, RSL studies on the northern Northwest Coast mainland have been limited in scope compared to other parts of the region (see summaries in Engelhart et al. 2015 and Shugar et al. 2014).

This paper presents new data refining our understanding of the postglacial RSL history of the area around Prince Rupert, on the north coast of British Columbia, Canada (Figure 1). We use diverse methods for studying RSL change to generate a robust RSL curve based on a large dataset of limiting and index points. We discuss what this information tells us about postglacial dynamics and coastline change through the Holocene, demonstrate its utility for locating evidence for early human occupation in the study area, and outline the importance of this new data for modelling of glacio-isostatic changes in northern British Columbia.

1.1 Study Area

The study area (Figure 2) is on the northern margin of the Hecate Lowlands, a 15-60 km wide area of low relief that extends about 600 km along the northern mainland coast between an offshore coastal trough and the Coast Mountains, and includes many low islands close to the mainland. The surficial geology of the study area is primarily organic (usually peat) veneers or blankets over patches of glaciomarine sediments (clays, silts and dropstones) which in turn overlie metamorphic bedrock (Clague 1984; Massey et al. 2005). In a few areas there are massive deposits of glacial till. Shorelines are crenulated, particularly along the northern shore of Prince Rupert Harbour and through Venn Pass, where there are many sheltered bays, small inlets, and tidal channels. These shorelines often have sand and mud flats extending hundreds of meters at low tides. The Prince Rupert Harbour itself is a deep waterway, one of many glacially carved inlets and valleys in the wider region, the largest of which are Portland Inlet and the Nass River valley to the north and the Skeena River valley to the south.

Today the two principal communities in the study area are the city of Prince Rupert and the reserve town of Metlakatla, but prior to European contact the area included dozens of contemporaneously occupied villages inhabited by the ancestors of the Tsimshian peoples (MacDonald and Inglis 1981; Ames 2005). Archaeological remains of these villages dot the shorelines along bays and passes. These ancient inhabitants had an intimate relation with the sea, and understanding how shorelines have changed through time is important for locating and interpreting past peoples' material remains. The rich archaeological record indicates that Prince Rupert Harbour was one of the most densely occupied areas of the Northwest Coast by around 3000 years ago (Ames and Martindale 2014). However, even with a century of archaeological

research that includes intensive radiocarbon dating (e.g. Ames 2005; Archer 1992; 2001; Coupland 1988, 2006; Coupland et al. 1993, 2001, 2003, 2009, 2010; Drucker 1943; MacDonald 1969; MacDonald and Cybulski 2001; MacDonald and Inglis 1981; Smith 1909), no archaeological sites dating earlier than 6000 years BP had been identified prior to our research. Elsewhere on the northern coast, terminal Pleistocene and early Holocene archaeological remains are being found with increasing frequency on paleoshorelines in the wake of detailed RSL reconstructions (Carlson and Baichtal 2015; Fedje and Christensen 1999; Fedje et al. 2005a, 2011; Josenhans et al. 1997; Mackie et al. 2011; McLaren et al. 2011). Our research objectives are similar, and include using RSL data to survey for evidence of earlier occupation in this archaeologically-important place. We also seek to refine the understanding of postglacial landform dynamics in northern British Columbia, which we review next.

1.2 Regional Setting: Glacial History and RSL Change

1.2.1 General Patterns for Coastal British Columbia

Recent compilations of known RSL data for the west coast of North America (Engelhart et al. 2015; Shugar et al. 2014) display a previously recognized (Clague et al. 1982) general pattern for the British Columbia coast in which postglacial RSL histories are largely mirrored between the offshore outer coast and the mainland coast, though these same compilations also demonstrate a high degree of RSL variation through time and space. As with other glaciated areas and their immediate peripheries (see Pirazzoli 1996), terminal Pleistocene RSL change on the Northwest Coast was governed by the location and thickness of ice sheets during the Fraser Glaciation (the most recent glacial period in western North America, ~30-12 kya, and the latter part of what is more broadly termed the Wisconsin Glaciation in North America, ~110-12 kya)

and subsequent isostatic adjustments during and following deglaciation. The general trend is that mainland and inner coast areas were depressed downward tens to more than 200 meters by an ice sheet hundreds to several thousand meters thick during the Last Glacial Maximum (LGM). At the same time unglaciated areas of the outer coast were bulged upwards by asthenosphere material displaced outwards by this depression (Clague and James 2002; Fedje et al. 2005b; Hetherington and Barrie 2004). Additionally, during this time global sea level was as much as 125 m lower as a result of ocean water locked up in the ice sheets (Fairbanks 1989).

Deglaciation of the region began around 18,000 or 19,000 cal. BP ¹ (Blaise et al. 1990) and the ice sheets retreated inland sequentially from the coast (Clague and James 2002; Clague 1984). At this time, RSL was much lower on the outer coast and much higher on the inner coast. Meltwater caused a rise in global (eustatic) sea level, although this was quickly outpaced by isostatic readjustments caused by the unloading of ice from the land. The uplifted area collapsed, producing an overall rise in RSL on the outer coast, while the once-depressed inner coast rebounded upward, causing rapid RSL fall there. These effects were most pronounced at their outer and inner extremities, and recent work by McLaren and colleagues (2011; 2014) has identified a ‘sea level hinge’ area between the elevated outer coast and the isostatically depressed mainland where RSL position was generally stable through the Holocene.

1.2.2 Northern British Columbia

Figure 1 depicts RSL curves for northern British Columbian locations running west-east. In this region the Cordilleran ice sheet reached its maximum extent sometime after 27,300 – 25,400 cal. BP (Blaise et al. 1990). Isostatic depression was greatest in the areas with the thickest ice cover, and during this time ice sheets extended out across the northern Hecate Strait into Dixon Entrance (Hetherington et al. 2004). Prince Rupert Harbour was fully glaciated. Offshore,

¹ All dates are discussed in Calendar Years Before Present (i.e. before 1950).

the combined eustatic lowering of the sea level and uplift due to the forebulge resulted in RSL at least 150 m lower at southern Haida Gwaii, and the shallow Dogfish Bank and Laskeek Bank in western Hecate Strait were emerged as a wide coastal plain (Hetherington et al. 2003, 2004; Fedje et al. 2005b; Josenhans et al. 1997).

During deglaciation, glaciers retreated inland and from higher elevations first; the last glaciers to retreat were those that filled the deep inlets and river valleys (Clague and James 2002). This process was rapid, but not constant. There were temperature fluctuations that may have paused glacial retreat periodically, such as the Younger Dryas period between 12,900 and 11,700 cal. BP (Fedje et al. 2011). In the Nass River Valley, McCuaig (2000; McCuaig and Roberts 2006) found several pauses in RSL regression at various highstands that formed now-relict deltas between 230 m asl and 130 m asl during glacial retreat in the area. Melting glaciers caused eustatic sea level to rise until the mid-Holocene (Fairbanks 1989; Smith et al. 2011).

As opposed to the forebulged outer coast, shorelines closer to the depressed mainland and up the valleys were submerged where isostatic depression was greater than the lowered eustatic sea level. Marine mollusc shells dating to 15,000 cal. BP found around Prince Rupert and Port Simpson on the north end of Tsimpsan Peninsula indicate that this part of the outer mainland coast was deglaciated by this time and that RSL was at least 50 m higher (Clague 1984). Radiocarbon dates on shells from Zymagotitz River, near Terrace, 110 km inland from Prince Rupert, indicate that this region was not deglaciated until several thousand years later, around 11,500 cal. BP, but that RSL was 170 m higher at this time in the Kitsumkalum-Kitimat trough (Clague 1984, 1985). The highstands in the Nass River Valley remain undated, though their general elevation and distance from the coast are similar to those of the Kitsumkalum-Kitimat trough (McCuaig 2000; McCuaig and Roberts 2006). This illustrates that the timing and pace of

deglaciation also caused time-transgressive RSL change. There was considerable discrepancy in deglaciation and RSL position between the outer coast and the heads of the inlets and valleys. Each of these flooded areas experienced rapid RSL drops caused by isostatic uplift, though the rates and timing varied.

The tilting of the crust surface from the uplifted forebulge to the heavily depressed mainland meant that the Dundas Islands, located 40 km northwest of Prince Rupert and 60 km northeast of the northeastern tip of Haida Gwaii, were near to the midway ‘hinge’ point on the deformed continental plate, and maximally submerged by RSL 14.5 m above its current position (Letham et al. 2015; McLaren 2008; McLaren et al. 2011). After 14,000 BP, isostatic uplift and eustatic rise caused RSL to drop gradually from 14.5 m asl to its current position through the Holocene, with a still stand at 7.5 m asl between 8900 cal. BP and 6000 cal. BP. Meanwhile, on Haida Gwaii, isostatic collapse of the forebulge combined with the eustatic sea level rise caused RSL to rise 15 or 16 m above current sea level around 10,000-9500 cal. BP and stabilize there for about 4000 years before slowly dropping towards their current elevation, likely as a result of tectonic uplift (Clague et al. 1982; Fedje et al. 2005b:25).

More recent RSL changes are less known and less well understood in the region, as they were much more subtle in comparison to early rapid isostatic and eustatic changes. Late Holocene RSL change is still occurring by way of low-amplitude isostatic, eustatic, steric, and tectonic changes; as well as much more localized processes such as catastrophic tectonic events (earthquakes), sedimentation, compaction, and erosion (Pirazzoli 1996). Late Holocene RSL changes are likely to be more localized, but tracking these smaller scale shifts is relevant for considering their impacts on the shorter timescales of human generations, as well as for understanding the potential impacts of RSL change in the present day.

1.3 Previous Sea-Level Work around Prince Rupert

Previous RSL research around Prince Rupert was conducted by John Clague for the Geological Survey of Canada (Clague 1984, 1985; Clague et al. 1982), and briefly reassessed by Millennia Research Ltd. (Eldridge and Parker 2007). Clague suggested that RSL dropped from 50 m asl sometime after 15,000 cal. BP and passed below its current elevation sometime after 10,000 cal. BP, before rising again to its current position at 5700 cal. BP (Figure 1D). The hypothesis for an early-to-mid Holocene lowstand was based on negative evidence: extensive radiocarbon dating of archaeological sites in the area during the 1970s did not yield any ages older than 5700 cal. BP (Ames 2005; MacDonald and Inglis 1981), leading to the suggestion that RSL had stabilized by this time and that older sites were submerged.

Millennia Research Ltd. tested this hypothesized early Holocene lowstand by examining three core samples from intertidal contexts in the area, and concluded that “sea levels never fell substantially lower than present”; though they allow that even in the absence of evidence, “sea level may still have fallen by a metre or two below modern levels” (Eldridge and Parker 2007:17). Our refined RSL curve for Prince Rupert Harbour includes data from this previous research but demonstrates a fairly different RSL history.

2. Data and Methods

From 2012 to 2015 we conducted field work to identify RSL index points and limiting points. All RSL data points include location, elevation, age, and indicative meanings.

2.1 Limiting Points, Index Points, and Indicative Meanings

Sea level index points are data directly indicating the position of RSL at a particular time and space (Hijma et al. 2015; Shennan 2015); they are usually *in situ* macrofossils or sediments with a known and restricted elevation range relative to the tidal range. For RSL reconstruction, the possible elevation range over which an index point could have formed is calculated and then the difference between that range and current position of the indicator is measured (Table 1). Sea level limiting points are fossil or sedimentary indicators of either terrestrial (upper limiting) or marine environments (lower limiting) and constrain but do not directly indicate the position of RSL (Table 1). Most of our data are limiting points.

2.2 Measuring Elevation and RSL Change

The datum against which all elevations are measured relative to is geodetic mean sea level measured by the Canadian Geodetic Vertical Datum of 1928 (CGVD28) benchmark at Prince Rupert, which is 3.85 +/- 0.01 m above Chart Datum (<http://www.meds-sdmm.dfo-mpo.gc.ca/isdm-gdsi/twl-mne/benchmarks-reperes/station-eng.asp?T1=9354®ion=PAC>). Conveniently, this elevation nearly coincides with Mean Water Level (MWL, 3.849 m above Chart Datum) at Prince Rupert, which is the average of all hourly water levels, and coincides with Mean Tide Level (MTL), the average of High Water Mean Tide (HWMT) and Low Water Mean Tide (LWMT) (Table 2; Canadian Hydrographic Survey, personal communication, 2015). Because of this coincidence, geodetic mean sea level, MWL, and MTL are treated as equivalent, and variations around this zero point are expressed as ‘m asl’.

The tidal range at Prince Rupert is 7.40 m, which is very large compared to other areas of the British Columbia coast (Canadian Hydrographic Survey, personal communication, 2015). This introduces uncertainty to measurements on indicators from marine or intertidal contexts that

are not *in situ*, such as re-worked shells or diatoms, which can be pushed to the highest tidal limits by waves or moved below the tidal range by currents or debris flows. *In situ* indicators, such as molluscs in growth position or salt marsh sediments provide more accurate estimates of RSL position within this wide tidal range.

The elevations of all data were measured using a variety of instruments and methods, including an RTK GPS unit and base station, a Leica Total Station, a clinometer and stadia rod, and hand held GPS units. Elevations were often derived from or double checked against LiDAR digital terrain models (DTMs) of the study area (Airborne Imaging 2013), and all field-derived elevations cross-checked against this dataset showed very good consistency. All measured elevations were converted to m asl on the CGVD28 datum. Vertical measurement errors are applied to all data points in the final dataset and expressed as 95% confidence intervals (see Hijma et al. 2015 for error types and equations).

2.3 Measuring Age

All RSL limiting and index points in this study have ages measured by radiocarbon dating. All dates have been calibrated using OxCal 4.2 (Bronk Ramsey 2009, 2014), and are presented as 95% (2 sigma) probability ranges in calibrated years before present (BP, i.e. the year 1950). The marine reservoir effect was accounted for by applying a ΔR of 273 \pm 38, which is a conservative estimate for at least the last 5000 years in the Prince Rupert area (Edinburgh et al. 2016). It has been demonstrated elsewhere that ΔR values can fluctuate through time (e.g. Deo et al. 2004), and that marine organisms from immediate postglacial contexts may have larger offsets than subsequent times as a result of increased deep-water mixing from isostatic depression (Hutchinson et al. 2004b). However we lack any controlled baseline data from prior to 5000 BP to assess these effects for the study area. We therefore consistently apply a $\Delta R=273$

+/- 38, acknowledging that this value could have been different in the past and some of our early shell dates may be younger than presented. However, most of our calibrated very early shell dates are in accord with early dates on terrestrial material.

Bulk samples of sediment or multiple fragments of macrofossil material were dated when single samples of the appropriate size were not available. Following Tornqvist et al. (2015), in these cases we applied an additional error of +/- 100 years before calibration. Bulk organic sediment from immediate postglacial times likely contains carbon taken up from underlying glacial sediments (Hutchinson et al. 2004b). Hutchinson et al. (2004b) find a difference of 625 +/-60 years between postglacial bulk sediments and macrofossils for the southern mainland coast, though this effect varies locally based on the composition of local glacial substrates, and, as with the early postglacial marine shell, no baseline study has been conducted in the study area.

2.4 Field and Lab Methods

Index and limiting points were derived from sediment cores from bodies of water that contain transitions to or from marine conditions, relict marine sediments identified in geological traverses, and the lowest (earliest) components of archaeological sites identified through excavations or percussion coring.

2.4.1 Livingstone Sediment Cores

We collected 13 sediment cores from bogs, bays, and isolation basins ranging +49.7 to -1.36 m asl using a hand-driven Livingstone piston corer (Wright 1967). Isolation basins are water-filled basins with a measurable sill over which water drains. In instances of RSL change, these basins are 'isolated' from marine conditions when highest high tide levels are below the elevation of the sill, but will be brackish or marine environments during times when tides wash

over the sill or the sill is submerged. The bottoms of these basins accumulate sediments containing paleoenvironmental proxies (e.g. diatoms, pollen, foraminifera, ostracods, plant or animal macrofossils) over time. The point at which sediments record a change from a marine to fresh water depositional environment (or vice versa) approximates the time at which water containing those proxies passed over the sill elevation. Dating these transitions is a means of accurately measuring RSL position at certain times (Engelhart et al. 2015; Hafsten 1979, 1983a, 1983b; Hafsten and Tallantire 1978; Hutchinson et al. 2004a; James et al. 2009a; Kjemperud 1981; McLaren et al. 2011; Romundset et al. 2009; Rundgren et al. 1997).

In two instances we cored sphagnum bogs with standing water in which upward-growing peat obscured any definite sill; the surface elevation of standing water is used as a best estimate of elevation. For a tidal bay where a definite sill was not observable due to water depth we selected a well-sheltered location that we anticipated to have good sediment sequence preservation. For estimating the elevation of data points at this location we subtract the depth of dated samples from the elevation of the beach surface at the core location.

We cored basins until we reached an impenetrable obstruction or glacial sediments, which, in the study area, consist of either till or a distinctive blue-gray coloured glacio-marine clay (Clague 1984). Environmental transitions were identified using a combination of lithostratigraphic analyses (physical characteristics of the sediments), diatom microfossil analyses, and sediment stable carbon and nitrogen isotope analyses. Samples were selected for AMS radiocarbon dating from points in the cores that were indicative of transitions.

2.4.1.1 Diatom Analyses of Core Sediment

Preserved diatom microfossils from core sediment were used as a proxy for changing water salinity and RSL transitions (Battarbee 1986; Zong and Sawai 2015). See Supplemental

Text for a detailed description of sample selection and preparation. A minimum of 300 identifications were made for each sample; species were identified using multiple reference guides (Campeau et al. 1999; Cumming et al. 1995; Fallu et al. 2000; Foged 1981; Hein 1990; Krammer and Lange-Bertalot 1986a, b, c, and d.; Laws 1988; Pienitz et al. 2003; Rao and Lewin 1976; Tynni 1986). Diatom species were placed in a five-part salinity classification scheme based on the ‘halobian system’ (Hustedt 1953; Kolbe 1927, 1932) outlined by Zong and Sawai (2015:234): 1 = halophobic (salt intolerant freshwater) species, 2 = oligohalobous indifferent (freshwater) species, 3 = oligohalobous halophilic (freshwater but tolerant of salinity levels up to 2‰) species, 4 = mesohalobous (brackish water with salinity levels ranging from 2‰ to 30‰) species, and 5 = polyhalobous (marine water with salinity > 30‰) species.

2.4.1.2 Stable Isotope Analyses of Core Sediment

For key strata where diatom evidence was lacking, we measured stable carbon ($\delta^{13}\text{C}$) and nitrogen ($\delta^{15}\text{N}$) isotope compositions and elemental carbon-to-nitrogen (C/N) ratios of the organic fraction of sediments as a proxy for paleoenvironmental salinity (for review see Khan et al. 2015; Lamb et al. 2006). Organic sediments derived from autochthonous inputs of C_3 -dominated terrestrial materials should have lower $\delta^{13}\text{C}$ values as well as higher and more variable C/N ratios relative to sediments containing organics derived from marine algae and plants (Khan et al. 2015). Intertidal and salt marsh areas have $\delta^{13}\text{C}$ values and C/N ratios that are transitional, reflecting contributions of organic matter from both terrestrial and marine environments (Lamb et al. 2006; Mackie et al. 2005; Khan et al. 2015). Our results also suggest that $\delta^{15}\text{N}$ values from organic sediments can be useful for discriminating between marine and terrestrial/freshwater samples as the latter have consistently lower values.

We measured $\delta^{13}\text{C}$ and $\delta^{15}\text{N}$ values and elemental compositions of Holocene sediment samples from select cores with known freshwater/terrestrial ($n=8$) contexts and marine/intertidal contexts ($n=12$) as a comparative baseline for assessing paleosalinity of sediments that lack diatom evidence. Stable isotope compositions were measured using an Elementar vario MICRO cube elemental analyzer (EA) coupled to an Isoprime isotope ratio mass spectrometer in continuous flow mode. Detailed sample contextual details, preparation methods, sample calibration, and analytical uncertainty are discussed in the Supplemental Text. Known freshwater sediment samples yielded lower average $\delta^{13}\text{C}$ and $\delta^{15}\text{N}$ values and exhibit a wider range of $\text{C}_{\text{ORG}}/\text{N}_{\text{TOTAL}}$ ratios than known marine samples (Table 3 and Supplementary Table 1).

2.4.2 Relict paleomarine sediments in exposures and raised shoreline landforms

Six exposures of marine deposits with abundant marine mollusc shells located above their current habitat range were identified through traverses up creeks or along shorelines and dated. Previous studies in the area have identified an additional four such exposures that we include (Archer 1998; Clague 1984, 1985; Fedje et al. 2005b).

In addition to identifying paleomarine sediments in exposures, LiDAR DTMs were used to identify landforms that could represent relict raised shorelines. These included linear stretches of steeper slope relative to adjacent higher and lower elevations that run parallel to the modern shoreline, which could represent relict wave-cut backbeach berms. These locations were ground-truthed and flat landforms immediately above them were tested for archaeological material.

2.4.3 Basal dates from archaeological sites

We collected Environmentalist Soil Probe (ESP) percussion core samples from large shell-bearing archaeological sites and dated the lowest instances of cultural material in these cores, operating on the assumption that the dated material represents human occupation on land

and therefore above or near the contemporary higher high water mean tide (HHWMT) level (2.32 m asl), which we select as the most meaningful of the highest tide averages on the scale of human lifetimes (see Table 2). Several dates on the lowest cultural material from auger samples and test excavations conducted on hypothesized raised paleoshorelines are also included. 62 dates from 28 sites are included as upper limiting constraints on RSL.

Earlier compilations of RSL data points for Prince Rupert (Clague 1984, 1985; Shugar et al. 2014) include up to 40 dates from previously excavated archaeological sites, but provenience information for these dates is not available to assign elevations with the level of accuracy that we required (Dan Shugar, personal communication, 2015). We therefore do not include these dates in our analysis; all archaeological data points were collected in this study and carefully controlled for elevation.

3. Results

One-hundred and twenty-three index and limiting points constrain the inferred RSL curve (Table 4, Figure 3). Five of these are from previous studies; the rest are new. All index points and key limiting points are reported individually in this section. A summary of diatom analyses is presented on the core log Figures and Table 5. An RSL curve is interpreted from the entire collection of points, their association to one another, and judgement of their reliability in Section 4.

3.1 Livingstone Sediment Cores

3.1.1 Tsook Lake Core (TL#1, 49.7 m asl)

The highest elevation core is from Tsook Lake, north of Metlakatla on the Tsimpsean Peninsula. The elevation of the basin's sill is 49.7 m asl. Core TL#1 (Figure 4) contains a

sequence of marine sand and silt transitioning to freshwater gyttja and fragmental herbaceous peat and fragmental granular peat (following the terminology of Schnurrenberger et al. 2003:151, and henceforth ‘peat’). An *Arctostaphylos* sp. seed (a shrub species known as an initial colonizer of deglaciated landscapes [Mann and Streveler 2008:207]) from a brackish and marine-diatom dominated context dates 15,090-14,365 cal. BP (D-AMS 009956). Seeds from a freshwater diatom-dominated zone with minor brackish/marine influence located below the transition to gyttja and peat date 14,782-13,714 cal. BP (D-AMS 009955), indicating that the Tsook Lake basin was likely only being flooded by exceptionally high tides at this time. A relatively gradual transition from marine/brackish to freshwater diatom assemblages over as much as 1,200 years between these two dated samples may be indicative of a gradual RSL decline at this time. Twigs and a small cone from just above the transition to dark brown decomposed peat/gyttja date 13,971-13,330 cal. BP (D-AMS 009954) and provide a latest possible date for the full isolation of this basin from marine influence.

3.1.2 Rifle Range Lake 1 Core (RR1#2, 35 m asl)

Rifle Range Lake 1 is located on the east side of Kaien Island, the furthest east of any of our core samples. It has an estimated sill elevation of 35 m asl. Core RR1#2 (Figure 5) contains a sharp transition from brackish and marine diatom-dominated sand and silt to freshwater gyttja and peat. Mixed but indistinguishable plant matter from a thin dark lens of bedded organics about 15 cm below the transition dates to 14,090-13,458 cal. BP (D-AMS 008741). Several small twig fragments from 11 cm above the transition date 14,055-13,345 cal. BP (D-AMS 008740). The very tight chronological succession of these two dates, along with the abrupt transition to fully freshwater conditions indicates that RSL passed very quickly over this elevation. However,

the date in the brackish/marine sediment contradicts other dates in this study that suggest that RSL had passed well below 35 m asl at or before this time. Possible reasons for this are discussed in Section 4.2.1.

3.1.3 Cores from Bogs on northern Digby Island (DIB1#1, 17.2 m asl; and NDB#1, 17 m asl)

DIB1#1 (17.2 m asl) and NDB#1 (17 m asl) are sphagnum bogs with standing water on northern Digby Island (Figure 2). Cores from each contain basal blue-gray clay resembling the glacio-marine sediment observed in the study area overlain by sharp transitions to peat (Supplemental Figures 1 and 2). However, no diatoms were observed in samples from near to these transitions. A stick of wood lying diagonally in the lowest instance of peat in DIB1#1 yielded a relatively recent age of 8295-8028 cal. BP (D-AMS-005844), suggesting that it is intrusive from above or indicating an erosional unconformity. Two dates on samples from higher up in the peat in NDB#1 yielded ages of 8169-7626 cal. BP (D-AMS 009950) and 10,171-9521 cal. BP (D-AMS 009948). These three dates serve as upper limiting points for RSL during the early Holocene.

3.1.4 Digby Island Lake 1 Core (DL1#1, 15.2 m asl)

Digby Island Lake 1 is one of several lakes in a larger basin at the center of Digby Island that would have been isolated from the ocean by a long and narrow channel that runs to the south end of the island with a maximum sill height of 15.2 m asl. Core DL1#1 (Figure 6) contains a transition from marine and brackish diatom-dominated clayey sandy silt to brown silty mud with a transitional sequence of mixed diatom assemblages to fully freshwater assemblages, overlain by freshwater peat and gyttja. Organic macrofossils of sufficient size for radiocarbon dating were

not found in the marine or brackish sediment. Several small twig fragments from just above the transition to medium brown silty sand produced a date of 15,013-13,859 cal. BP (D-AMS 008745). Sediment from 2 cm above these twigs contains only 3.5 percent brackish and marine diatoms, indicating that this date is a reasonable approximation of the time just before the basin became isolated from marine incursions.

3.1.5 Bencke Lagoon Cores (BL#1 and BL#4, 2.4 m asl)

Bencke Lagoon is a shallow 'L'-shaped body of water located in a low-relief area at the end of Scott Inlet, east of Metlakatla (Figure 7). The lagoon currently drains over a 2.4 m asl sill, putting it within the upper tidal range for the Prince Rupert area (i.e. just above higher high water mean tide [HHWMT], Table 2), and therefore flooded by several high tides each month. The result is slightly brackish water within the lagoon.

Two cores taken several meters from each other (BL#1 and BL#4) contain a sequence beginning with coarse clastic material that is likely glacial till overlain by laminated gray silty sand transitioning to clay with marine mollusc shells that coarsens upwards to sand with marine mollusc shells. Sand without marine mollusc shells but with reworked fragments of marine diatoms overlies these layers. Subsequent to the deposition of the till, this sequence likely indicates a low energy subtidal environment transitioning to intertidal, and eventually to high intertidal. The upper section of core BL#1 (Figure 8) contains a sharp transition to gyttja with a remarkably diverse freshwater diatom assemblage, indicating a transition to a pond or slow-moving creek. The last few centimeters of sediment above this are light brown/tan silty mud containing a freshwater diatom assemblage similar to the gyttja below with the addition of the brackish-marine species *Paralia sulcata* and small *Fallacia* spp.. The inclusion of these

brackish-marine species into an otherwise diverse freshwater species-dominated context suggests that they are allochthonous, carried in by either very high tides or by storm surges. Stable isotope and elemental composition measurements of this gyttja yielded values that are intermediate between the average values for known marine and freshwater/terrestrial baseline samples (Table 3, Figure 9). This suggests that the organic matter at the top of the core is composed of a mixture of both freshwater and marine-derived materials, and was deposited under conditions similar to those of today.

A *Balanus* sp. shell from the lowest instance of shell in BL#4 dates 14,970-14,190 cal. BP (D-AMS 008752), and a *Mytilus* sp. shell and a *Balanus* sp. shell from the highest instance of shell in BL#1 date 15,284-14,675 cal. BP (D-AMS 008751) and 14,980-14,230 cal. BP (D-AMS 009953), respectively, though marine molluscs from early postglacial times may be slightly younger than measured if they are affected by more deep water mixing from isostatic depression (Section 2.3, Hutchinson et al. 2004b). A bulk sample of organic-rich sediment from the lowest instance of freshwater gyttja dates 14,833-13,738 cal. BP (UBA-29065) suggesting that the highest tides passed below 2.4 m asl (and therefore below their current position) by this time, although again, there may be an element of immediate-postglacial old carbon effect affecting this age (see Sections 2.3 and 4.1).

Seeds from just below the transition from freshwater gyttja to the silty mud with apparent marine incursions date 13,722-13,160 cal. BP (D-AMS 009952), and a twig from directly above this transition dates 13,255-13,065 cal. BP (D-AMS 009951). The proximity of these very old sediments to the surface indicates that the Holocene sediment sequence has been truncated in this location.

3.1.6 Optimism Bay Cores (OB#1 and OB#2, -1.36 m asl)

A well-sheltered bay with an extensive intertidal mudflat located north of the entrance to Scott Inlet, about 1 km northwest of Bencke Lagoon, was given an informal name of Optimism Bay (Figure 7). Intertidal sediment obscures any sill that may exist at the mouth of the bay, so data point elevations are subtracted from the elevation of the beach surface at the core location (-1.36 m asl).

Cores OB#1 and OB#2 (Figure 10) are only a few meters apart. Both contain a dark reddish brown organic-rich layer (-5 m asl to -4.86 m asl in OB#1 and -6.36 m asl to -6.0 m asl in OB#2) beneath several meters of intertidal or nearshore marine sand with marine shell hash. The buried organic-rich layer contains only a few poorly preserved oligohalobous indifferent and oligohalobous halophilic diatoms that could be allochthonous in OB#1, and no preserved diatoms in OB#2. Stable isotope analyses of two samples from the organic-rich layer in OB#1 and four samples in OB#2 yielded $\delta^{13}\text{C}$ and $\delta^{15}\text{N}$ values within the range values for our known freshwater/terrestrial sediments (Table 3, Figure 9 and Figure 10). Combined with the notable scarcity of diatoms, these results suggest that this deposit was subaerially exposed near to the shore but without direct tidal influence, and that the deposit is a paleosol or peat.

The sediment directly above this layer contains a diverse assemblage of primarily brackish and marine diatom species, though samples also contain between 4 and 18% freshwater diatom species. Stable isotope values of four samples from this zone all differ from those of the peat/paleosol, though exhibit both $\delta^{13}\text{C}$ values and C/N ratios closer to freshwater/terrestrial samples than the rest of the marine samples that we tested (Supplementary Table 1), suggesting some degree of mixing of organic sediments. In both cores, the diatom assemblage and stable isotope results indicate a marine transgression over a terrestrial peat or soil; the 3-4 m of shelly

sands above these sequences indicate a full transition to intertidal or nearshore marine environment. There is no indication of terrestrial conditions in either of the cores again.

Eight radiocarbon dates from both cores date the sequence. A bulk sample of organic rich-sediment from the very lowest instance of terrestrial material in OB#2 dates 14,163-13,436 cal. BP (UBA-29067), though, as with the gyttja in Bencke Lagoon, this sample may also be up to several centuries younger if a postglacial hard water reservoir effect has affected the carbonates in the sediment. The degree of this effect is constrained, however, by the age of the large piece of wood several centimeters above the bottom of the terrestrial layer: 13,772-13,572 cal. BP (D-AMS 008750). A bulk sample of organic-rich sediment from before the transition from freshwater/terrestrial conditions to the brackish diatom-dominated sediment dates 12,700-11,823 cal. BP (UBA-29066), providing an estimate for the last time this area was above tidal influence. In the brackish/marine sediments above the transition in both cores, four dates on plant macrofossils (D-AMS 008747, D-AMS 008749) and shell (D-AMS 008753, D-AMS 008754) all have calibrated age ranges between about 11,230 cal. BP and 10,700 cal. BP.

Notable amongst the diatom assemblage of the marine transgressive sediment in OB#2 was a single specimen of *Didymosphenia geminata* (Supplemental Figure 3), a nuisance species once considered invasive to the Northwest Coast, though argued by Bothwell and colleagues (2014; Taylor and Bothwell 2014) to be native to North America. This specimen is in stratigraphically secure context and well constrained by the radiocarbon dates to between 12,000 and 11,000 years old (Figure 10), making it the oldest identified specimen in North America and having significant implications for our understanding of the origins of this species' presence on the continent (Max Bothwell, personal communication, 2016).

3.1.7 Other isolation basin cores at or around current sea level (SL#1, 2.2 m asl; PL#1, 0.75 m asl; RA#2, 0 m asl; GLP#1, 0 m asl)

We cored four other basins at or near current sea level: Salt Lake, Russell Arm, Philip's Lagoon, and an unnamed lagoon east of Auriol Point (Figure 2). Cores from the latter two contained only marine and intertidal sediment sequences and provide only limited RSL lower constraining information (Supplemental Figures 4 and 5). Core SL#1 (Supplemental Figure 6) from Salt Lake, an isolated body of water with a 2.2 m asl sill and a minor tidal influence, contained laminated blue-gray clay, silt, and fine sand directly overlain by coarse sand with marine mollusc shells that date only 2660-2345 cal. BP (D-AMS 005839). Salt Lake is currently too high above sea level to support marine shellfish, so this date indicates that RSL was at least high enough for this area to be fully intertidal in the later Holocene. The lower laminated sediments in the core appear marine and suggest higher RSL earlier than the dated shell, though they resemble glacio-marine sediment observed in other cores. If this is the case then there is a significant erosional unconformity at the contact between these sediments and the shelly sand above, perhaps caused by Holocene RSL fluctuations.

Salt Lake drains into Russell Arm, which has an isolation basin with a bedrock sill that is 0 m asl. The ~4 m sediment sequence sitting on bedrock in core RA#2 contained only intertidal and marine sediment from the last 3400 years; a shell-rich sandy layer at the bottom dates 3394-3143 cal. BP (D-AMS 005843) and 3448-3343 cal. BP (D-AMS 005842), a massive bed of shell-free well-sorted silt rich with marine diatoms above this dates 2148-1998 cal. BP (D-AMS 005841), and an overlying shell-rich layer at the top of the sequence dates 1147-924 cal. BP (D-AMS 005840) (Supplemental Figure 7). While minimally indicating RSL at or above 0 m asl for the last 3400 years, there is some evidence for a slight upwards fluctuation in this sequence.

Low-tide and subtidal sediment in the immediate area is fine gray silt, while the higher intertidal zone (i.e. the adjacent depositional environment) has sand and shell hash pushed up by wave action. These facies provide a modern analogue for the facies in the core, and lateral migration of these facies in response to RSL change is suggested by their vertical succession. Therefore, the transition from sediment rich with intertidal molluscs to well-sorted silt with marine diatoms and then back between 3400 BP and 1150 BP suggests a slight rise and then fall in RSL. This pattern is also suggested by late Holocene archaeological data and discussed in Section 4.1.

3.2 Paleomarine deposits in geological exposures and relict paleoshoreline landforms

Two previously identified and two newly identified paleomarine sediment beds contain raised terminal Pleistocene-aged deposits. Marine mollusc shells exposed in marine sediment 53.6 m asl near Port Simpson, 30 km north of Prince Rupert date 14,863-14,080 cal. BP (Beta-14465) and 14,649-14,019 cal. BP (Beta-14464) (Archer 1998; Fedje et al. 2004; 2005b). Clague (1984, 1985; Lowdon and Blake Jr. 1979) dated a *Mya truncata* shell exposed at 11 m asl on the west side of Kaien Island that produced a calibrated age of 14,211-13,569 cal. BP (GSC-2290). We identified a terminal Pleistocene paleomarine deposit in a terrestrial ESP core from a 16 m asl terrace on the isthmus between Russell Arm and Philip's Lagoon; two marine shell samples from this core dated 15,187-14,574 cal. BP (D-AMS 005852) and 15,011-14,241 cal. BP (D-AMS 004470). Another large bed of reworked marine mollusc shells was found exposed at 3.83 m asl in the bank of Swamp Creek on the west side of Tsimpsean Peninsula. A shell from this exposure dated 14,510-14,000 cal. BP (D-AMS 007879).

Seventeen dated samples from seven exposed paleomarine sediment deposits ranging from -0.6 m to 9 m asl have ages ranging from 11,700 cal. BP to 9000 cal. BP. These show a

general trend of increasing elevation with time, tracking a marine transgression above the current sea level position in the early Holocene. Several of these samples were located within the current tidal range but were identified tens to hundreds of meters up creeks and buried under several meters of alluvial sediment and forest soil, indicating that these areas had once been intertidal under higher RSL conditions, and then that a subsequent drop in RSL caused a transition to estuarine and then terrestrial conditions (Figure 11). Several other locations contained molluscs dead in growth position (i.e. articulated valves sitting vertically in the sediment) within the current tidal range but above their habitat range, indicating higher sea level.

In two cases, we dated *in situ* butter clam (*Saxidomus gigantea*) specimens that provide RSL index points because of their known habitat range relative to the tidal range (Table 1; Carlson and Baichtal 2015:125; Foster 1991). A specimen from a shell bed containing large senile *Protothaca staminea*, *Clinocardium nuttalli*, *Tresus capax*, and *Saxidomus gigantea* in growth position exposed by a creek that has incised the intertidal zone in an unnamed estuary north of Optimism Bay dated 10,250-9952 cal. BP (D-AMS 007880, Figure 7). The mean elevation of this shell bed is 0.058 m asl, though butter clams are known to prefer living between 0.46 m above and 0.91 m below Lower Low Water Mean Tide (LLMWT, -2.528 m asl at Prince Rupert) (Carlson and Baichtal 2015:125²; Foster 1991), or -2.07 to -3.44 m asl around Prince Rupert. This indicates that RSL was 3.5 to 2.1 m higher when the *S. gigantea* were alive. An *in situ* *S. gigantea* shell from Tea Bay Creek that dates 10,196-9901 cal. BP (D-AMS 004468) was recovered 2.4 m asl indicates that RSL was 5.8-4.5 m higher at that time (Figure 11). Assuming a constant tidal range through time, these estimates place highest astronomical tide (3.66 m asl, Table 2) as high as 9.46 m asl by ~10,000 years ago.

² Carlson and Baichtal use the range -0.91 and +0.46 m above MLLW (mean lower low water), which is a US measurement based on observed data and generally equivalent to LLMWT, a Canadian measure based on predicted tidal levels (Canadian Hydrographic Survey, personal communication, September 28, 2015).

In addition to these paleomarine sediments, frequent 7-10 m asl steep-sloped linear ridges that run parallel to the modern shoreline throughout the study area are visible in LiDAR bare earth DTMs (Figure 12). These features resemble relict backbeach berms, and their prominence in the regional topography suggests that RSL was once stable at these positions. Archaeological deposits associated with these paleoshorelines indicate that these features were shorelines during the early Holocene (Section 3.3), which is consistent with the 5.8-4.5 m higher RSL indicated by the Tea Bay Creek *S. gigantea*.

3.3 Archaeological Sites

Sixty-two dates from 28 archaeological habitation sites constrain RSL position during the Holocene. Preliminary archaeological survey of flat landforms immediately above the 7-10 m asl paleoshoreline ridges resulted in the identification of three of the oldest archaeological sites yet recorded in the Prince Rupert area. P011-1, on a 10-12 m asl terrace (Figure 12), contains evidence of concentrated and repeatedly-used campfires or hearths and stone tool making dating 9304-9028 cal. BP (D-AMS 011950) and 8348-8186 cal. BP (D-AMS 011949). Two more sites on 8-9 m asl terraces, GbTo-82 and P009-1, have small cultural shell-bearing components that date 6728-6463 cal. BP (D-AMS 011956) and 6635-6445 cal. BP (D-AMS 011948), respectively. A paleosol directly below the cultural component at P009-1 provides a further 7.95 m asl upper limiting RSL point at 7170-6960 cal. BP (D-AMS 011947).

The majority of archaeological data points ($n=57$) come from the basal components of large shell-bearing sites and date between 5000 cal. BP and 1000 cal. BP. These data are spread between 3.1 m asl and 10 m asl, and in general suggest RSL close to, but slightly higher than that of today (Figure 3).

Several archaeological sites dating 3500-1500 cal. BP were identified on paleoshorelines associated with higher RSL. Three previously unrecorded large shell-bearing sites (T623-1, T717-1, T722-1) were identified 60-130 m back from the modern shoreline in LiDAR DTMs. GcTo-28 is a similar previously recorded village 30 m back from the shoreline. These sites are all located on 5.5-6.5 m asl terraces fronted by low-lying 3.5-4.5 m slopes toward the modern shoreline (e.g. Figure 12). Basal dates from these sites vary from about 3500 BP to 1700 BP, but they all appear to have been abandoned between 2000 and 1500 BP. Sandy deposits with marine shell that we interpret to be intertidal or storm surge deposits were identified beneath the cultural layers at three of these sites. Shells from a natural deposit 2.38 m asl and 2.92 m asl beneath T623-1, 130 m back from the current shoreline, date 2762-2495 cal. BP (OS-119874) and 2315-2071 cal. BP (OS-119876), respectively, while a shell from 5.36 m asl beneath T722-1, 60 m back from the current shoreline, dates 3201-2736 cal. BP (D-AMS 007890). Taken together, the archaeological data from the last 5000 years suggests slightly higher RSL in the late Holocene, with some potential fluctuations, discussed in Section 4.1.

4. Discussion

4.1 Prince Rupert RSL History and the Processes Driving RSL Change

The age-altitude relations of our dated samples and an inferred RSL curve are shown in Figure 13. The RSL curve is the most parsimonious interpretation of the data. The calibrated ranges of radiocarbon dates add uncertainty to the timing of inflections and potentially more subtle nuances within the curve, especially for the terminal Pleistocene.

RSL was at least 50 m higher than at present when the area was deglaciated. Marine sediment in Tsook Lake (49.7 m asl) demonstrates that this occurred at by least 15,090-14,365

cal. BP (D-AMS 009956). A gradual transition from marine to freshwater diatoms between 15,090-14,365 cal. BP (D-AMS 009956) and 14,782-13,714 cal. BP (D-AMS 009955) in Tsook lake indicates a relatively slow RSL regression between these times, though a date of 14,163-13,436 cal. BP (UBA-29067) on the first instance of paleosol/peat -6.3 m asl at Optimism Bay indicates very rapid isostatic uplift of the deglaciated landscape after Tsook Lake was isolated from marine influence. This rapid RSL drop is also indicated or constrained by dates from the paleomarine deposit near Port Simpson (53.55 m asl) and on the isthmus between Russell Arm and Philip's lagoon (15.9 m asl), the transition from marine to freshwater conditions Digby Island Lake 1 (15.2 m asl), the paleomarine exposures on west Kaien Island (11 m asl) and in Swamp Creek (3.83 m asl), and the transition from marine to freshwater conditions in Bencke Lagoon (2.4 m asl).

There is a large degree of overlap between the date on the freshwater bulk sediment samples from Bencke Lagoon (14,833-13,738 cal. BP, UBA-29065) and Optimism Bay (14,163-13,436 cal. BP, UBA-29067) and the transition from marine to freshwater conditions nearly 50 meters higher at Tsook Lake (14,782-13,714 cal. BP, D-AMS 009955), which was dated using plant macrofossils. It is likely that the bulk sample ages have been influenced by an immediate postglacial old carbon effect (Hutchinson et al. 2004b). Even if this effect pushes the dates ahead several centuries, these data demonstrate that around Prince Rupert the immediate postglacial RSL drop caused by isostatic rebound likely took less than 1000 years, and as little as a few centuries. This rapid uplift rate is in line with those observed at other near-field/glaciated areas on the west coast of North America, particularly on the southern British Columbia coast (e.g. Clague et al. 1982; Hutchinson et al. 2004a; James et al. 2005, 2009a; Shugar et al. 2014).

A RSL lowstand below -6.3 m asl following initial isostatic rebound lasted for about a 2000 year interval that encompassed the Younger Dryas period (12,900-11,700 BP). This lowstand is indicated by the transition to fully freshwater conditions in Bencke Lagoon at 14,833-13,738 cal. BP (UBA-29065) and by the buried peat/paleosol in Optimism Bay, 6.3 m below current sea level. The extent of this lowstand below sea level is not constrained by any lower limiting points (Figure 13), though stable isotope values for the Optimism Bay peat/paleosol suggest very minor mixing of marine-derived organic material, suggesting that the lowstand did not extend much below -6.3 m asl (Section 3.1.6, Table 3, Figure 9). Evidence for the terminal Pleistocene lowstand is not apparent in the other low elevation cores from Philip's Lagoon (PL#1, 0.75 m asl sill) and the lagoon east of Auriol Point (GLP#1, 0 m asl sill), likely due to the erosion of sediment from this time during the subsequent RSL transgression; erosional unconformities are often produced by slow RSL rise (Green et al. 2014). The preservation of lowstand sediment at Optimism Bay and Bencke Lagoon is likely attributable to fortuitous preservation contexts. The re-introduction of marine diatoms in Bencke Lagoon at 13,255-13,065 cal. BP (D-AMS 009951, Section 3.1.5), the middle of the lowstand, may be indicative of fluctuations during this time that are not evident within the Optimism Bay cores, irregular storm events or very high tides, mixing of lower freshwater sediments with younger sediment during the RSL transgression, or a laboratory error. All other radiocarbon dates suggest that RSL did not rise up to and above the lowstand peat/paleosol until after 12,700-11,823 cal. BP (UBA-29066), when intertidal sediments are present in both Optimism Bay cores.

A marine transgression caused RSL to rise to 6-8 m asl between 11,700 and 9000 cal. BP. Four dates on the brackish and marine diatom-rich sediments above the Optimism Bay peat/paleosol and seventeen dates on seven relict paleomarine deposits indicate that Optimism

Bay was again intertidal by 11,500 BP, that RSL passed over its current position just before 11,000 BP, and that it continued upward several meters in the early Holocene. Because the elevations of these samples are not controlled by sill elevations, and because marine mollusc shells can be moved anywhere within or below the tidal range by waves, tides, and currents, these data have more elevation scatter (Figure 13). This may also partly be attributable to varying marine reservoir effects (Hutchinson et al. 2004b). We lend the most weight to the growth position *S. giganteas* from the estuary north of Optimism Bay (indicating an RSL 3.5-2.1 m asl) and from Tea Bay Creek (indicating an RSL of 5.8-4.5 m asl) for the position of the inferred RSL curve during this transgression. The similar dates on these samples, 10,250-9952 cal. BP (D-AMS 007880) and 10,196-9901 cal. BP (D-AMS 004468), respectively, and the 2.4 m elevation difference between the two suggest that the transgression was rapid. It occurred earlier and more abruptly than post-lowstand transgressions recorded on the south coast of British Columbia. The RSL rise is likely related to a well-recorded global increase in eustatic sea level between 11,650 and 7000 cal. BP (Smith et al. 2011), which includes a particularly rapid increase at the termination of the Younger Dryas associated with a meltwater pulse (Glacial Meltwater Pulse 1B) caused by dramatic warming at this time (Green et al. 2014; Liu and Milliman 2004; Smith et al. 2011). This eustatic sea level rise outpaced isostatic rebound, even though the now-slower isostatic crustal response continued upward.

The early Holocene is characterized by a RSL highstand, primarily constrained by abundant 7-10 m paleoshoreline berms and newly identified archaeological sites on terraces associated with these berms, and loosely constrained by 17 m asl upper limiting dates from the Digby Island bogs and 0 m asl lower limiting dates from Pillsbury Cove and the lagoon east of Auriol point. The Tea Bay Creek *S. giganteas* indicate that RSL rose to at least 5.8-4.5 m above

its current position by 10,196-9901 cal. BP (D-AMS 004468). Taking into account a high tide of up to 3.66 m above this (Table 2), the 9000-8000 BP archaeological remains 10-12 m asl at P011-1 suggest that RSL may have continued rising another 1 or 2 meters by that time. Taking into account the 6500 cal. BP archaeological remains from 8-9 m asl terraces at GbTo-82 and P009-1, these data suggest that RSL reached 6-8 m asl by 9000 years ago and remained relatively stable above its current position for the duration of the early Holocene, dropping only a couple of meters by 6500 cal. BP. This contradicts earlier RSL reconstructions for the area that inferred that RSL was below its current position between 10,000 and 5700 cal. BP (see Section 1.3; Clague 1984, 1985; Clague et al. 1982; Eldridge and Parker 2007).

RSL dropped to within a few meters of its current position after 6500 cal. BP and continued dropping slowly, albeit with some potential fluctuations. This may have been driven by continuing slower isostatic crustal response overtaking the slowing post-glacial eustatic sea level rise, the latter of which completed around 6000 BP. The last 6000 years are primarily constrained by basal dates on archaeological sites that display a wide degree of scatter. There are no lower limiting data between 7525-7225 cal. BP (Beta-221626, Pillsbury Cove) and 3448-3343 cal. BP (D-AMS 005842, Russell Arm). There is only a single data point between just after 6500 BP and 5000 BP: a basal date of 6006-5733 cal. BP (OS-101646) from site GcTo-6 at 4.18 m asl suggests that RSL continued to fall from the early Holocene highstand, perhaps at a slightly increased rate. The data from 5000 cal. BP onward can be interpreted in several ways, depending on the weight attributed to specific indicators. Figure 14 presents two options, a more conservative general pattern of slow RSL regression that smooths out potential noise in the data, and a second option that attempts to fit all the data so that the lowest basal archaeological dates are close to or above a 2.32 m HHWMT and all lower limiting dates above RSL are at least

704 within the relative tidal range. The latter is an exaggerated curve, but illustrates the maximum
705 inflections from known data. Between 5000 and 3200 cal. BP the majority of archaeological
706 basal dates are 5-6 m asl but show a subtle overall decrease in elevation until 3000 cal. BP, at
707 which time three different sites (GbTo-4, GbTo-24, GbTo-64) have dated basal samples at or
708 below modern HAT. This suggests a continued fall, but that RSL was still 1.5-2.5 m higher than
709 its current position during this period.

710 The period between 3200 cal. BP and 1600 cal. BP has the largest vertical spread of data
711 (Figure 14). An increase in the overall range of basal elevations during this time indicates that
712 people are initiating settlements on higher ground. There is a slight increase in elevations of the
713 lowest basal archaeological dates in the middle of this age range compared to those immediately
714 preceding and following. The four large shell-bearing sites identified on 5.5-6.5 m terraces 60-
715 130 m back from the modern shoreline (GcTo-28, T623-1, T717-1, T722-1) are all occupied
716 during this time and are all abandoned between 2000 and 1500 years ago. There are five lower
717 limiting data points that suggest higher RSL between 3000 and 2000 years ago from stranded
718 paleomarine deposits beneath archaeological sites GcTo-52, T623-1, and T722-1, and from the
719 Salt Lake Core. The facies sequence in the Russell Arm core also suggest a slight RSL rise
720 sometime between 3394-3143 cal. BP (D-AMS 005843) and 1147-924 cal. BP (D-AMS
721 005840).

722 Minimally, these data indicate that RSL continued to be several meters higher into the
723 late Holocene (Figure 14, dotted line), though, depending on how much weight is put on the
724 correlation between archaeological basal dates and RSL changes, they could be suggestive of a
725 modest RSL dip and then rise (~1-2 m) around 3200 cal. BP before ultimately falling to very
726 close to its current position between 2000 and 1500 years ago (Figure 14, dashed line). The

overall trend of slow RSL fall from the early Holocene highstand is likely attributed to the final influence of isostatic crustal rebound in the region. More data is required to test possible subtle late Holocene RSL fluctuations and their driving mechanisms, though they may be associated with climate fluctuations or neoglacial periods in the Coast Mountains (i.e. Clague and Mathewes 1996; Desloges and Ryder 1990; Lamoureux and Cockburn 2005).

Most recently, historical tidal records from 1937-2000 indicate that RSL is rising in Prince Rupert Harbour by a rate of 1.72 ± 0.06 mm/yr, and that this is a result primarily of global eustatic sea level rise and a very slight (possibly zero) local subsidence rate of 0.7 ± 1.0 mm/yr (Larsen et al. 2003; see also James et al. 2014 for similar calculations). The measured eustatic sea level rise over the last century is likely partly attributable to anthropogenically accelerated global warming. The effects of this recent RSL rise are visible on actively eroding archaeological sites throughout the area.

4.2 Significance for Regional Studies

4.2.1 Regional Glacial and RSL Histories

This research highlights spatial variation in the timing of RSL changes not previously anticipated in the study area, particularly immediately after deglaciation. A tightly dated transition from marine conditions to freshwater conditions in the Rifle Range Lake 1 core RR1#2 suggests that RSL passed below 35 m asl between 14,090-13,458 cal. BP (D-AMS 008741) and 14,055-13,345 cal. BP (D-AMS 008740), but at the same time, samples from cores in Bencke Lagoon and Optimism Bay indicate that RSL was below its current position in those locations. One explanation for this discrepancy is a time-transgressive lag in isostatic rebound mediated by the position of eastward-retreating ice sheets. Rifle Range Lake is 12 km east-southeast of

Optimism Bay, in a glacially carved channel on the fringe of the transition from the Hecate Lowlands to the Coast Mountain Range (Figure 2). Ice sheet cover may have been thicker at Rifle Range Lake 1, and may have melted slightly later than the western edge of the study area, causing a lag of several hundred years before this area experienced full isostatic uplift. This implies at least 3.1 m/km of crustal tilt at this ice margin, a high value that suggests a thin lithosphere in this area (see James et al. 2000 for a discussion of the relationship between crustal tilt and lithosphere thickness at the northern Cascadia subduction zone).

The pattern holds for radiocarbon dated barnacle shells found in growth position 30 m asl near the mouth of Khyex River entering the Skeena River, a further 30 km east of Rifle Range Lake 1. Two samples from this location both date about 12,700-12,200 cal. BP (Blackwell et al. 2010), indicating that RSL was still well above its current position here during its lowstand around Prince Rupert. Finally, another 80 km east of Khyex River, the Kitsumkalum-Kitimat Trough south of Terrace was not deglaciated until at least 11,500 BP (Clague 1984, 1985), and RSL dropped rapidly because of isostatic uplift there at the same time as the RSL transgression was taking place at Prince Rupert.

Clearly, RSL position at single points in time can vary greatly with short distances depending on glacial loading, particularly on axes perpendicular to continental margins. As a result, RSL data may need to be gathered and compiled from relatively spatially limited areas, particularly if it is being used for guiding archaeological surveys for terminal Pleistocene material. Furthermore, compiling multiple RSL histories for more discrete spatial units has the potential to contribute to more robust glacial-isostatic modelling of coastal British Columbia (Hetherington et al. 2003, 2004; Hetherington and Barrie 2004), such as that conducted by James and colleagues (2009b) for the northern Cascadia subduction zone.

4.2.2 Implications for Early Human Occupation and Archaeological Survey

Understanding the history of RSL change in the Prince Rupert area is critical for developing surveys for terminal Pleistocene and early Holocene archaeological sites in the area, as well as for understanding the impact of RSL change on the archaeological record.

Furthermore, the archaeological potential of paleoshorelines away from the current shoreline has important implications for heritage conservation in and around Prince Rupert Harbour, a major port and hub of industrial development. Detailed archaeological impact assessments that include potential paleoshoreline locations above and below current sea level that may be impacted by future development will help to mitigate the potential destruction of early archaeological sites.

Support for a coastal migration route for the first peopling of the Americas is gaining traction (Dixon 2013; Dixon and Monteleone 2014; Fedje and Mathewes 2005; Fedje et al. 2011; Mackie et al. 2011; Mandryk et al. 2001), and there is now evidence for people having lived on the BC coast as early as 13,500 cal. BP near Calvert Island, 350 km south of Prince Rupert (McLaren et al. 2015). Elsewhere on the Northwest Coast, Late Pleistocene and early Holocene sites are being identified with increasing frequency on paleoshorelines, though very few early sites are recorded on or near the mainland, especially on the northern Northwest Coast (Mackie et al. 2011). The paucity of very early sites on the inner coast may be related to a lag in deglaciation time as well as more extreme isostatic adjustments, but our data indicates that the Prince Rupert area was deglaciated and supporting edible marine molluscs by at least 15,090-14,365 cal. BP (D-AMS 009956), was vegetated shortly after, and had completed its most dramatic period of shoreline change by 14,000-13,500 years ago. We suggest that the study area was amenable to human occupation by at least this time; the presence of humans 350 km south

on Calvert Island by 13,500 BP means that it is reasonable to hypothesize contemporaneous human occupation of the Prince Rupert area.

Our data suggest that archaeological evidence of habitation around Prince Rupert immediately after deglaciation is likely to be thinly scattered between 50 m asl and current sea level, and from between 13,500 and 11,000 years ago is likely to be below current sea level, potentially buried beneath several meters of intertidal sediment. Furthermore, preservation in well-sheltered areas like Optimism Bay is likely to be excellent, whereas other archaeological material may have eroded away during the marine transgression after the Younger Dryas.

Early Holocene archaeological sites will be stranded on raised terraces above a high tide line that was minimally 8 m asl. P011-1 is the earliest currently recorded radiocarbon dated archaeological site on the inner northern coast of British Columbia, though an abundance of terraces associated with the 7-10 m paleoshoreline ridges visible in LiDAR DTMs of the study area suggests a high potential for more early Holocene sites. The refined RSL curve provides an important tool for archaeologists working in the region, and will be necessary for exploring the possibilities for early human dispersals through northern British Columbia, as well as developing an understanding of early- and mid-Holocene occupation, which was until now unknown for the Prince Rupert area.

5. Conclusion

This paper describes RSL history around Prince Rupert since deglaciation, constrained by 123 RSL index and limiting points gathered from Livingstone sediment cores, geological surveys, and archaeological investigations. The area was deglaciated sometime before 15,090-14,365 cal. BP (D-AMS 009956), after which there was a rapid RSL drop from at least 50 m asl

to at least -6.3 m asl between 14,500 BP and 13,500 BP in as little as a few centuries. After a lowstand below current sea level for about 2000 years during the terminal Pleistocene, RSL rose again to at least 6 m asl - and as high as 8 m asl - after the Younger Dryas. RSL slowly dropped towards its current position through the Holocene, though it appears to have remained 1-3 m higher until between 2000 and 1500 years ago. There is equivocal evidence for slight fluctuations on the order of several meters between 3200 and 1500 BP. By collecting a large dataset over a relatively small geographical area we are able to distinguish variable RSL histories across relatively short distances. This detailed dataset contributes to a refined understanding of glacio-isostatic dynamics in the region. We identify what is currently the earliest dated archaeological site on the inner northern BC coast, a small 8000-9000 year old campsite on a 10-12 m asl terrace, though we suggest that the study area could have been inhabited by humans by at least 14,500-13,500 years ago, when we have the first dated evidence for vegetation of the landscape. The new inferred RSL curve for Prince Rupert indicates the probable elevations of early human settlement in the region at different times and gives potential targets for future research.

Acknowledgments

We gratefully acknowledge Lax Kw'alaams and Metlakatla Indian Bands for supporting our research. We thank Duncan McLaren and Daryl Fedje for allowing us to use the Livingstone Coring equipment, for training in diatom analysis methods, and for providing a legacy of sea level and archaeological field work along the north coast of BC on which this study builds. This project could not have been completed without the field expertise of John Maxwell and Steven Dennis, nor could it have been done without the field assistance of Erika Leighton, Tony

841 Leighton, Kisha Supernant, Justin Junge, Jacob Kinze Earnshaw, Steve Mozarowski, Brian
842 Pritchard and Dave Doolan. We thank Ian Hutchinson and Eric Letham for advice along the way
843 and comments on an earlier draft of this paper, and we are immensely grateful to Thomas James
844 and John Clague for their detailed reviews and suggestions that improved the final product. Eric
845 Letham helped design and create Figures 3, 4, 5, 6, 8, 10, 13 and 14. We thank Audrey
846 Dallimore and Malcolm Nichol for photographing our cores and allowing us to do sampling at
847 the Pacific Geoscience Centre in Sidney, BC. We thank Nexen Energy for generously providing
848 us with the LiDAR data used in this project. This project was funded by SSHRC Grant # 410-
849 2011-0414 (PI: Martindale) and NSF Grant # 1216847 (PI: Ames).

850

References

- Airborne Imaging
2013 *Final Project Report for Digby Island LiDAR*. Unpublished report prepared for Nexen Energy.
- Ames, K.M.
2005 *The North Coast Prehistory Project Excavations in Prince Rupert Harbour, British Columbia: The Artifacts*. BAR International Series, 1342. British Archaeological Reports, Oxford.
- Ames, K.M., A. Martindale
2014 Rope Bridges and Cables: A Synthesis of Prince Rupert Harbour Archaeology. *Canadian Journal of Archaeology* 38(1):140-178.
- Archer, D.J.W.
1992 *Results of the Prince Rupert Radiocarbon Dating Project*. Report on File, British Columbia Heritage Trust.
- 1998 Early Holocene Landscapes on the North Coast of British Columbia. Paper presented at the 31st annual meeting of the Canadian Archaeological Association, Victoria.
- 2001 Village Patterns and the Emergence of Ranked Society in the Prince Rupert Area. In *Perspectives on the Northern Northwest Coast Prehistory*, edited by J.S. Cybulski, pp. 203–222. Mercury Series, Archaeology Survey of Canada Paper 160, Canadian Museum of Civilization, Hull, Quebec.
- Battarbee, R.W.
1986 Diatom Analysis. In *Handbook of Holocene Palaeoecology and Palaeohydrology*, edited by B.E. Berglund, pp. 527-570. John Wiley and Sons, Chichester.
- Blackwell, B.A., J.J. Gong, A.R. Skinner, A. Blais-Stevens, R.E. Nelson, J.I. Blickstein
2010 ESR Dating Pleistocene Barnacles from BC and Maine: A New Method for Tracking Sea Level Change. *Health Physics* 98(2):417-426.
- Blaise, B., J.J. Clague, R.W. Mathewes
1990 Time of the Maximum Late Wisconsin Glaciation, West Coast of Canada. *Quaternary Research* 34:282-295.
- Bothwell, M.L., B.W. Taylor, C. Kilroy
2014 The Didymo story: the tale of low dissolved phosphorus in the formation of *Didymosphenia geminata* blooms. *Diatom Research*, DOI: 10.1080/0269249X.2014.889041
- Bronk Ramsey, C.
2009 Bayesian analysis of radiocarbon dates. *Radiocarbon* 51(1):337-360.

- 2014 OxCal Program, Version 4.2.3. <http://c14.arch.ox.ac.uk/embed.php?File=oxcal.html>.
- Campeau, S., R. Pienitz, A. Héquette
 1999 *Diatoms from the Beaufort Sea Coast, Southern Arctic Ocean (Canada): Modern Analogues for Reconstructing Late Quaternary Environments and Relative Sea Levels*. Bibliotheca Diatomologica No. 42. J. Cramer Inc., Berlin.
- Carlson, R.J., J.F. Baichtal
 2015 A Predictive Model for Locating Early Holocene Archaeological Sites Based on Raised Shell-Bearing Strata in Southeast Alaska, USA. *Geoarchaeology: An International Journal* 30:120-138.
- Clague, J.J.
 1984 *Quaternary Geology and Geomorphology: Smithers-Terrace-Prince Rupert Area, British Columbia*. Memoir No. 413, Geological Survey of Canada, Ottawa, Ontario.
 1985 Deglaciation of the Prince Rupert-Kitimat Area, British Columbia. *Canadian Journal of Earth Sciences* 22:256-265.
- Clague, J.J., J.R. Harper, R.J. Hebda, D.E. Howes
 1982 Late Quaternary Sea Levels and Crustal Movements, Coastal British Columbia. *Canadian Journal of Earth Science* 19:597-618.
- Clague, J.J., T.S. James
 2002 History and Isostatic Effects of the Last Ice Sheet in Southern British Columbia. *Quaternary Science Reviews* 21:71-87.
- Clague, J.J., R.W. Mathewes
 1996 Neoglaciation, Glacier-Dammed Lakes, and Vegetation Change in Northwestern British Columbia, Canada. *Arctic and Alpine Research* 28(1):10-24.
- Coupland, G.
 1988 Prehistoric Economic and Social Change in the Tsimshian Area. *Research in Economic Anthropology* 3:211-245.
 2006 A Chief's House Speaks: Communicating Power on the Northern Northwest Coast. In *Household Archaeology on the Northwest Coast*, edited by E. Soepel, D. Ann Trieu Gahr, and K.M. Ames, pp. 80-96. International Monographs in Prehistory, Archaeological Series 16, Ann Arbor, Michigan.
- Coupland, G., C. Bissell, S. King
 1993 Prehistoric Subsistence and Seasonality at Prince Rupert Harbour: Evidence from the McNichol Creek Site. *Canadian Journal of Archaeology* 17:59-73.
- Coupland, G., T. Clark, A. Palmer

- 2009 Hierarchy, Communalism and the Spatial Order of Northwest Coast Houses: a Comparative Study. *American Antiquity* 74:77-106.
- Coupland, G., R.H. Colten, R. Case.
- 2003 Preliminary Analysis of Socioeconomic Organization at the McNichol Creek Site, British Columbia. In *Emerging from the Mist: Studies in Northwest Coast Culture History*, edited by R.G. Matson, G. Coupland, and Q. Mackie, pp. 152–169. UBC Press, Vancouver.
- Coupland, G., A. Martindale, S. Marsden
- 2001 Does Resource Abundance Explain Local Group Rank among the Coast Tsimshian? In *Perspectives in Northern Northwest Coast Prehistory*, Mercury Series Archaeological Survey of Canada Paper 160. J.S. Cybulski ed. pp. 221-248. Ottawa: National Museum of Canada.
- Coupland, G., K. Stewart, K. Patton
- 2010 Do you never get tired of salmon? Evidence for extreme salmon specialization at Prince Rupert harbour, British Columbia. *Journal of Anthropological Archaeology* 29(2): 189-207.
- Cumming, B.F., S.E. Wilson, J.P. Smol
- 1995 *Diatoms from British Columbia (Canada) Lakes and their Relationship to Salinity, Nutrients, and other limnological variables*. Bibliotheca Diatomologica No. 31. J. Cramer, Berlin.
- Deo, J.N., J.O. Stone, J.K. Stein
- 2004 Building confidence in shell: variations in the Marine Reservoir Correction for the Northwest Coast over the past 3000 years. *American Antiquity* 69(4):771-786.
- Desloges, J.R., J.M. Ryder
- 1990 Neoglacial history of the Coast Mountains near Bella Coola, British Columbia. *Canadian Journal of Earth Sciences* 27:281-290.
- Dixon, E.J.
- 2013 Late Pleistocene colonization of North America from Northeast Asia: new insights from large-scale paleogeographic reconstructions. *Quaternary International* 285:57-67.
- Dixon, E.J., K. Monteleone
- 2014 Gateway to the Americas: Underwater Archaeological Survey in Beringia and the North Pacific. In *Prehistoric Archaeology on the Continental Shelf*, edited by A.M Evans et al., pp. 95-114. Springer Science, New York.
- Drucker, P.
- 1943 Archaeological Survey on the Northern Northwest Coast. In *Bureau of American Ethnology Bulletin*, pp. 17–132. vol. 133. The Smithsonian Institution, Washington D.C.

- 988 Edinborough, K., A. Martindale, G.T. Cook, K. Supernant, K.M. Ames
 989 2016 A Marine Reservoir Effect ΔR Value for Kitandach, in Prince Rupert Harbour, British
 990 Columbia, Canada. *Radiocarbon* DOI:10.1017/RDC.2016.46.
 991
- 992 Eldridge, M., A. Parker
 993 2007 *Fairview Container Terminal Phase II Archaeological Overview Assessment*. Report
 994 prepared for Fairview Container Terminal, Prince Rupert Port Authority by Millennia
 995 Research Ltd.
 996
- 997 Engelhart, S.E., M. Vacchi, B.P. Horton, A.R. Nelson, R.E. Kopp
 998 2015 A Sea-Level Database for the Pacific Coast of Central North America. *Quaternary*
 999 *Science Reviews* 113: 78-92.
 1000
- 1001 Fairbanks, R.G.
 1002 1989 A 17,000-year glacio-eustatic sea level record: influence of glacial melting rates on the
 1003 Younger Dryas event and deep-ocean circulation. *Nature* 342:637-642.
 1004
- 1005 Fallu, M.A., N. Allaire, R. Pienitz
 1006 2000 *Fresh Water Diatoms from Northern Quebec and Labrador (Canada)*. Bibliotheca
 1007 Diatomologica No. 45. J. Cramer, Berlin.
 1008
- 1009 Fedje, D.W., and T. Christensen
 1010 1999 Modeling Paleoshorelines and Locating Early Holocene Coastal Sites in Haida Gwaii.
 1011 *American Antiquity* 64(4):635-652.
 1012
- 1013 Fedje, D.W., T. Christensen, H. Josenhans, J.B. McSporran, J. Strang
 1014 2005a Millennial Tides and Shifting Shores: Archaeology on a Dynamic Landscape. In *Haida*
 1015 *Gwaii: Human History and Environment from the Time of Loon to the Time of the Iron*
 1016 *People*, edited by D.W. Fedje and R.W. Mathewes, pp. 163-186. UBC Press, Vancouver.
 1017
- 1018 Fedje, D.W., H. Josenhans, J.J. Clague, J.V. Barrie, D.J. Archer, J.R. Southon
 1019 2005b Hecate Strait Paleoshorelines. In *Haida Gwaii: Human History and Environment from*
 1020 *the Time of Loon to the Time of the Iron People*, edited by D.W. Fedje and R.W.
 1021 Mathewes, pp. 21-37. UBC Press, Vancouver.
 1022
- 1023 Fedje, D.W., Q. Mackie, T. Lacourse, D. McLaren
 1024 2011 Younger Dryas Environments and Archaeology on the Northwest Coast of North
 1025 America. *Quaternary International* 242:452-462.
 1026
- 1027 Fedje, D.W., R.F. Mathewes (eds.)
 1028 2005 *Haida Gwaii: Human History and Environment from the Time of the Loon to the Time of*
 1029 *the Iron People*. University of British Columbia Press, Vancouver.
 1030
- 1031 Fedje, D.W., D. McLaren, R. Wigen
 1032 2004 *Preliminary Archaeological and Peleocological Investigations of Late Glacial to Early*
 1033 *Holocene Landscapes of Haida Gwaii, Hecate Strait and Environs*. BC Archaeology

- 1034 Branch Permit 2001-172, Haida Nation Permit 2002 (renewed 2003) for Haida Gwaii
1035 Karst Research.
1036
- 1037 Foged, N.
1038 1981 *Diatoms in Alaska*. Bibliotheca Phycologica No. 53. J. Cramer, Berlin.
1039
- 1040 Foster, N.R.
1041 1991 *Intertidal bivalves: a guide to the common marine bivalves of Alaska*. University of
1042 Alaska Press, Fairbanks.
1043
- 1044 Green, A.N., J.A.G. Cooper, L. Salzmänn
1045 2014 Geomorphic and stratigraphic signals of postglacial meltwater pulses on continental
1046 shelves. *Geology* 42(2):151-154.
1047
- 1048 Hafsten, U.
1049 1979 Late and post-Weichselian shore level changes in south Norway. In *The Quaternary*
1050 *History of the North Sea*, edited by Oele, E., R.T.E. Schüttenhelm, A.J. Wiggers, pp. 45-
1051 59. Acta Universitatis Upsala, Symposia Universitatis Upsaliensis Annum
1052 Quingentesimum Celebrantis 2, Uppsala.
1053
- 1054 1983a Biostratigraphical evidence for late Weichselian and Holocene sea-level changes in
1055 southern Norway. In *Shorelines and Isostasy*, edited by Smith, D.E., A.G. Dawson, pp.
1056 161-181. Institute of British Geographers, Special Publication 16, London.
1057
- 1058 1983b Shore-level changes in south Norway during the last 13,000 years, traced by
1059 biostratigraphical methods and radiometric datings. *Norsk Geografisk Tidsskrift* 37:63-
1060 79.
1061
- 1062 Hafsten, U., P.A. Tallantire
1063 1978 Palaeoecology and post-Weichselian shore-level changes on the coast of Møre, western
1064 Norway. *Boreas* 7:109-122.
1065
- 1066 Hein, M.F.
1067 1990 *Flora of Adak Island, Alaska: Bacillariophyceae (Diatoms)*. Bibliotheca
1068 Diatomologica No. 21. J. Cramer, Berlin.
1069
- 1070 Hetherington, R., J.V. Barrie
1071 2004 Interaction between local tectonics and glacial unloading on the Pacific margin of
1072 Canada. *Quaternary International* 120: 65-77.
1073
- 1074 Hetherington, R., J.V. Barrie, R.G.B. Reid, R. MacLeod, D.J. Smith
1075 2004 Paleogeography, glacially induced crustal displacement, and Late Quaternary coastlines
1076 on the continental shelf of British Columbia, Canada. *Quaternary Science Reviews*
1077 23:295-318.
1078
- 1079 Hetherington, R., J.V. Barrie, R.G.B. Reid, R. MacLeod, D.J. Smith, T.S. James, R. Kung

- 1080 2003 Late Pleistocene coastal paleogeography of the Queen Charlotte Islands, British
 1081 Columbia, Canada, and its implications for terrestrial biogeography and early postglacial
 1082 human occupation. *Canadian Journal of Earth Science* 40:1755-1766.
 1083
- 1084 Hijma, M.P., S.E. Engelhart, T.E. Törnqvist, B.P. Horton, P. Hu, D.F. Hill
 1085 2015 A protocol for a geological sea-level database. In *Handbook of Sea-Level Research*,
 1086 edited by Shennan, I., A.J. Long, B.P. Horton, pp. 536-553. John Wiley and Sons, West
 1087 Sussex, UK.
 1088
- 1089 Hustedt, F.
 1090 1953 Die Systematik der Diatomeen in ihren Beziehungen zur Geologie und Ökologie nebst
 1091 einer Revision des Halobien-Systems. *Svensk Botanisk Tidskrift* 47:509-519.
 1092
- 1093 Hutchinson, I., T.S. James, J.J. Clague, J.V. Barrie, K.W. Conway
 1094 2004a Reconstruction of Late Quaternary Sea-level Change in Southwestern British Columbia
 1095 from Sediments in Isolation Basins. *Boreas* 33:183-194.
 1096
- 1097 Hutchinson, I., T.S. James, P.J. Reimer, B.D. Bornhold, J.J. Clague
 1098 2004b Marine and limnic radiocarbon reservoir corrections for studies of late- and postglacial
 1099 environments in Georgia Basin and Puget Lowland, British Columbia, Canada and
 1100 Washington, USA. *Quaternary Research* 61:193-203.
 1101
- 1102 James, T.S., J.J. Clague, K. Wang, I. Hutchinson
 1103 2000 Postglacial rebound at the northern Cascadia subduction zone. *Quaternary Science*
 1104 *Reviews* 19:1527-1541.
 1105
- 1106 James, T.S., E.J. Gowan, I. Hutchinson, J.J. Clague, J.V. Barrie, K.W. Conway
 1107 2009a Sea-level Change and Paleogeographic Reconstructions, Southern Vancouver Island,
 1108 British Columbia, Canada. *Quaternary Science Reviews* 28:1200-1216.
 1109
- 1110 James, T.S., E.J. Gowan, I. Wada, K. Wang
 1111 2009b Viscosity of the asthenosphere from glacial isostatic adjustment and subduction dynamics
 1112 at the northern Cascadia subduction zone, British Columbia, Canada. *Journal of*
 1113 *Geophysical Research* 114:B04405, doi:10.1029/2008JB006077.
 1114
- 1115 James, T.S., J.A. Henton, L.J. Leonard, A. Darlington, D.L. Forbes, M. Craymer
 1116 2014 *Relative Sea-level Projections in Canada and the Adjacent Mainland United States*.
 1117 Geological Survey of Canada, Open File 7737, doi:10.4095/295574.
 1118
- 1119 James, T.S., I. Hutchinson, J.V. Barrie, K.W. Conway, D. Mathews
 1120 2005 Relative Sea-Level Change in the Northern Strait of Georgia, British Columbia.
 1121 *Géographie physique et Quaternaire* 59:113-127.
 1122
- 1123 Josenhans, H., D.W. Fedge, R. Pienitz, J. Southon
 1124 1997 Early Humans and Rapidly Changing Holocene Sea Levels in the Queen Charlotte
 1125 Islands-Hecate Strait, British Columbia, Canada. *Science* 277:71-74.

- 1126
 1127 Khan, N.S., C.H. Vane, B.P. Horton
 1128 2015 Stable Carbon Isotope and C/N Geochemistry of Coastal Wetland Sediments as a Sea-
 1129 Level Indicator. In *Handbook of Sea-Level Research*, edited by Shennan, I., A.J. Long,
 1130 B.P. Horton, pp. 295-311. John Wiley and Sons, West Sussex, UK.
 1131
 1132 Kjemperud, A.
 1133 1981 Diatom changes in sediments of basins possessing marine/lacustrine transitions in Frosta,
 1134 Nord-Troendelag, Norway. *Boreas* 10:27-38.
 1135
 1136 Kolbe, R.W.
 1137 1927 Zur Ökologie, Morphologie und Systematik der Brackwasser-Diatomeen.
 1138 *Pflanzenforschung* 7:1-146.
 1139
 1140 1932 Grundlinien einer allgemeinen Ökologie der Diatomeen. *Ergebnisse der Biologie* 8:221-
 1141 348.
 1142
 1143 Krammer, K., H. Lange-Bertalot
 1144 1986a Bacillariophyceae 1. Teil: Naviculaceae. In *Süsswasser flora von Mitteleuropa*, edited by
 1145 Ettl, H., Gerloff, J., Heynig, H. and Mollenhauer, D., Band 2/1, 876 pp.. Gustav Fischer
 1146 Verlag, Stuttgart, Germany.
 1147
 1148 1986b Bacillariophyceae 2. Teil: Bacillariaceae, Epithemiaceae, Surirellaceae. In *Süsswasser*
 1149 *flora von Mitteleuropa*, edited by Ettl, H., Gerloff, J., Heynig, H. and Mollenhauer, D.,
 1150 Band 2/2, 596 pp.. Gustav Fischer Verlag, Stuttgart, Germany.
 1151
 1152 1986c Bacillariophyceae 3. Teil: Centrales, Fragilariaceae, Eunotiaceae. . In *Süsswasser flora*
 1153 *von Mitteleuropa*, edited by Ettl, H., Gerloff, J., Heynig, H. and Mollenhauer, D., Band
 1154 2/3, 598 pp.. Gustav Fischer Verlag, Stuttgart, Germany.
 1155
 1156 1986d Bacillariophyceae 4. Teil: Achnanthaceae, Kritische Ergänzungen zu Achnanthes s.l.,
 1157 Navicula s. str., Gomphonema. In *Süsswasserflora von Mitteleuropa*, edited by Ettl, H.,
 1158 Gärtner, G., Gerloff, J., Heynig, H. and Mollenhauer, D., Band 2/4, 468 pp.. Gustav
 1159 Fischer Verlag, Stuttgart, Germany.
 1160
 1161 Lamb, A.L., G.P. Wilson, M.J. Leng
 1162 2006 A Review of Coastal Palaeoclimate and Relative Sea-Level Reconstructions using $\delta^{13}\text{C}$
 1163 and C/N Ratios in Organic Material. *Earth Science Reviews* 75:29-57.
 1164
 1165 Lamoureux, S.F., J.M.H. Cockburn
 1166 2005 Timing and climatic controls over Neoglacial expansion in the northern Coast Mountains,
 1167 British Columbia, Canada. *The Holocene* 15(4):619-624.
 1168
 1169 Larsen, C.F., K.A. Echelmeyer, J.T. Freymueller, R.J. Motyka

- 1170 2003 Tide gauge records of uplift along the northern Pacific-North American plate boundary,
 1171 1937 to 2001. *Journal of Geophysical Research* 108(B4), 2216,
 1172 doi:10.1029/2001JB001685.
 1173
- 1174 Laws, R.A.
 1175 1988 Diatoms (Bacillariophyceae) from surface sediments in the San Francisco Bay Estuary.
 1176 *Proceedings of the California Academy of Sciences* 45:133-254.
 1177
- 1178 Letham, B., A. Martindale, D. McLaren, T. Brown, K.M. Ames, D.J.W. Archer, S. Marsden
 1179 2015 Holocene Settlement History of the Dundas Islands Archipelago, Northern British
 1180 Columbia. *BC Studies* 187:51-84.
 1181
- 1182 Liu, P.J., J.D. Milliman
 1183 2004 Reconsidering melt-water pulses 1A and 1B: global impacts of rapid sea-level rise.
 1184 *Journal of Ocean University of China* 3(2):183-190.
 1185
- 1186 Lowdon, J.A., W. Blake Jr.
 1187 1979 *Geological Survey of Canada Radiocarbon Dates XIX*. Geological Survey of Canada
 1188 Paper 79-7, Ottawa, Canada.
 1189
- 1190 MacDonald, G.F.
 1191 1969 Preliminary Culture Sequence from the Coast Tsimshian Area, British Columbia.
 1192 *Northwest Anthropological Research Notes* 3:240-254.
 1193
- 1194 MacDonald, G.F., J.S. Cybulski
 1195 2001 Introduction: the Prince Rupert Harbour Project. In *Perspectives on Northern Northwest*
 1196 *Coast Prehistory*, edited by J.S. Cybulski, pp. 1-23. Mercury Series Archaeology Paper
 1197 160. Canadian Museum of Civilization, Gatineau, Quebec.
 1198
- 1199 MacDonald, G.F., R.I. Inglis
 1200 1981 An Overview of the North Coast Prehistory Project (1966-1980). *BC Studies* 48:37-63.
 1201
- 1202 Mackie, E.A.V., M.J. Leng, J.M. Lloyd, C. Arrowsmith
 1203 2005 Bulk organic $\delta^{13}\text{C}$ and C/N ratios as palaeosalinity indicators within a Scottish isolation
 1204 basin. *Journal of Quaternary Science* 20(4):303-312.
 1205
- 1206 Mackie, Q., D.W. Fedje, D. McLaren, N. Smith, I. McKechnie
 1207 2011 Early Environments and Archaeology of Coastal British Columbia. In *Trekking the*
 1208 *Shore: Changing Coastlines and the Antiquity of Coastal Settlement*, edited by N.F.
 1209 Bicho, J.A. Haws, L.G. Davis, pp. 51-103. Interdisciplinary Contributions to
 1210 Archaeology, Springer, New York.
 1211
- 1212 Mandryk, C.A.S., H. Josenhans, D.W. Fedje, R.W. Mathewes
 1213 2001 Late Quaternary Paleoenvironments of Northwestern North America: Implications for
 1214 Inland versus Coastal Migration Routes. *Quaternary Science Reviews* 20:301-314.
 1215

- 1216 Mann, D.H., G.P. Streveler
 1217 2008 Post-glacial Relative Sea Level, Isostasy, and Glacial History in Icy Strait, Southeast
 1218 Alaska, USA. *Quaternary Research* 69:201-216.
 1219
- 1220 Massey, N.W.D., D.G. MacIntyre, J.W. Haggart, P.J. Desjardins, C.L. Wagner, R.T. Cooney
 1221 2005 Digital Map of British Columbia: Tile NN8-9 North Coast and Queen Charlotte
 1222 Islands/Haida Gwaii, B.C. Ministry of Energy and Mines, GeoFile 2005-5.
 1223
- 1224 Mathews, R.K., Fyles J.G., Nasmith H.W.
 1225 1970 Postglacial crustal movements in southwestern British Columbia and adjacent
 1226 Washington state. *Canadian Journal of Earth Sciences* 7:690-702.
 1227
- 1228 McCuaig, S.J.
 1229 2000 *Glacial History of the Nass River Region*. Unpublished PhD Dissertation, Department of
 1230 Geography, Simon Fraser University.
 1231
- 1232 McCuaig, S.J., M.C. Roberts
 1233 2006 Nass River on the move: radar facies analysis of glaciofluvial sedimentation and its
 1234 response to sea-level change in northwestern British Columbia. *Canadian Journal of*
 1235 *Earth Science* 43:1733-1746.
 1236
- 1237 McLaren, D.
 1238 2008 *Sea Level Change and Archaeological Site Locations on the Dundas Island Archipelago*
 1239 *of North Coastal British Columbia*. Unpublished PhD Dissertation, Department of
 1240 Anthropology, University of Victoria.
 1241
- 1242 McLaren, D., D.W. Fedje, M.B. Hay, Q. Mackie, I.J. Walker, D.H. Shugar, J.B.R. Eamer, O.B.
 1243 Lian, C. Neudorf
 1244 2014 A post-glacial sea level hinge on the central Pacific Coast of Canada. *Quaternary Science*
 1245 *Reviews* 97(1):148-169.
 1246
- 1247 McLaren, D., A. Martindale, D.W. Fedje, Q. Mackie
 1248 2011 Relict Shorelines and Shell Middens of the Dundas Island Archipelago. *Canadian*
 1249 *Journal of Archaeology* 35: 86-116.
 1250
- 1251 McLaren, D., F. Rahemtulla, Gitla (E. White), D.W. Fedje
 1252 2015 Prerogatives, Sea Level, and the Strength of Persistent Places: Archaeological Evidence
 1253 for Long-Term Occupation of the Central Coast of British Columbia. *BC Studies* 187:
 1254 155-191.
 1255
- 1256 Pienitz, R, D.W. Fedje, M. Poulin
 1257 2003 *Marine and Non-Marine Diatoms from the Haida Gwaii Archipelago and Surrounding*
 1258 *Coasts, Northeastern Pacific, Canada*. Bibliotheca Diatomologica 48. J. Cramer Inc.,
 1259 Berlin.
 1260
- 1261 Pirazzoli, P.A.

- 1262 1996 *Sea-level changes: the last 20 000 years*. Wiley, Chichester, England.
- 1263
- 1264 Rao, V.N.R., J. Lewin
- 1265 1976 Benthic marine diatom flora of False Bay, San Juan Island, Washington. *Syesis* 9:173-
- 1266 213.
- 1267
- 1268 Reimer, P.J., E. Bard, A. Bayliss, J.W. Beck, P.G. Blackwell, C. Bronk Ramsey, C.E. Buck, H.
- 1269 Cheng, R.L. Edwards, M. Friedrich, P.M. Grootes, T.P. Guilderson, H. Haflidason, I. Hajdas, C.
- 1270 Hatté, T.J. Heaton, D.L. Hoffmann, A.G. Hogg, K.A. Hughen, K.F. Kaiser, B. Kromer, S.W.
- 1271 Manning, M. Niu, R.W. Reimer, D.A. Richards, E.M. Scott, J.R. Southon, R.A. Staff, C.S.M.
- 1272 Turney, J. van der Plicht
- 1273 2013 IntCal 13 and Marine 13 Radiocarbon Age Calibration Curves 0-50,000 Years Cal BP.
- 1274 *Radiocarbon* 55:1869-1887.
- 1275
- 1276 Romundset, A., Ø.S. Lohne, J. Mangerud, J.I. Svendsen
- 1277 2009 The First Holocene Relative Sea-Level Curve from the Middle Part of Hardangerfjorden,
- 1278 Western Norway. *Boreas* 39:87-104.
- 1279
- 1280 Rundgren, M., Ó. Ingólfsson, S. Björk, H. Haflidason
- 1281 1997 Dynamic sea-level change during the last deglaciation in northern Iceland. *Boreas*
- 1282 26:201-215.
- 1283
- 1284 Schnurrenberger, D., J. Russell, K. Kelts
- 1285 2003 Classification of lacustrine sediments based on sedimentary components. *Journal of*
- 1286 *Paleolimnology* 29:141-154.
- 1287
- 1288 Shennan, I.
- 1289 2015 Handbook of sea-level research: framing research questions. In *Handbook of Sea-Level*
- 1290 *Research*, edited by Shennan, I., A.J. Long, B.P. Horton, pp. 3-25. John Wiley and Sons,
- 1291 West Sussex, UK.
- 1292
- 1293 Shugar, D.H., I.J. Walker, O.B. Lian, J.B.R. Eamer, C. Neudorf, D. McLaren, D.W. Fedje
- 1294 2014 Post-glacial sea-level change along the Pacific coast of North America. *Quaternary*
- 1295 *Science Reviews* 97(1):170-192.
- 1296
- 1297 Smith, D.E., S. Harrison, C.R. Firth, J.T. Jordan
- 1298 2011 The early Holocene sea level rise. *Quaternary Science Reviews* 30:1846-1860.
- 1299
- 1300 Smith, H.I.
- 1301 1909 Archaeological Remains on the Coast of Northern British Columbia and Southern
- 1302 Alaska. *American Anthropologist* 11:595-600.
- 1303
- 1304 Taylor, B.W., M.L. Bothwell
- 1305 2014 The origin of invasive microorganisms matters for science, policy, and management: the
- 1306 case of *Didymosphenia geminata*. *Bioscience*, 64(6):531-538.
- 1307

- 1308 Törnqvist, T.E., B.E. Rosenheim, P. Hu, A.B. Fernandez
1309 2015 Radiocarbon dating and calibration. In *Handbook of Sea-Level Research*, edited by
1310 Shennan, I., A.J. Long, B.P. Horton, pp. 349-360. John Wiley and Sons, West Sussex,
1311 UK.
1312
1313 Tynni, R.
1314 1986 *Observations of Diatoms on the Coast of the State of Washington*. Geological Survey of
1315 Finland Report of Investigations 75. Espoo, Finland.
1316
1317 Wright Jr., H.E.,
1318 1967 A square-rod piston sampler for lake sediments. *Journal of Sedimentary Petrology*,
1319 37(3): 975-976.
1320
1321 Zong, Y., Y. Sawai
1322 2015 Diatoms. In *Handbook of Sea-Level Research*, edited by Shennan, I., A.J. Long, B.P.
1323 Horton, pp. 233-248. John Wiley and Sons, West Sussex, UK.

Table 1 - Data Point Types

Indicator Sample Type	Indicative Meaning	Indicative Range for Database	Reference Water Level for Database	Explanation
Index Points				
Transitional (mixed fresh and brackish/marine) diatom assemblage in isolation basin sediments	Basin sill is either nearly below high tide influence (dropping RSL) or just being inundated by high tides (rising RSL)	HAT to MTL	$(\text{HAT} + \text{MTL})/2$	Conservatively assumes that the dated sample represents the time at which the sill of the basin was between mean tide level and the highest astronomical tide level and was on the verge of being isolated/inundated.
Growth position butter clam (<i>Saxidomus gigantea</i>) shells	Sediment from which the specimen was taken was within the habitat elevation range of <i>S. gigantea</i> when the specimen was alive	LLWMT +46 cm to LLWMT -91 cm	$((\text{LLWMT} + 46 \text{ cm}) + (\text{LLWMT} - 91 \text{ cm}))/2$	Modification of a method used by Carlson and Baichtal (2015) for estimating RSL based on the known growth range of <i>S. gigantea</i> (Foster 1991). Calculates the elevation range relative to tidal position within which the specimen could have lived.
Limiting Points	Indicative Meaning			
Marine shells in sediment, not in growth position	Sediment with shell is from within or below the tidal range.			
Only brackish/marine diatoms in sediments	Sediment was deposited in coastal/marine setting, or, in the case of isolation basin sediments, when the sill was below lowest tide level.			
Only freshwater diatoms in sediments	Sediment was deposited in fully freshwater setting, or, in the case of isolation basin sediments, when the sill was above highest tide level.			
Terrestrial peat/paleosol	Sediment was formed/deposited above high tide.			
Archaeological site with remains of habitation (shell midden, charcoal concentrations, architectural features)	Lowest instance of archaeological material was deposited above high tide.			

Table 1. RSL data point types used in the present study and descriptions of indicative meanings.

Table 2 - Tidal Parameters

Tidal Parameter	Abbreviation	Definition	Measurement above Chart Datum (m CD)	Equivalent elevation relative to geodetic mean sea level (m asl; used in this study)
Highest Astronomical Tide	HAT	Highest tide on an 18.6 year cycle.	7.514	3.664
Higher High Water Large Tide	HHWLT	The average of the highest high waters, one from each of 19 years of predictions.	7.407	3.557
Higher High Water Mean Tide	HHWMT	The average from all the higher high waters from 19 years of predictions.	6.17	2.32
High Water Mean Tide	HWMT	The average of the high water levels.	5.897	2.047
Mean Water Level	MWL	The average of all hourly water levels over the available period of record.	3.849	0
Mean Tide Level	MTL	The average of HWMT and LWMT.	3.8485	0
Low Water Mean Tide	LWMT	The average of the low water levels.	1.8	-2.05
Lower Low Water Mean Tide	LLWMT	The average of all the lower low waters from 19 years of predictions.	1.322	-2.528
Lower Low Water Large Tide	LLWLT	The average of the lowest low waters, one from each of 19 years of predictions.	0.006	-3.844
Lowest Astronomical Tide	LAT	Lowest tide on an 18.6 year cycle.	-0.125	-3.975

Table 2. Tidal Parameters and their definitions for Canadian Hydrographic Survey Benchmark Station 9354, predicted over 19 years, start year 2010 (Canadian Hydrographic Survey, personal communication, September 28, 2015). Note that MWL and MTL are essentially the same and are equal to 0 m asl. Note that in Canada, tidal parameters are calculated based on predicted tides, whereas in the USA tidal parameters are calculated based on observed data.

Table 3 - Stable Isotope Results

	$\delta^{13}\text{C}$ Average	$\delta^{13}\text{C}$ Range	$\delta^{15}\text{N}$ Average	$\delta^{15}\text{N}$ Range	$\text{C}_{\text{ORG}}/\text{N}_{\text{TOTAL}}$ Average	$\text{C}_{\text{ORG}}/\text{N}_{\text{TOTAL}}$ Range
Known Marine Samples (n=12)	-23.60±2.38‰	-26.51‰ to -19.90‰	+5.3±0.9‰	+4.0‰ to +6.5‰	17.0±4.8	10.1 to 24.9
Known Freshwater Samples (n=8)	-28.78±1.32‰	-31.18‰ to -27.23‰	+0.4±1.1‰	-1.5‰ to +2.0‰	26.8±16.1	13.3 to 54.4
Bencke Lagoon Sample (n=1)	-26.61‰	n/a	+2.2‰	n/a	15.3	n/a
Optimism Bay Samples (n=6)	-28.08±0.76‰	-28.76‰ to -26.86‰	+1.7±0.52‰	+1.1‰ to +2.5‰	19.15±2.1	17.5 to 23.0

Table 3. Stable carbon ($\delta^{13}\text{C}$) and nitrogen ($\delta^{15}\text{N}$) isotope compositions and elemental carbon-to-nitrogen (C/N) ratios of known marine sediments and known freshwater sediments from the study area. Bencke Lagoon sample and Optimism Bay samples were of unknown environmental salinity origin and tested against the knowns. Bencke Lagoon is intermediate between fresh and marine values (though closer to freshwater) and suggests a mixture of inputs. Optimism Bay samples fall within the range of known freshwater samples.

Table 4 - Data Points

Map ID (see Figure 2)	Lab # ¹	Site	Method and Test	14C Age BP	+/-	Calendar Range (older, 2 sigma) ²	Calendar Range (recent, 2 sigma) ²	Calibrated Median	Easting	Northing	Material	Proxy Indicator	Elevation/(Index Point Paleo RSL Elevation), m asl	Source
Index Points														
TL	D-AMS 009955	Tsook Lake	Livingstone Core TL#1	12167	47	14782 ⁺	13714 ⁺	14087 ⁺	406914	6023855	Seeds	Lake core sediments - mixed diatom assemblage (fresh and brackish)	49.7/(47.87)	This study
DL	D-AMS 008745	Digby Island Lake 1	Livingstone Core DL1#1	12312	41	15013 ⁺	13859 ⁺	14380 ⁺	406751	6017482	Twigs - charred	Lake core sediment: freshwater diatom assemblage with slight mixing of brackish/marine diatoms	15.2/(13.37)	This study
BL	D-AMS 009951	Bencke Lagoon	Livingstone Core BL#1	11292	46	13255	13065	13142	408247	6021605	Twig	Lagoon core sediment: mixed diatom assemblage (fresh and brackish/marine diatoms)	2.4/(0.57)	This study
B	D-AMS 004468	Tea Bay Creek	Bulk sample from exposure	9526	34	10196	9901	10073	405524	6022967	Butter/horse clam shell	Marine mollusc shells in gray silty sand and clay	2.4/(5.15)	This study
C	D-AMS 007880	Estuary north of Optimism Bay	Bulk sample from exposure	9589	32	10250	9952	10159	407411	6022741	<i>Tresus capax</i> shell	Marine molluscs in growth position	0.058/(2.81)	This study
Lower Limiting Points, intertidal														
4	OS-101336	Biogenic shell deposit beneath GcTo-52	CT 2012-515	3010	30	2645	2327	2454	404301	6024878	<i>Saxidomus gigantea</i> or <i>Tresus</i> spp. shell	ESP core test: marine mollusc shells in sand below archaeological site	5.02	This study
6	OS-119876	Biogenic shell deposit beneath T623-1	CT 2013-035	2800	25	2315	2071	2201	404990	6022028	Clam shell	ESP core test: marine mollusc shells in sand below archaeological site	2.92	This study
6	OS-119874	Biogenic shell deposit beneath T623-1	CT 2013-035	3170	30	2762	2495	2676	404990	6022028	Clam shell	ESP core test: marine mollusc shells in sand below archaeological site	2.38	This study
13	D-AMS	Biogenic	CT 2014-	3426	91	3201	2736	2952	408012	6012786	<i>Saxidomus</i>	ESP core test:	5.36	This

	007890	shell deposit beneath T722-1	526															marine mollusc shells in sand below archaeological site		study
OB	D-AMS 008753	Optimism Bay	OB#1	10350	47	11214	10880	11079	407593	6022454	Shell, unknown marine snail	Bay core sediment: brackish and marine diatom assemblage, marine mollusc shells	-4.76	This study						
OB	D-AMS 008747	Optimism Bay	OB#1	9586	37	11123	10751	10932	407593	6022454	Wood (bark)	Bay core sediment: brackish and marine diatom assemblage, marine mollusc shells	-4.76	This study						
OB	D-AMS 008748	Optimism Bay	OB#1	9866	46	11391	11201	11262	407593	6022454	Plant fibre	Bay core sediment: interface between intertidal sediments and peat/gyttja, reedy plant macrofossil with brackish/marine plant $\delta^{13}C$ ratio (-19.4)	-4.86	This study						
OB	D-AMS 008754	Optimism Bay	OB#2	10365	38	11219	10923	11098	407593	6022454	<i>Mytilus</i> sp. shell	Bay core sediment: brackish and marine diatom assemblage, marine mollusc shells	-5.26	This study						
OB	D-AMS 008749	Optimism Bay	OB#2	9568	40	11100	10735	10932	407593	6022454	Wood (charcoal?)	Bay core sediment: brackish and marine diatom assemblage, marine mollusc shells	-5.26	This study						
SL	D-AMS 005838	Salt Lake	SL#1	2080	30	2140	1952	2050	411213	6021611	Wood/Charcoal (twig)	Lake core sediment: brackish diatom assemblage	2.2	This study						
E	D-AMS 007877	Shell exposure in creek north of Bencke Lagoon #1	Bulk sample	9908	33	10666	10371	10523	408272	6022534	<i>Mytilus</i> sp. shell	Marine molluscs in gravelly sand	1.58	This study						
E	D-AMS 007893	Shell exposure in creek north of Bencke Lagoon #1	Bulk sample	8962	32	10224	9928	10161	408272	6022534	Green wood, twig	Marine molluscs in gravelly sand	1.58	This study						
D	D-AMS	Shell	Bulk	10154	34	11023	10669	10830	408314	6022730	<i>Clinocardium</i>	Marine molluscs in	1.8	This						

Off map (see Fig. 1)	Beta-14464	Port Simpson					50	12970			14649	14019	14240		407339 (approximate)	6045499 (approximate)	Marine Mollusc Shell	Marine mollusc shell in gray clay	53.55	2004:51
Off map	CAMS-3390	Ridley Island					70	9480			10198	9731	9998		415331 (approximate)	6008382 (approximate)	Marine Mollusc Shell	Marine mollusc shell in gray clay exposed in a road cut	7.05	Fedje et al. 2005; Fedje et al. 2004:46-47
RR	D-AMS 008741	Rifle Range Lake 1	RR1#2				42	11908			14090*	13458*	13749*		417608	6015559	Mixed plant matter, appears charred and/or decomposing	Lake core sediments - brackish and marine diatoms	35	This study
RA	D-AMS 005842	Russell Arm	RA#2				26	3158			3448	3343	3385		411094	6021336	Green wood, twig	Lagoon core sediment: marine mollusc shells	0	This study
RA	D-AMS 005843	Russell Arm	RA#2				29	3681			3394	3143	3276		411094	6021336	Clam shell	Lagoon core sediment: marine mollusc shells	0	This study
RA	D-AMS 005841	Russell Arm	RA#2				29	2105			2148	1998	2077		411094	6021336	Tree cone (charred?)	Lagoon core sediment: marine diatoms and marine $\delta^{13}C$ and $\delta^{15}N$ values	0	This study
RA	D-AMS 005840	Russell Arm	RA#2				26	1751			1147	924	1026		411094	6021336	Clam shell	Lagoon core sediment: marine mollusc shells	0	This study
F	D-AMS 005852	Russell Arm/Philip's Lagoon Isthmus	CT 2013-503				43	13263			15187	14574	14929		410980	6021304	Marine mollusc shell	ESP core test: marine mollusc shells	15.9	This study
F	D-AMS 004470	Russell Arm/Philip's Lagoon Isthmus	CT 2013-503				45	13141			15011	14241	14620		410980	6021304	<i>Balanus</i> sp. Shell	ESP core test: marine mollusc shells	15.78	This study
SL	D-AMS 005839	Salt Lake	SL#1				28	3034			2660	2345	2491		411213	6021611	Clam shell	Lake core sediment: marine mollusc shells	2.2	This study
A	D-AMS 007879	Swamp Creek	Bulk sample				33	12954			14510	14000	14194		404395	6026537	Marine Mollusc Shell	Marine mollusc shell in gray silty clay	3.83	This study
B	D-AMS 004469	Tea Bay Creek	Bulk sample				35	8472			9533	9447	9495		405524	6022967	Small green wood cone	Marine mollusc shells in gray silty	2.4	This study

B	D-AMS 005846	Tea Bay Creek	CT 2013- 513	9559	39	11090	10730	10932	405507	6022978	Green wood	sand and clay ESP core test: marine mollusc shells	1.5	This study
B	D-AMS 005845	Tea Bay Creek	CT 2013- 513	9508	43	10197	9862	10045	405507	6022978	Clam Shell	ESP core test: marine mollusc shells	1.5	This study
B	D-AMS 005847	Tea Bay Creek	CT 2013- 513	9665	37	10386	10133	10229	405507	6022978	<i>Mytilus</i> sp. shell	ESP core test: marine mollusc shells	1.2	This study
B	D-AMS 005849	Tea Bay Creek	CT 2013- 513	9748	38	10480	10201	10323	405507	6022978	Barnacle shell	ESP core test: marine mollusc shells	0.3	This study
B	D-AMS 005850	Tea Bay Creek	CT 2013- 513	9989	41	11695	11268	11451	405507	6022978	Green wood	ESP core test: marine mollusc shells	-0.6	This study
B	D-AMS 005851	Tea Bay Creek	CT 2013- 513	10256	43	11133	10762	10966	405507	6022978	Barnacle shell	ESP core test: marine mollusc shells	-0.6	This study
TL	D-AMS 009956	Tsook Lake	TL#1	12514	50	15090	14365	14778	406914	6023855	<i>Arctostaphylos</i> sp. seed	Lake core sediments - brackish and marine diatoms	49.7	This study
Upper Limiting Points, non-archaeological														
BL	UBA- 29065	Bencke Lagoon	BL#1	12199	49	14833	13738	14148	408247	6021605	Organic-rich sediment	Lagoon core sediment: freshwater diatom assemblage	2.4	This study
BL	D-AMS 009952	Bencke Lagoon	BL#1	11589	37	13722	13160	13420	408247	6021605	Seeds	Lagoon core sediment: freshwater diatom assemblage	2.4	This study
DIB	D-AMS 005844	Digby Island Bog 1	DIB#1	7345	35	8295	8028	8147	409292	6017796	Green wood	Bog core sediment: Terrestrial plant macrofossils	17.2	This study
H	D-AMS 007892	McNichol Creek	Bulk sample	8149	29	9241	9009	9075	413052	6022825	Green wood, stick	Terrestrial plant macrofossils and freshwater diatom assemblage	18.5	This study
NDB	D-AMS 009948	North Digby Bog	NDB#1	8718	33	10171	9521	9771	405388	6018934	Multiple chunks of wood	Bog core sediment - peat/gyttja	17	This study
NDB	D-AMS 009950	North Digby Bog	NDB#1	7055	41	8169	7624	7879	405388	6018934	Twigs and mixed plant matter	Bog core sediment - peat/gyttja	17	This study
OB	UBA- 29067	Optimism Bay	OB#2	11922	60	14163	13436	13773	407593	6022454	Organic-rich sediment	Bay core sediment: peat/gyttja with terrestrial plant	-6.31	This study

OB	D-AMS 008750	Optimism Bay	OB#2	11876	42	13772	13572	13677	407593	6022454	Wood	macrofossils Bay core sediment: peat/gyttja with terrestrial plant macrofossils	-6.31	This study
OB	UBA- 29066	Optimism Bay	OB#2	10450	56	12700	11823	12307	407593	6022454	Organic-rich sediment	Bay core sediment: peat/gyttja with terrestrial plant macrofossils	-6.31	This study
18	D-AMS 011947	Paleosol beneath P009-1	ST 2015- 030	6175	35	7170	6960	7077	407969	6022226	Charcoal	Shovel test: terrestrial paleosol beneath shell midden	7.95	This study
RR	D-AMS 008740	Rifle Range Lake 1	RR1#2	11826	59	14055	13345	13666	417608	6015559	Twig fragments, potentially charred	Lake core sediments - freshwater diatom assemblage	35	This study
TL	D-AMS 009954	Tsook Lake	TL#1	11785	42	13971	13330	13623	406914	6023855	Twigs and a cone	Lake core sediments - freshwater diatom assemblage	49.7	This study
Upper Limiting Points, archaeological														
5	D-AMS 009643	GbTo-24	CT 2014- 525	3518	27	3204	2919	3063	402621 .3	6021540	Clam shell	ESP core test: lower boundary of archaeological shell midden	5.26	This study
5	D-AMS 009641	GbTo-24	CT 2014- 522	3585	29	3312	3007	3155	402628 .7	6021537	Clam shell	ESP core test: lower boundary of archaeological shell midden	3.8	This study
20	OS- 108969	GbTo-34	CT 2012- 030	2350	25	1780	1535	1650	407855 .8	6021318	Clam Shell	ESP core test: lower boundary of archaeological shell midden	9.53	This study
20	OS- 108967	GbTo-34	CT 2012- 017	3460	25	3132	2851	2984	407849 .1	6021321	<i>Mytilus</i> sp. shell	ESP core test: lower boundary of archaeological shell midden	9.06	This study
20	OS- 108970	GbTo-34	CT 2012- 019	2910	25	2459	2172	2324	407862 .3	6021358	Clam Shell	ESP core test: lower boundary of archaeological shell midden	8.86	This study
20	OS- 108964	GbTo-34	CT 2012- 024	3620	25	3335	3065	3204	407847 .9	6021278	<i>Mytilus</i> sp. shell	ESP core test: lower boundary of archaeological shell midden	7.57	This study
20	OS- 108968	GbTo-34	CT 2012- 031	4570	25	4552	4274	4421	407839 .4	6021327	<i>Mytilus</i> sp. shell	ESP core test: lower boundary of	7.36	This study

20	SUERC Average	GbTo-34	CT 2012-005	n/a	n/a				4696.5	407830.6	6021331	Mytilus sp. shell and charcoal	ESP core test: lower boundary of archaeological shell midden	6.04	This study; Edinborough et al. 2016
20	OS-108926	GbTo-34	CT 2012-009	4600	30				4459	407844.9	6021367	Mytilus sp. shell	ESP core test: lower boundary of archaeological shell midden	5.6	This study
20	OS-109689	GbTo-34	CT 2012-002	4300	20				4042	407812	6021293	Mytilus sp. shell	ESP core test: lower boundary of archaeological shell midden	5.12	This study
20	OS-109085	GbTo-34	CT 2012-037	1910	30				1200	407864.3	6021233	Mytilus sp. shell	ESP core test: lower boundary of archaeological shell midden	3.26	This study
21	D-AMS 009629	GbTo-4	CT 2012-535	3603	25				3180	408570	6020202	Clam shell	ESP core test: lower boundary of archaeological shell midden	5.4	This study
21	D-AMS 009635	GbTo-4	CT 2014-504	3549	26				3104	408706	6020197	Clam shell	ESP core test: lower boundary of archaeological shell midden	3.2	This study
24	OS-108830	GbTo-57	CT 2013-021	3210	25				2719	409965	6021274	Mytilus sp. shell	ESP core test: lower boundary of archaeological shell midden	10.01	This study
23	OS-108829	GbTo-59	CT 2013-014	4470	25				4288	409704	6021142	Mytilus sp. shell	ESP core test: lower boundary of archaeological shell midden	5.92	This study
22	OS-108828	GbTo-6	CT 2013-040	2710	25				2077	408172	6019197	Mytilus sp. shell	ESP core test: lower boundary of archaeological shell midden	4.8925	This study
7	D-AMS 011954	GbTo-63	AT 2015-049	3350	29				2845	403172	6020154	Protothaca staminea shell	Auger test: lower boundary of archaeological shell midden	9.98	This study
14	D-AMS 013864	GbTo-64	CT 2014-508	3590	24				3162	405966	6020930	Clam Shell	ESP core test: lower boundary of archaeological shell midden	3.34	This study

9	OS-101344	GbTo-66	CT 2012-556	4650	40	4766	4380	4525	405015.5	6020414	<i>Mytilus</i> sp. shell	ESP core test: lower boundary of archaeological shell midden	5.97	This study
9	OS-101352	GbTo-66	CT 2012-554	4780	25	4821	4562	4707	405001.6	6020395	<i>Saxidomus gigantea</i> or <i>Tresus</i> spp. shell	ESP core test: lower boundary of archaeological shell midden	5.84	This study
9	OS-101350	GbTo-66	CT 2012-555	4230	30	4095	3815	3950	405000.1	6020410	<i>Saxidomus gigantea</i> or <i>Tresus</i> spp. shell	ESP core test: lower boundary of archaeological shell midden	5.29	This study
12	OS-101572	GbTo-70	CT 2012-042	2900	25	2439	2158	2312	406785.9	6014176	<i>Saxidomus gigantea</i> or <i>Tresus</i> spp. shell	ESP core test: lower boundary of archaeological shell midden	6.8	This study
12	OS-101569	GbTo-70	CT 2012-053	3000	25	2640	2318	2437	406798.8	6014181	<i>Mytilus</i> sp. shell	ESP core test: lower boundary of archaeological shell midden	6.55	This study
12	OS-101567	GbTo-70	CT 2012-051	2910	30	2465	2165	2324	406792.2	6014200	Marine mollusc shell	ESP core test: lower boundary of archaeological shell midden	6.49	This study
12	OS-101656	GbTo-70	CT 2012-044	2590	25	2061	1814	1932	406793.4	6014158	<i>Mytilus</i> sp. shell	ESP core test: lower boundary of archaeological shell midden	6.49	This study
12	OS-101571	GbTo-70	CT 2012-047	3320	25	2930	2728	2814	406778.1	6014195	<i>Mytilus</i> sp. shell	ESP core test: lower boundary of archaeological shell midden	6.225	This study
26	D-AMS 009639	GbTo-76	CT 2013-003	2509	26	1955	1710	1839	412957	6021122	Clam shell	ESP core test: lower boundary of archaeological shell midden	7.49	This study
26	D-AMS 009637	GbTo-76	CT 2013-001	2479	24	1922	1686	1804	412948.7	6021073	<i>Mytilus</i> sp. shell	ESP core test: lower boundary of archaeological shell midden	3.13	This study
10	OS-101580	GbTo-78	CT 2012-062	2560	20	2021	1786	1898	404667.1	6018835	<i>Saxidomus gigantea</i> or <i>Tresus</i> spp. shell	ESP core test: lower boundary of archaeological shell midden	7.87	This study
10	OS-101578	GbTo-78	CT 2012-064	2250	25	1664	1404	1535	404619.3	6018856	<i>Mytilus</i> sp. shell	ESP core test: lower boundary of archaeological shell midden	5.28	This study

10	OS-101575	GbTo-78	CT 2012-065	3580	30	3308	2997	3147	404625.2	6018815	<i>Saxidomus gigantea</i> or <i>Tresus</i> spp. Shell	midden ESP core test: lower boundary of archaeological shell midden	5.03	This study
11	D-AMS 011956	GbTo-82	AT 2015-007	6436	34	6728	6463	6596	404466	6017411	<i>Balanus</i> sp. and other marine mollusc fragments	Auger test: lower boundary of archaeological shell midden	9.39	This study
8	OS-101346	GbTo-89	CT 2012-549	2440	25	1873	1624	1759	405102.4	6020577	<i>Mytilus</i> sp. shell	ESP core test: lower boundary of archaeological shell midden	9.2	This study
8	OS-101338	GbTo-89	CT 2012-551	3010	35	2650	2325	2456	405091	6020557	<i>Mytilus</i> sp. shell	ESP core test: lower boundary of archaeological shell midden	6.19	This study
8	OS-101340	GbTo-89	CT 2012-550	3470	25	3141	2860	2998	405100.2	6020618	<i>Mytilus</i> sp. shell	ESP core test: lower boundary of archaeological shell midden	5.44	This study
8	OS-101342	GbTo-89	CT 2012-547	3020	25	2650	2336	2467	405088.9	6020581	<i>Mytilus</i> sp. shell	ESP core test: lower boundary of archaeological shell midden	4.8	This study
19	OS-101330	GcTo-1	CT 2012-525	3160	25	2749	2494	2665	407641.4	6021772	<i>Mytilus</i> sp. shell	ESP core test: lower boundary of archaeological shell midden	8.81	This study
19	OS-101328	GcTo-1	CT 2012-522	3820	30	3562	3327	3436	407607.5	6021725	<i>Mytilus</i> sp. shell	ESP core test: lower boundary of archaeological shell midden	4.21	This study
27	OS-101356	GcTo-27	CT 2012-508	3540	35	3245	2931	3092	403664.6	6025041	<i>Saxidomus gigantea</i> or <i>Tresus</i> spp. shell	ESP core test: lower boundary of archaeological shell midden	9.12	This study
27	OS-101360	GcTo-27	CT 2012-506	4380	25	4314	3995	4160	403530	6025000	<i>Saxidomus gigantea</i> or <i>Tresus</i> spp. shell	ESP core test: lower boundary of archaeological shell midden	5.66	This study
27	OS-101358	GcTo-27	CT 2012-507	4040	25	3830	3574	3704	403543	6025015	<i>Saxidomus gigantea</i> or <i>Tresus</i> spp. shell	ESP core test: lower boundary of archaeological shell midden	5.29	This study
1	OS-	GcTo-28	CT 2012-	2990	40	2644	2303	2431	403393	6025179	<i>Saxidomus</i>	ESP core test: lower	5.15	This

25	OS-101555	GcTo-6	CT 2012-557	4490	30	4437	4147	4312	412686	6021480	<i>Mytilus</i> sp. shell	ESP core test: lower boundary of archaeological shell midden	3.58	This study
6	OS-119875	T623-1	CT 2013-035	2410	35	1858	1584	1724	404990	6022028	Clam shell	ESP core test: lower boundary of archaeological shell midden	3.22	This study
18	D-AMS 011948	P009-1	ST 2015-030	5732	33	6635	6445	6527	407969	6022226	Charcoal	Shovel test: lower boundary of archaeological shell midden	8.14	This study
15	D-AMS 007906	T717-1	CT 2014-515	3243	28	3560	3393	3463	405353	6020650	Charcoal	ESP core test: lower boundary of archaeological shell midden	6.86	This study
13	D-AMS 007889	T722-1	CT 2014-526	2853	24	2346	2126	2250	408012	6012786	<i>Saxidomus gigantea</i> or <i>Tresus</i> spp. Shell	ESP core test: lower boundary of archaeological shell midden	5.51	This study
13	D-AMS 013865	T722-1	CT 2014-527	3034	26	2660	2345	2491	408020	6012763	<i>Saxidomus gigantea</i> or <i>Tresus</i> spp. shell	ESP core test: lower boundary of archaeological shell midden	4.62	This study
28	OS-101563	T627-2	CT 2012-574	4860	25	4925	4645	4805	410002.9	6016085	<i>Mytilus</i> sp. shell	ESP core test: lower boundary of archaeological shell midden	5.876	This study
16	D-AMS 011949	P011-1	ST 2015-034	7445	35	8348	8186	8266	405975	6020487	Charcoal	Shovel test: archaeological material on raised terrace	11.35	This study
16	D-AMS 011950	P011-1	ST 2015-034	8220	40	9304	9028	9186	405975	6020487	Charcoal	Shovel test: archaeological material on raised terrace	11.25	This study

* indicates date on a bulk sample of material that has been calibrated with an additional +/-100 year uncertainty modifier.

¹ Labs are indicated by Lab Number prefixes as follows: D-AMS=DirectAMS, Bothell, WA; OS= National Ocean Sciences Accelerator Mass Spectrometry, Woods Hole Oceanographic Institute, Woods Hole, MA; SUERC=Scottish Universities Environmental Research Centre, Glasgow, Scotland; UBA=Queen's University Belfast 14Chrono Centre for Climate, the Environment, and Chronology, Belfast, UK; Beta=Beta Analytic Inc., Miami, FL; CAMS=Center for Accelerator Mass Spectrometry, Livermore, CA; GSC=Geological Survey of Canada Radiocarbon Dating Laboratory, Ottawa, ON.

² All terrestrial samples were calibrated using the INTCAL13 calibration curve, and all marine samples were calibrated using the MARINE13 calibration curve (Reimer et al. 2013).

Table 4. Radiocarbon dates for RSL Index and Limiting Points used to constrain the Prince Rupert Harbour area RSL curve. Map ID letters and numbers refer to locations on Figure 2.

Table 5 - Diatom Log

Location and Core	Sample Depth	Total diatoms confidently identified ([total IDs], [total <i>n</i> species])	Diatom species contributing >2.5% to assemblage ([Salinity Class], [Percent Abundance])	Paleoenvironment/ Paleosalinity
Tsook Lake, TL#1	72 cm	299, 17	<i>Frustulia rhomboides</i> (1, 3.7%), <i>Fragilaria</i> sp. cf. <i>elliptica</i> or <i>pinnata</i> (2, 35.8%), <i>Nitzschia amphibioides</i> (2, 19.7%), <i>Fragilaria construens</i> (2, 10.0%), <i>Navicula</i> sp. cf. <i>radiosa</i> or <i>leptostriata</i> (2, 8.7%), <i>Pseudostaurosira brevistriata</i> (3, 9.0%); also <i>Eunotia</i> spp. and <i>Gomphonema</i> spp. (all salinity class 1-2)	Freshwater pond or lake
Tsook Lake, TL#1	74 cm	294, 36	<i>Fragilaria</i> sp. cf. <i>elliptica</i> or <i>pinnata</i> (2, 25.3%), <i>F. construens</i> (2, 21.8%), <i>Staurosirella leptostauron</i> (2, 6.1%), <i>Stauroneis phoenicenteron</i> (2, 2.7%), <i>Pseudostaurosira brevistriata</i> (3, 29.3%), <i>Fragilaria construens</i> var. <i>subsalina</i> (3, 3.4%), <i>Coscinodiscus</i> sp.* (5, 1%)	Freshwater pond or lake, newly isolated
Tsook Lake, TL#1	76 cm	278, 32	<i>Fragilaria construens</i> (2, 15.1%), <i>F. sp. cf. elliptica</i> or <i>pinnata</i> (2, 8.6%), <i>Staurosirella leptostauron</i> (2, 5.0%), %, <i>Pseudostaurosira brevistriata</i> (3, 43.9%), <i>Fragilaria construens</i> var. <i>subsalina</i> (3, 4.0%), <i>Thalassiosira</i> sp. or <i>Coscinodiscus</i> sp.* (5, 1.1%)	Freshwater pond or lake, newly isolated
Tsook Lake, TL#1	78 cm	287, 36	<i>Fragilaria construens</i> (2, 22.3%), <i>Gyrosigma acuminatum</i> (2, 7.3%), <i>Staurosirella leptostauron</i> (2, 4.5%), <i>Stauroneis phoenicenteron</i> (2, 3.1%), <i>Fragilaria</i> sp. cf. <i>elliptica</i> or <i>pinnata</i> (2, 3.1%), <i>Pseudostaurosira brevistriata</i> (3, 16.7%), <i>Cocconeis placentula</i> (3, 5.9%), <i>Epithemia adnata</i> (3, 4.2%), <i>Amphora libyca</i> (3, 3.1%), <i>Tabularia fasciculata</i> * (4, 2.4%), <i>Thalassiosira</i> sp. or <i>Coscinodiscus</i> sp. (5, 4.5%), <i>Cocconeis costata</i> * (5, 2.4%)	Newly isolated freshwater pond, upper estuary, or freshwater-dominant lagoon with marine incursions
Tsook Lake, TL#1	82 cm	277, 29	<i>Cymatopleura elliptica</i> (2, 17.7%), <i>Fragilaria neoproducta</i> (2, 5.8%), <i>F. sp. cf. elliptica</i> or <i>pinnata</i> (2, 3.2%), <i>F. construens</i> var. <i>subsalina</i> (3, 17.7%), <i>Epithemia adnata</i> (3, 13.0%), <i>Amphora libyca</i> (3, 5.4%), <i>Cocconeis placentula</i> (3, 4.0%), <i>Craticula cuspidata</i> (3, 2.5%), <i>Navicula digitoradiata</i> (4, 8.7%), <i>Opephora olsenii</i> (4, 4.0%), <i>Thalassiosira</i> sp. or <i>Coscinodiscus</i> sp. (5, 6.1%), <i>Cocconeis costata</i> (5, 2.9%)	Mixed fresh, brackish, and marine assemblage, environment transitioning from nearshore/ lagoon/estuary to freshwater
Tsook	84 cm	265, 31	<i>Cymatopleura elliptica</i> (2, 10.9%), <i>Fragilaria neoproducta</i> (2, 4.5%), <i>F. sp. cf.</i>	Mixed fresh,

Lake, TL#1			<i>elliptica</i> or <i>pinnata</i> (2, 4.5%), <i>F. construens</i> var. <i>subsalina</i> (3, 9.8%), <i>Epithemia adnata</i> (3, 7.9%), <i>Amphora libyca</i> (3, 4.5%), <i>Navicula digitoradiata</i> (4, 21.1%), <i>Rhopalodia acuminata</i> (4, 3.8%), <i>Cocconeis scutellum</i> (4, 3.0%), <i>Thalassiosira</i> sp. or <i>Coscinodiscus</i> sp. (5, 5.3%), <i>Cocconeis costata</i> (5, 3.0%)	brackish, and marine assemblage, environment transitioning from nearshore/ lagoon/estuary to freshwater
Tsook Lake, TL#1	87 cm	294, 22	<i>Navicula digitoradiata</i> (4, 68.7%), <i>Cocconeis scutellum</i> (4, 7.8%), <i>C. costata</i> (5, 5.4%), <i>Thalassiosira</i> sp. or <i>Coscinodiscus</i> sp. (5, 2.7%)	Brackish/Marine, likely nearshore coastal
Tsook Lake, TL#1	95 cm	197, 15	<i>Navicula digitoradiata</i> (4, 68.7%), <i>Scoliopleura tumida</i> (4, 7.1%), <i>Tabularia fasciculata</i> (4, 2.5%), <i>Cocconeis costata</i> (5, 22.8%), <i>Rhabdonema arcuatum</i> (5, 20.8%), <i>Thalassiosira decipiens</i> (5, 5.6%), <i>Thalassiosira</i> sp. or <i>Coscinodiscus</i> sp. (5, 5.6%), <i>Trachyneis aspera</i> (5, 2.5%)	Brackish/Marine, likely nearshore coastal
Rifle Range Lake 1, RR1#1	185 cm	272, 10	<i>Eunotia incisa</i> (1, 18.4%), <i>E. serra</i> var. <i>diadema</i> (1, 4.8%), <i>Aulacoseira</i> spp. (2, 33.1%), <i>Stauroneis phoenicenteron</i> (2, 12.13%), <i>Stauroneis</i> spp. (2, 9.6%), <i>Pinnularia maior</i> (2, 11.4%), <i>P. microstauron</i> (2, 8.5%)	Freshwater pond or lake
Rifle Range Lake 1, RR1#1	287 cm	292, 15	<i>Fragilaria construens</i> (2, 72.3%), <i>Sellaphora</i> sp. cf. <i>pupula</i> or <i>laevissima</i> (2, 9.9%), <i>Achnanthes exigua</i> (2, 6.5%), also several different <i>Gomphonema</i> spp. (2)	Freshwater pond or lake
Rifle Range Lake 1, RR1#1	289 cm	299, 28	<i>Fragilaria construens</i> (2, 33.8%), <i>F. sp.</i> cf. <i>elliptica</i> or <i>pinnata</i> (2, 26.1%), <i>Achnanthes exigua</i> (2, 4.3%), <i>Pseudostaurosira brevistriata</i> (3, 11.4%)	Freshwater pond or lake, newly isolated
Rifle Range Lake 1, RR1#1	291 cm	295, 34	<i>Tabellaria</i> spp. (<i>fenestrata</i> or <i>flocculosa</i>) (1, 5.8%), <i>Fragilaria construens</i> (2, 18.3%), <i>F. sp.</i> cf. <i>elliptica</i> or <i>pinnata</i> (2, 12.5%), <i>Pseudostaurosira robusta</i> (2, 2.7%), <i>P. brevistriata</i> (3, 25.1%), <i>Rhopalodia gibba</i> (3, 3.4%), also many different <i>Gomphonema</i> spp. (2) and <i>Cymbella/Encyonema</i> spp. (2)	Freshwater pond or lake, newly isolated

Rifle Range Lake 1, RR1#1	293 cm	290, 37	<i>Gyrosigma acuminatum</i> (2, 12.8%), <i>Fragilaria</i> sp. cf. <i>elliptica</i> or <i>pinnata</i> (2, 10.6%), <i>F. construens</i> var. <i>venter</i> (2, 9.3%), <i>F. construens</i> (2, 8.6%), <i>Pseudostaurisira brevistriata</i> (3, 15.9%), <i>Fragilaria construens</i> var. <i>subsalina</i> (3, 4.8%), <i>Fallacia pygmaea</i> (4, 7.6%), <i>Opephora olsenii</i> (4, 3.4%)	Newly isolated freshwater pond or lake with some brackish species
Rifle Range Lake 1, RR1#1	295 cm	289, 37	<i>Fragilaria construens</i> var. <i>subsalina</i> (3, 6.6%), <i>Cocconeis scutellum</i> var. <i>parva</i> (4, 12.5%), <i>C. scutellum</i> (4, 10.4%), <i>Opephora olsenii</i> (4, 11.4%), <i>Achnanthes delicatula</i> ssp. <i>hauckiana</i> (4, 8.0%), <i>Tabularia fasciculata</i> (4, 6.6%), <i>Mastogloia pumila</i> (4, 3.8%), <i>Campylodiscus clypeus</i> (4, 3.1%), <i>Navicula digitoradiata</i> var. <i>minima</i> (4, 3.1%), <i>Fallacia litoricola</i> (5, 8.7%), <i>Opephora marina</i> (5, 3.8%)	Brackish/Marine, likely nearshore coastal
Rifle Range Lake 1, RR1#1	297 cm	288, 32	<i>Gyrosigma acuminatum</i> (2, 3.1%), <i>Pseudostaurisira brevistriata</i> (3, 7.3%), <i>Tabularia fasciculata</i> (4, 13.9%), <i>Cocconeis scutellum</i> (4, 12.5%), <i>C. scutellum</i> var. <i>parva</i> (4, 5.9%), <i>Navicula digitoradiata</i> (4, 9.4%), <i>Nitzschia sigma</i> (4, 4.2%), <i>Opephora olsenii</i> (4, 3.1%), <i>Thalassiosira</i> sp. or <i>Coscinodiscus</i> sp. (5, 13.9%), <i>Cocconeis costata</i> (5, 6.9%), <i>Fallacia litoricola</i> (5, 2.8%)	Brackish/Marine, likely nearshore coastal
Digby Island Lake 1, DL#1	155 cm	295, 21	<i>Tabellaria</i> spp. (<i>fenestrata</i> or <i>flocculosa</i>) (1, 13.6%), <i>Frustulia rhomboides</i> (1, 12.5%), <i>Eunotia incisa</i> (1, 3.1%), <i>Aulacoseira</i> spp. (2, 43.7%), <i>Navicula</i> cf. <i>radiosa</i> (2, 4.7%), <i>Encyonema gracilis</i> (2, 3.7%), <i>Pinnularia interrupta</i> (2, 3.1%)	Freshwater pond/ or lake
Digby Island Lake 1, DL#1	215 cm	298, 26	<i>Eunotia incisa</i> (1, 10.7%), <i>E. cf. minor</i> (1, 5.4%), other <i>Eunotia</i> spp. (salinity classes 1-2, 6.4%), <i>Aulacoseira</i> spp. (2, 16.4%), <i>Navicula</i> cf. <i>radiosa</i> (2, 3.7%), <i>Encyonema gracilis</i> (2, 3.0%), <i>Gomphonema</i> spp. (2, 2.7%), <i>Cocconeis placentula</i> (3, 33.6%)	Freshwater pond/ or lake
Digby Island Lake 1, DL#1	220 cm	298, 42	<i>Aulacoseira</i> spp. (2, 31.2%), <i>Fragilaria</i> sp. cf. <i>elliptica</i> or <i>pinnata</i> (2, 18.4%), <i>F. construens</i> (2, 16.4%), <i>Cocconeis placentula</i> (3, 3.0%)	Freshwater pond/ or lake
Digby Island Lake 1,	225 cm	296, 22	<i>Fragilaria</i> sp. cf. <i>elliptica</i> or <i>pinnata</i> (2, 36.8%), <i>Achnanthes joursacense</i> (2, 8.8%), <i>A. oestrupii</i> (2, 4.7%), <i>Fragilaria construens</i> (2, 2.7%), <i>Pseudostaurisira brevistriata</i> (3, 17.9%), <i>Martyana martyi</i> (3, 16.2%)	Freshwater pond/ or lake, newly isolated

DL#1	230 cm	293, 26	<i>Fragilaria</i> sp. cf. <i>elliptica</i> or <i>pinnata</i> (2, 20.1%), <i>Achnanthes exigua</i> (2, 9.2%), <i>Amphora pediculus</i> (2, 5.1%), <i>Gyrosigma attenuatum</i> (2, 4.8%), <i>Fragilaria construens</i> (2, 4.4%), <i>Staurosirella leptostauron</i> (2, 3.4%), <i>Achnanthes jousacense</i> (2, 3.1%), <i>Pseudostaurosira brevistriata</i> (3, 34.8%), <i>Amphora libyca</i> (3, 2.7%), also one <i>Rhabdonema arcuatum</i> and one <i>Thalassiosira</i> sp. or <i>Coscinodiscus</i> sp. (both salinity class 5)	Freshwater pond/ or lake, newly isolated
Digby Island Lake 1, DL#1	232	279, 20	<i>Fragilaria</i> sp. cf. <i>elliptica</i> or <i>pinnata</i> (2, 23.0%), <i>F. construens</i> (2, 6.5%), <i>Gyrosigma attenuatum</i> (2, 6.5%), <i>Amphora pediculus</i> (2, 5.7%), <i>Pseudostaurosira brevistriata</i> (3, 41.2%), <i>Amphora libyca</i> (3, 6.1%), also one <i>Rhabdonema arcuatum</i> and several <i>Thalassiosira</i> sp. or <i>Coscinodiscus</i> sp. (both salinity class 5)	Newly isolated freshwater pond or lake
Digby Island Lake 1, DL#1	236	293, 29	<i>Fragilaria</i> sp. cf. <i>elliptica</i> or <i>pinnata</i> (2, 11.2%), <i>Amphora pediculus</i> (2, 3.1%), <i>Pseudostaurosira brevistriata</i> (3, 19.8%), <i>Amphora libyca</i> (3, 9.6%), <i>Fragilaria construens</i> var. <i>subsalina</i> (3, 6.8%), <i>Cocconeis placentula</i> (3, 3.8%), <i>Martiana martyi</i> (3, 3.1%), <i>Cocconeis scutellum</i> (4, 3.4%), <i>Thalassiosira</i> sp. or <i>Coscinodiscus</i> sp. (5, 17.7%), <i>Rhabdonema arcuatum</i> (5, 3.4%), <i>Cocconeis costata</i> (5, 2.7%)	Mixed fresh, brackish, and marine assemblage, environment transitioning from nearshore/ lagoon/estuary to freshwater
Digby Island Lake 1, DL#1	238	219, 29	<i>Amphora libyca</i> (3, 26.0%), <i>Epithemia adnata</i> (3, 2.7%), <i>Fragilaria construens</i> var. <i>subsalina</i> (3, 2.7%), <i>Cocconeis scutellum</i> (4, 5.0%), <i>Thalassiosira</i> sp. or <i>Coscinodiscus</i> sp. (5, 21.0%), <i>Thalassiosira decipiens</i> (5, 10.5%), <i>Rhabdonema arcuatum</i> (5, 6.4%), <i>Cocconeis costata</i> (5, 3.2%)	Mixed fresh, brackish, and marine assemblage, environment transitioning from nearshore/ lagoon/estuary to freshwater
Digby Island Lake 1, DL#1	245 cm	300, 20	<i>Cocconeis scutellum</i> (4, 13.7%), <i>Navicula digitoradiata</i> (4, 7.7%), <i>Scoliolepta tumida</i> (4, 3.3%), <i>Tabularia fasciculata</i> (4, 3.0%), <i>Rhabdonema arcuatum</i> (5, 32.3%), <i>Thalassiosira decipiens</i> (5, 13.3%), <i>Cocconeis costata</i> (5, 10.3%), <i>Thalassiosira</i> sp. or <i>Coscinodiscus</i> sp. (5, 3.7%), <i>Trachyneis aspera</i> (5, 2.7%)	Brackish/Marine, likely nearshore coastal
Benck	5 cm	296, 33	<i>Aulacoseira</i> spp. (2, 31.8%), <i>Fragilaria construens</i> (2, 3.0%), <i>Diploneis finnica</i> (2,	Freshwater pond,

e Lagoon, BL#1			2.7%), <i>Fallacia</i> spp. (4, 6.4%), <i>Paralia sulcata</i> (5, 37.8%)	upper estuary, or freshwater-dominant lagoon with marine incursions
Benck e Lagoon, BL#1	10 cm	293, 40	<i>Tabellaria</i> spp. (<i>fenestrata</i> or <i>flocculosa</i>) (1, 2.7%), <i>Aulacoseira</i> spp. (2, 30.4%), <i>Fragilaria construens</i> (2, 3.1%), <i>Diploneis finnica</i> (2, 3.1%), <i>Fallacia</i> spp. (4, 5.8%), <i>Paralia sulcata</i> (5, 26.6%)	Freshwater pond, upper estuary, or freshwater-dominant lagoon with marine incursions
Benck e Lagoon, BL#1	15 cm	303, 36	<i>Tabellaria</i> spp. (<i>fenestrata</i> or <i>flocculosa</i>) (1, 7.3%), <i>Aulacoseira</i> spp. (2, 34.7%), <i>Fragilaria construens</i> (2, 12.2%), <i>F. sp. cf. elliptica</i> or <i>pinnata</i> (2, 9.6%), <i>Cymbella cistula</i> (2, 3.0%), <i>Gomphonema subtile</i> (2, 2.6%), <i>Navicula radiosa</i> (2, 2.6%)	Freshwater pond, close to but above highest high tide
Benck e Lagoon, BL#1	20 cm	305, 46	<i>Tabellaria</i> spp. (<i>fenestrata</i> or <i>flocculosa</i>) (1, 3.0%), <i>Aulacoseira</i> spp. (2, 22.3%), <i>Fragilaria construens</i> (2, 11.8%), <i>F. sp. cf. elliptica</i> or <i>pinnata</i> (2, 6.9%), <i>Cymbella cistula</i> (2, 4.6%), <i>Achnanthes joursacense</i> (2, 4.3%), <i>Lindavia radiosa</i> (2, 3.3%), <i>Staurosirella lapponica</i> (2, 2.6%), <i>Rhopalodia gibba</i> (3, 4.9%), <i>Pseudostaurasira brevistriata</i> (3, 4.3%), also a small number of <i>Fallacia</i> spp. (4, 2.0%) and <i>Paralia sulcata</i> (5, 2.0%)	Freshwater pond, close to but above highest high tide
Benck e Lagoon, BL#1	25 cm	298, 39	<i>Tabellaria</i> spp. (<i>fenestrata</i> or <i>flocculosa</i>) (1, 10.0%), <i>Fragilaria construens</i> (2, 12.1%), <i>F. sp. cf. elliptica</i> or <i>pinnata</i> (2, 10.1%), <i>Aulacoseira</i> spp. (2, 9.7%), <i>Cocconeis pseudothumensis</i> (2, 8.1%), <i>Achnanthes oestrupii</i> (2, 6.0%), <i>Staurosirella lapponica</i> (2, 6.0%), <i>Pseudostaurasira brevistriata</i> (3, 10.1%), <i>Cocconeis placentula</i> (3, 5.0%)	Freshwater pond
Benck e Lagoon, BL#1	27 cm	286, 31	<i>Fragilaria</i> sp. <i>cf. elliptica</i> or <i>pinnata</i> (2, 14.6%), <i>Amphora pediculus</i> (2, 7.3%), <i>Achnanthes joursacense</i> (2, 5.9%), <i>Gyrosigma acuminatum</i> (2, 5.6%), <i>Cocconeis pseudothumensis</i> (2, 3.8%), <i>Fragilaria construens</i> (2, 3.8%), <i>Navicula aurora</i> (2, 3.1%), <i>Staurosirella pinnata</i> var. <i>intercedens</i> (2, 2.8%), <i>Pseudostaurasira brevistriata</i> (3, 29.7%)	Freshwater pond
Optim ism Bay, OB#1	300 cm	278, 38	<i>Tabularia fasciculata</i> (4, 7.6%), <i>Tryblionella aerophila</i> (4, 5.4%), <i>Gyrosigma balticum</i> (4, 5.0%), <i>Bacillaria socialis</i> (4, 4.7%), <i>Gyrosigma fasciola</i> (4, 4.7%), <i>Seminavis ventricosa</i> (4, 4.0%), <i>Nitzschia sigma</i> (4, 3.6%), <i>Psammodyctyon panduriforme</i> var. <i>delicatum</i> or <i>Tryblionella aerophila</i> (4, 2.9%), <i>Navicula</i>	Brackish/Marine, nearshore or intertidal

Optim ism Bay, OB#1	312 cm	296, 45	<p><i>transistans</i> (5, 27.7%), <i>Thalassiosira</i> sp. or <i>Coscinodiscus</i> sp. (5, 8.3%), <i>Cocconeis costata</i> (5, 2.5%), also several freshwater species such as <i>Gyrosigma acuminatum</i>*, <i>Fragilaria</i> sp. cf. <i>elliptica</i> or <i>pinnata</i>*, and <i>Surirella brebissonii</i>*</p> <p><i>Aulacoseira</i> spp. (2, 4.7%), <i>Craticula halophila</i> (3, 4.1%), <i>Achnanthes delicatula</i> ssp. <i>hauckiana</i> (4, 13.5%), <i>Navicula digitoradiata</i> (4, 7.8%), <i>Tabularia fasciculata</i> (4, 6.8%), <i>Psammodyctyon panduriforme</i> var. <i>delicatulum</i> or <i>Tryblionella aerophila</i> (4, 4.7%), <i>Melosira</i> sp. cf. <i>nummuloides</i> or <i>moniliformis</i> (4, 4.4%), <i>Amphora coffeaeformis</i> (4, 2.7%), <i>Diploneis interrupta</i> (4, 2.7%), <i>Navicula transistans</i> (5, 11.1%), <i>Thalassiosira</i> sp. or <i>Coscinodiscus</i> sp. (5, 5.7%), <i>Cocconeis costata</i> (5, 3.4%), <i>Odontella</i> sp. cf. <i>rhombus</i> or <i>aurita</i> (5, 3.4%)</p> <p>Nearly barren of diatoms, except for some very poorly preserved specimens that appear to be <i>Nitzschia dissipata</i> (2, 40%) and <i>Craticula halophiliodes</i> (3, 60%).</p> <p>Staple C and N analyses indicate that this is a terrestrial or freshwater peat/paleosol. Samples in the same strata below this and in core OB#2 were barren of diatoms.</p>	Brackish/Marine, marine transgressive intertidal zone or estuary
Optim ism Bay, OB#1	315 cm	5, 2		Terrestrial or freshwater
Optim ism Bay, OB#2	95 cm	301, 44	<p><i>Gyrosigma acuminatum</i> (2, 2.7%), <i>Craticula halophila</i> (3, 4.0%), <i>Navicula digitoradiata</i> (4, 12.6%), <i>Amphipleura</i> cf. <i>rutilans</i> (4, 7.3%), <i>Tabularia fasciculata</i> (4, 7.3%), <i>Achnanthes delicatula</i> ssp. <i>hauckiana</i> (4, 3.7%), <i>Gyrosigma fasciola</i> (4, 3.7%), <i>Nitzschia sigma</i> (4, 3.3%), <i>Bacillaria socialis</i> (4, 2.7%), <i>Psammodyctyon panduriforme</i> var. <i>delicatulum</i> (4, 2.7%), <i>Navicula transistans</i> (5, 14.3%), <i>Thalassiosira</i> cf. <i>eccentrica</i> (5, 3.7%)</p>	Brackish/Marine, marine transgressive intertidal zone or estuary
Optim ism Bay, OB#2	109 cm	299, 55	<p><i>Navicula digitoradiata</i> (4, 21.4%), <i>Tabularia fasciculata</i> (4, 8.0%), <i>Achnanthes delicatula</i> ssp. <i>hauckiana</i> (4, 3.3%), <i>A. brevipes</i> (4, 3.0%), <i>A. cf. parvula</i> (4, 3.0%), <i>Gyrosigma fasciola</i> (4, 3.0%), <i>Melosira</i> sp. cf. <i>nummuloides</i> or <i>moniliformis</i> (4, 3.0%), <i>Amphipleura</i> cf. <i>rutilans</i> (4, 2.7%), <i>Navicula transistans</i> (5, 6.4%), <i>Thalassiosira pacifica</i> (5, 3.3%), <i>T. cf. eccentrica</i> (5, 2.7%), <i>Thalassiosira</i> sp. or <i>Coscinodiscus</i> sp. (5, 2.7%), also 12.5% total freshwater species such as <i>Gyrosigma acuminatum</i>*, <i>Craticula halophila</i>*, <i>Fragilaria</i> spp.*</p>	Brackish/Marine, marine transgressive intertidal zone or estuary
Optim ism Bay, OB#2	111.5 cm	287, 42	<p><i>Navicula digitoradiata</i> (4, 13.9%), <i>Tabularia fasciculata</i> (4, 10.1%), <i>Achnanthes delicatula</i> ssp. <i>hauckiana</i> (4, 6.3%), <i>Melosira</i> sp. cf. <i>nummuloides</i> or <i>moniliformis</i> (4, 4.9%), <i>Achnanthes brevipes</i> (4, 3.1%), <i>Thalassiosira</i> sp. or <i>Coscinodiscus</i> sp. (5, 17.4%), <i>Navicula transistans</i> (5, 4.9%), <i>Thalassiosira</i> cf. <i>eccentrica</i> (5, 4.9%), <i>Achnanthes</i> cf. <i>groenlandica</i> (5, 3.8%), <i>Cocconeis costata</i> (5, 2.8%), <i>Tryblionella acuminata</i> (5, 2.8%), also a couple halophob <i>Tabularia</i> spp. (<i>fenestrata</i> or</p>	Brackish/Marine, marine transgressive intertidal zone or estuary

				<i>flocculosa</i>) and several other freshwater species	
Optim ism Bay, OB#2	113 cm	290, 29		<i>Navicula digitoradiata</i> (4, 52.4%), <i>Gyrosigma balticum</i> (4, 5.2%), <i>Scoliopleura tumida</i> (4, 4.1%), <i>Nitzschia sigma</i> (4, 3.8%), <i>Thalassiosira</i> sp. or <i>Coscinodiscus</i> sp. (5, 4.8%), <i>Thalassiosira</i> cf. <i>eccentrica</i> (5, 3.1%), <i>Tryblionella acuminata</i> (5, 3.1%), <i>Didymosphenia geminata</i> * (salinity class 2, 1 specimen)	Brackish/Marine, marine transgressive intertidal zone or estuary

Table 5. Detailed list of most common or key diatoms observed in Livingstone Core Samples. Salinity Class (1=halophobic, 2=oligohalobous indifferent, 3=oligohalobous halophilic, 4=mesohalobous, 5=polyhalobous) and percent of total sample assemblage given in parentheses after each species name.

Figure 1 Regional Map
[Click here to download high resolution image](#)

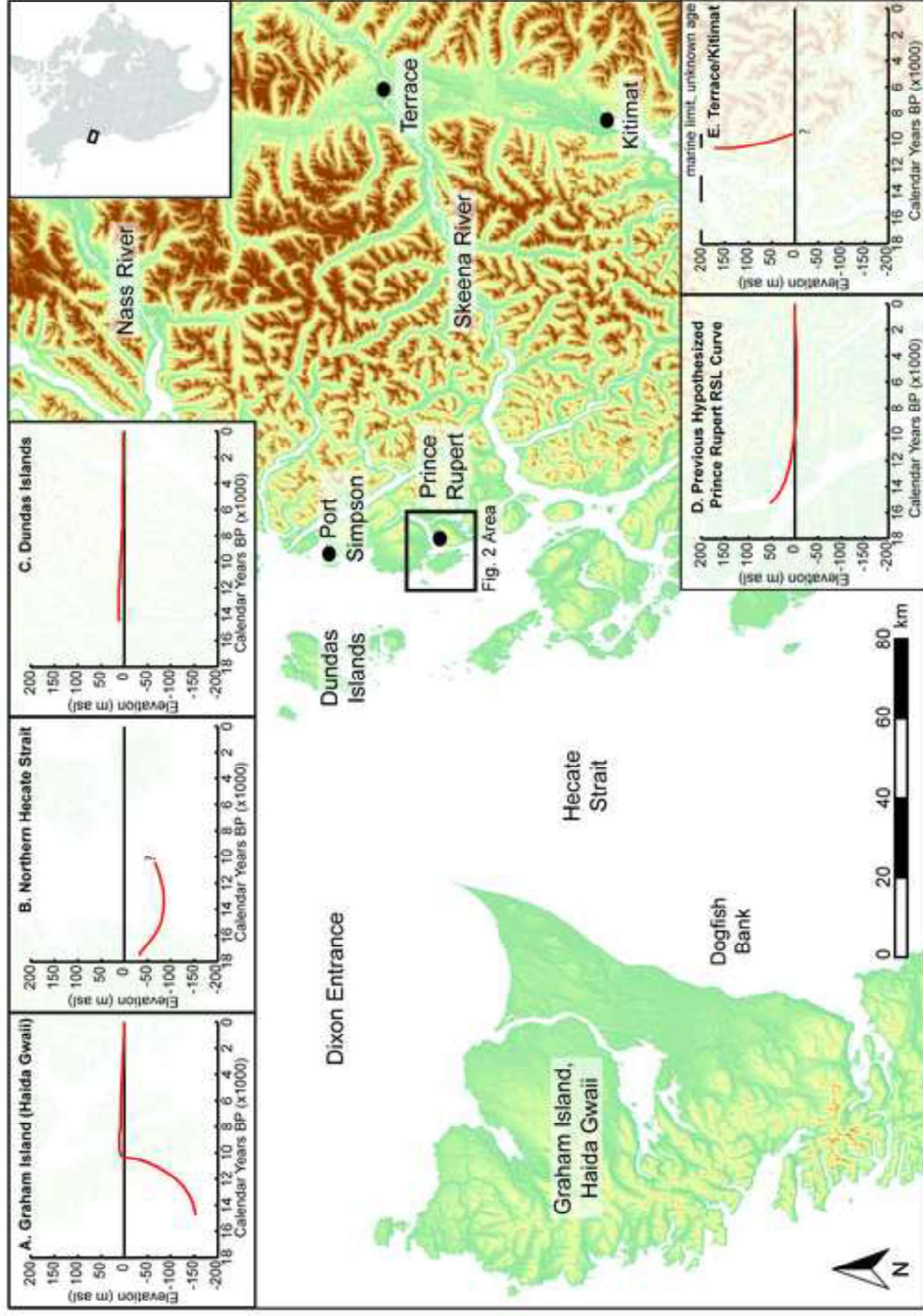


Figure 2 Data Points Map
[Click here to download high resolution image](#)

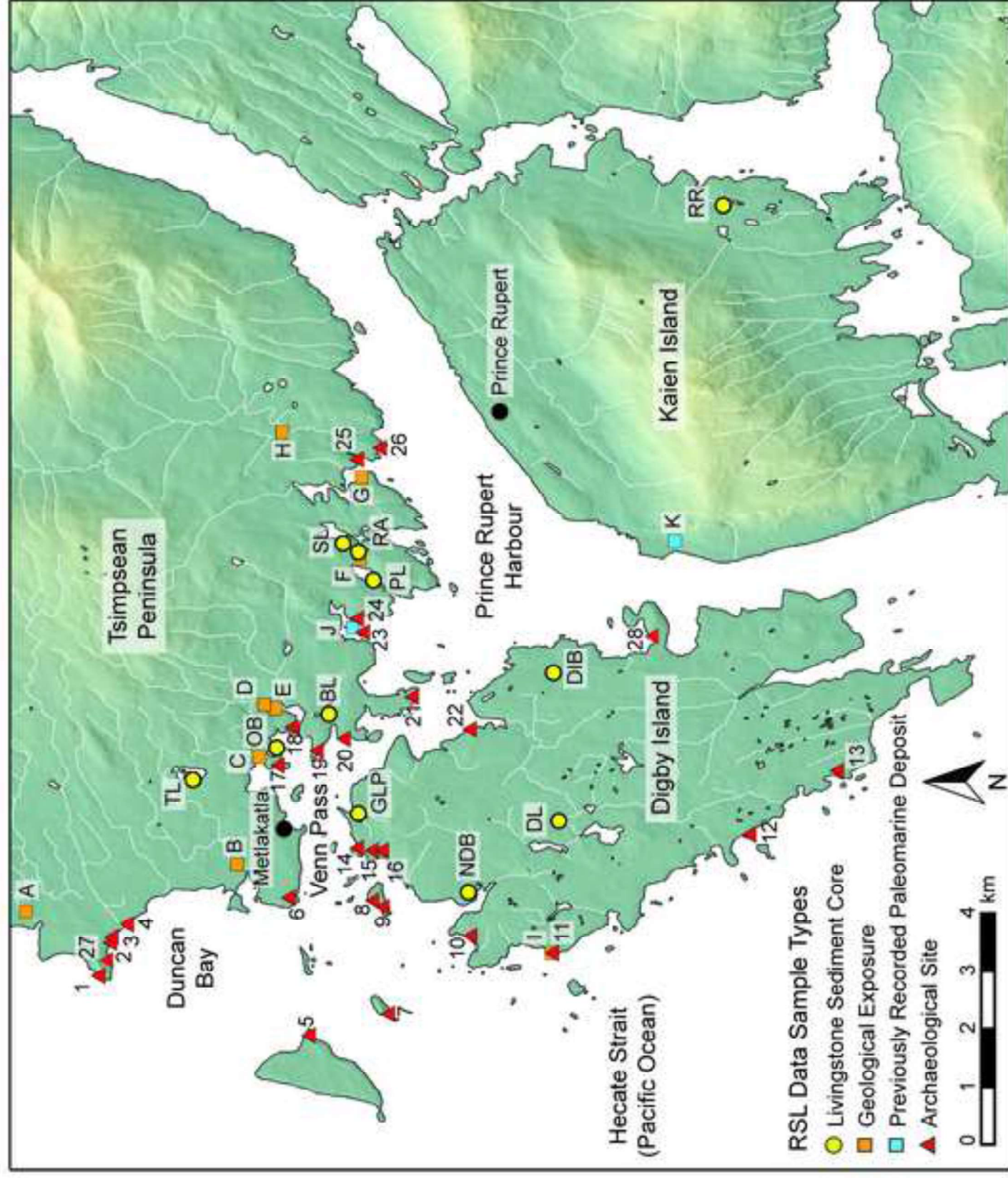


Figure 3 Age-Elevation Plot
[Click here to download high resolution image](#)

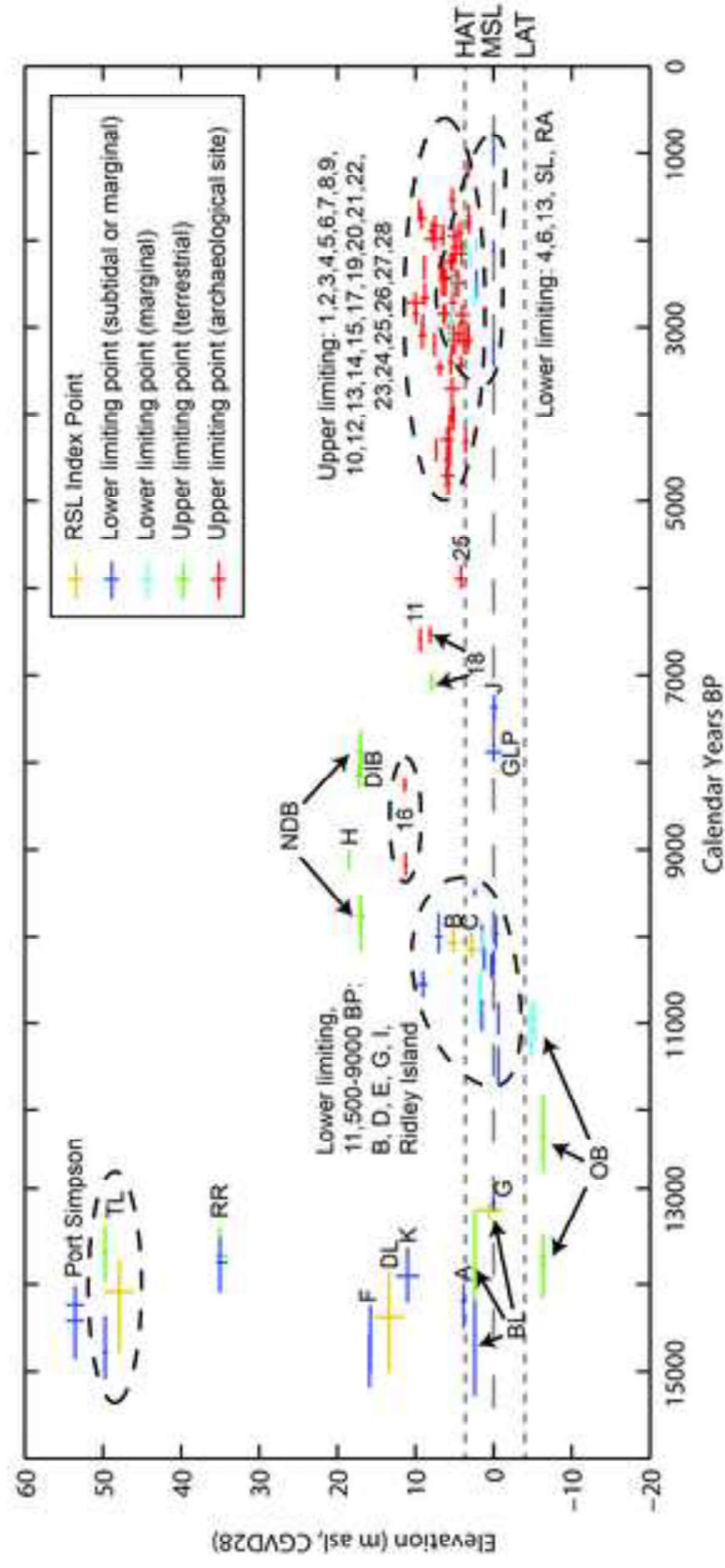


Figure 4 Tsook Lake Core

[Click here to download high resolution image](#)

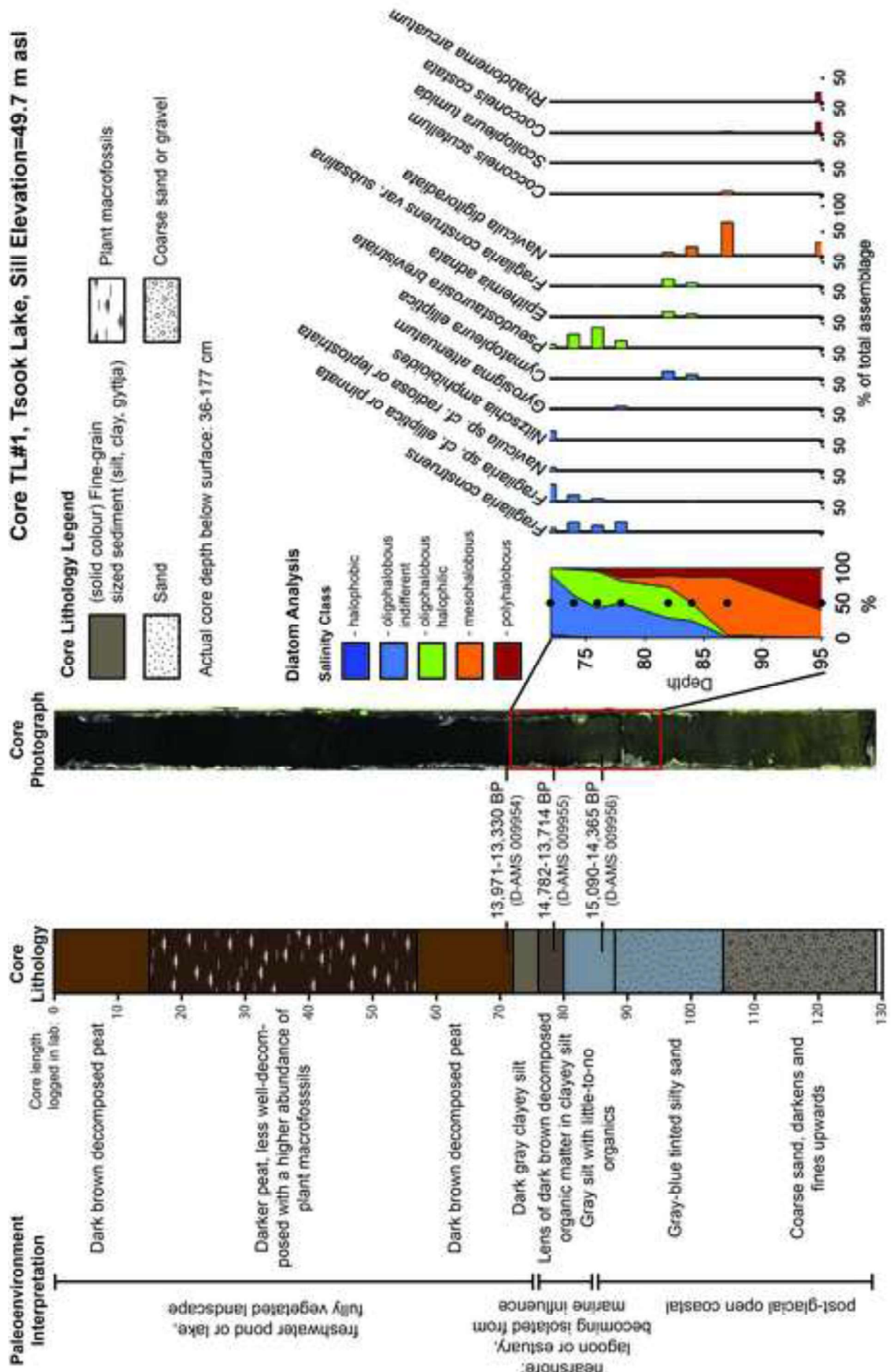


Figure 5 Rifle Range Lake Core

[Click here to download high resolution image](#)

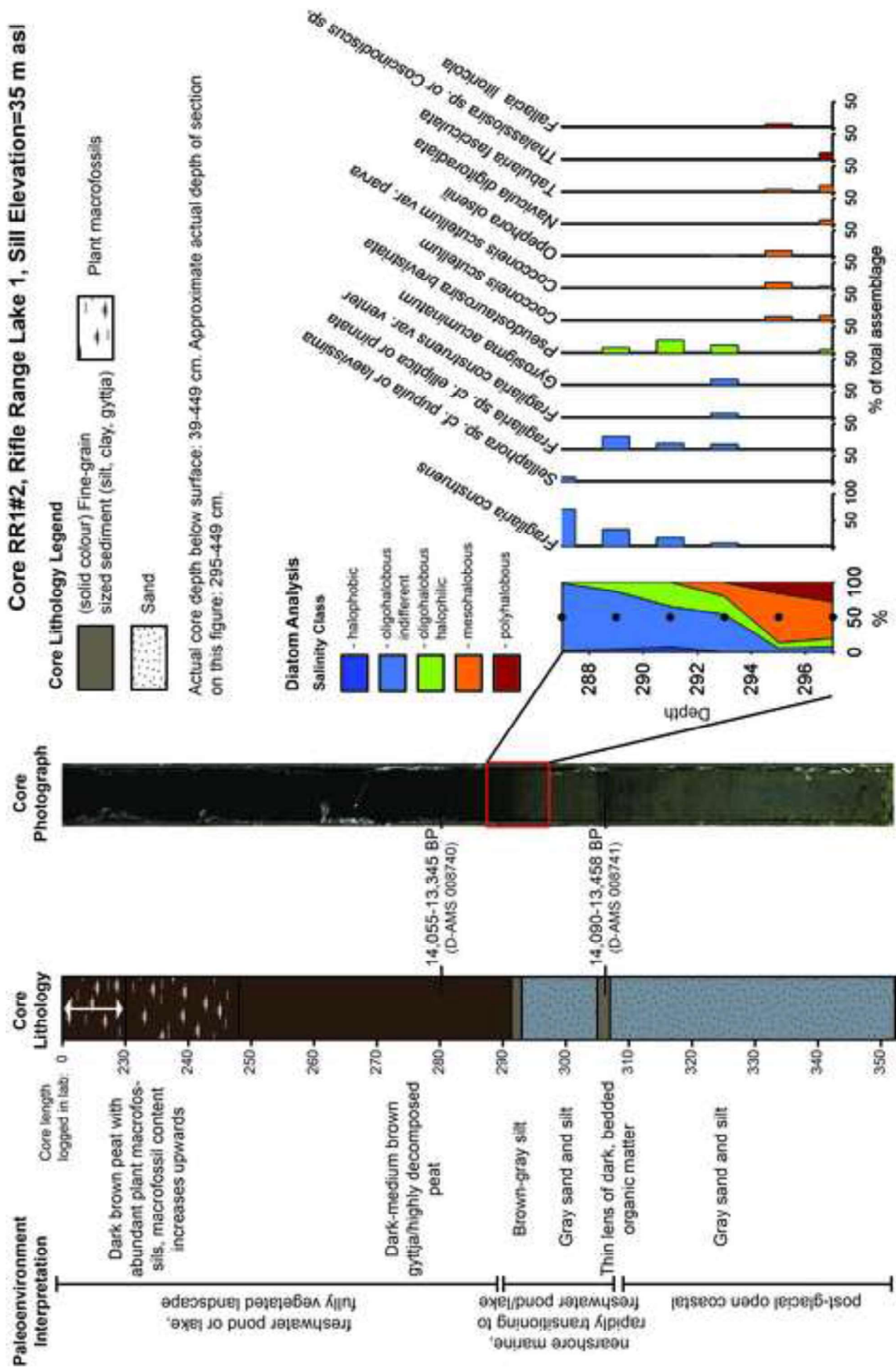


Figure 6 Digby Lake Core

[Click here to download high resolution image](#)

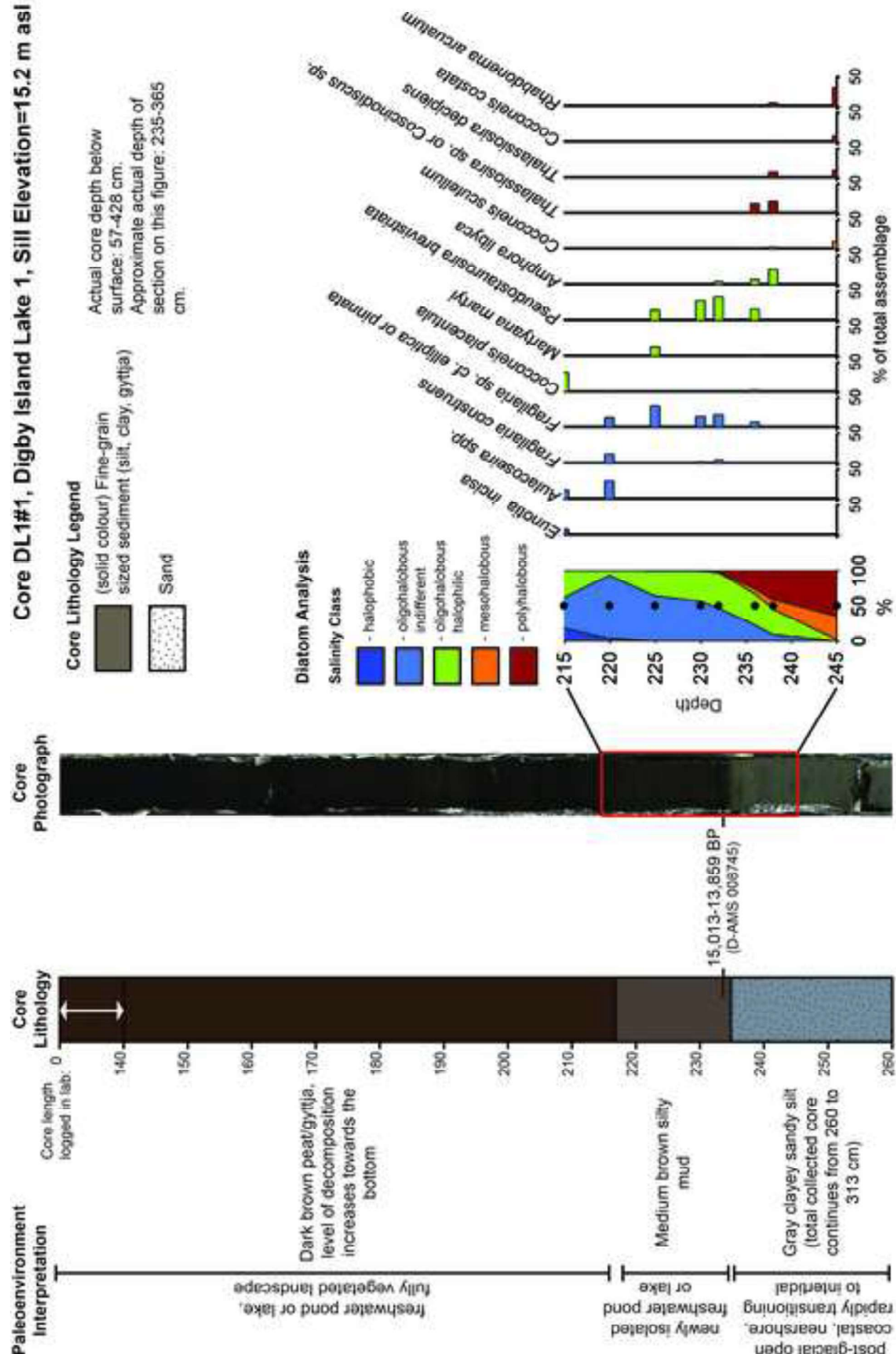


Figure 7 Scott Inlet Area
[Click here to download high resolution image](#)

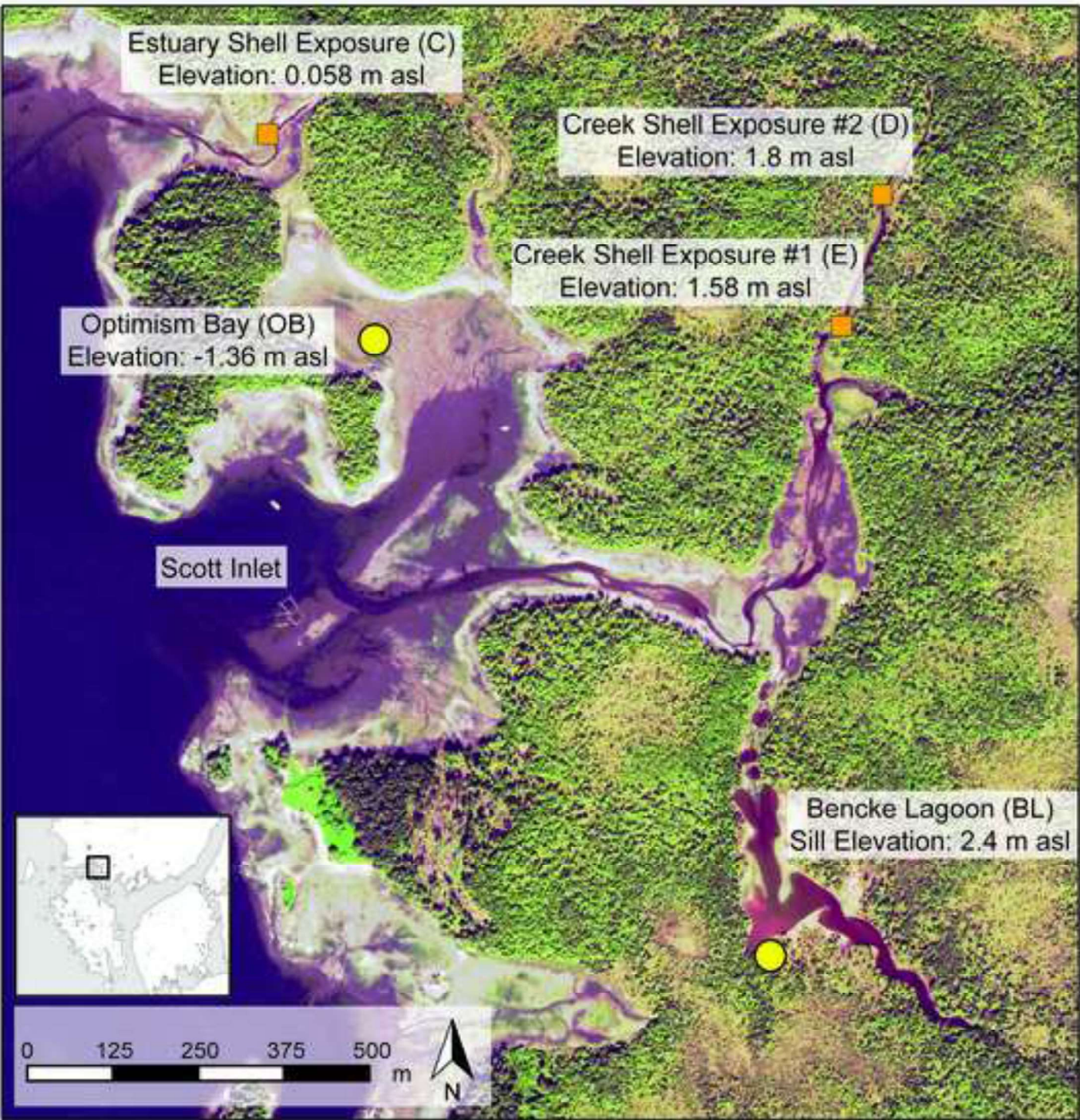


Figure 8 Bencke Lagoon Core

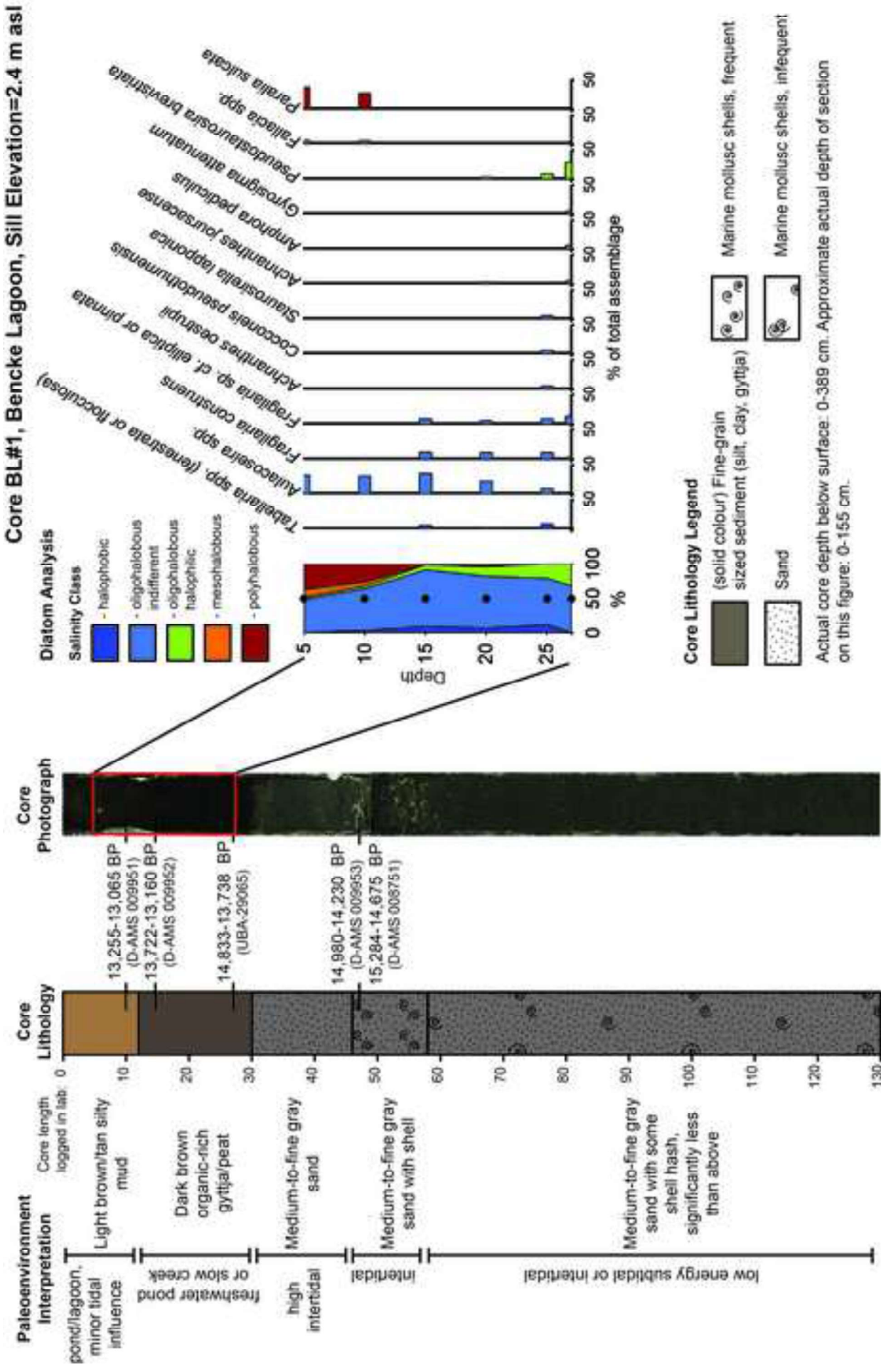


Figure 9 Stable Isotope Plot
[Click here to download high resolution image](#)

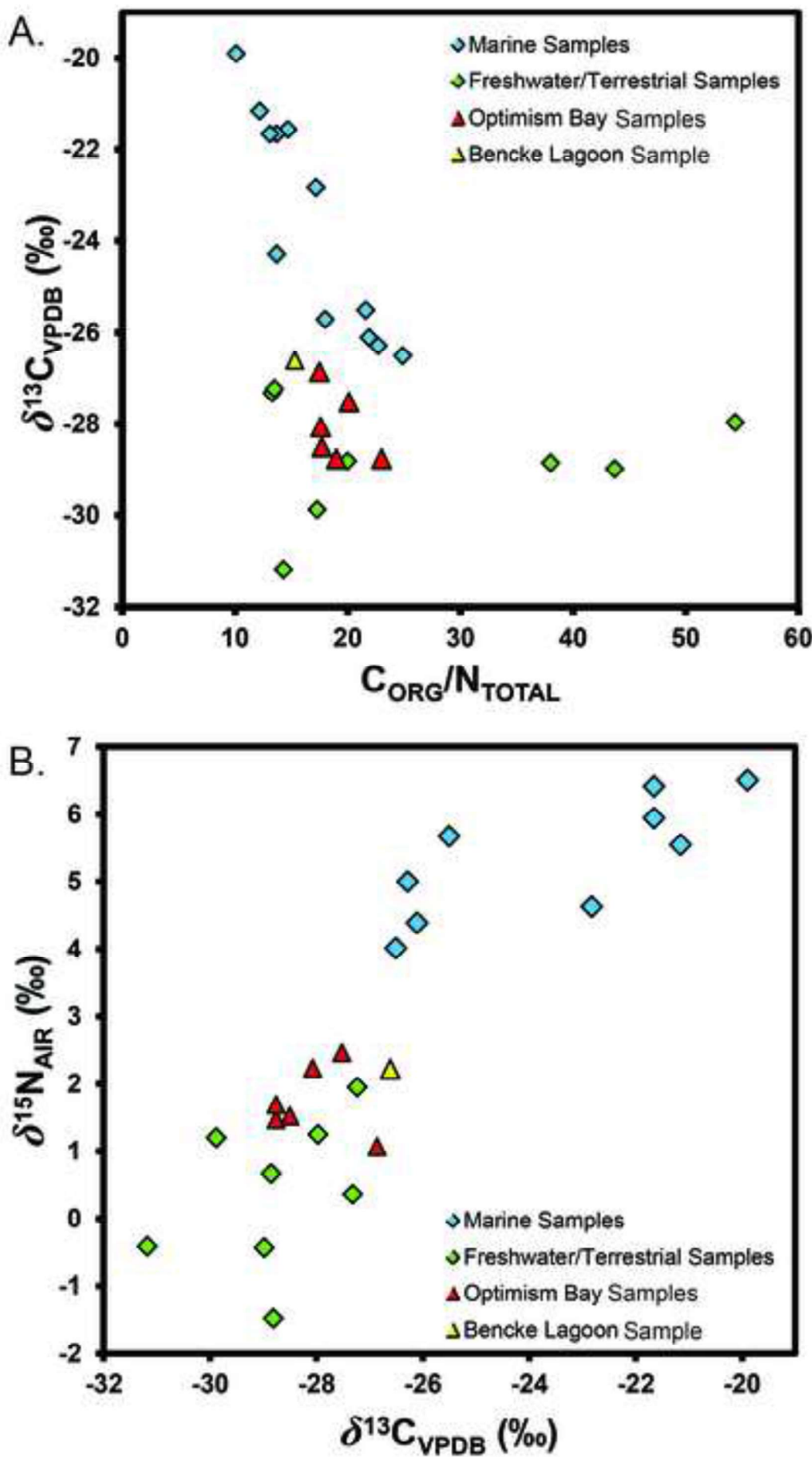
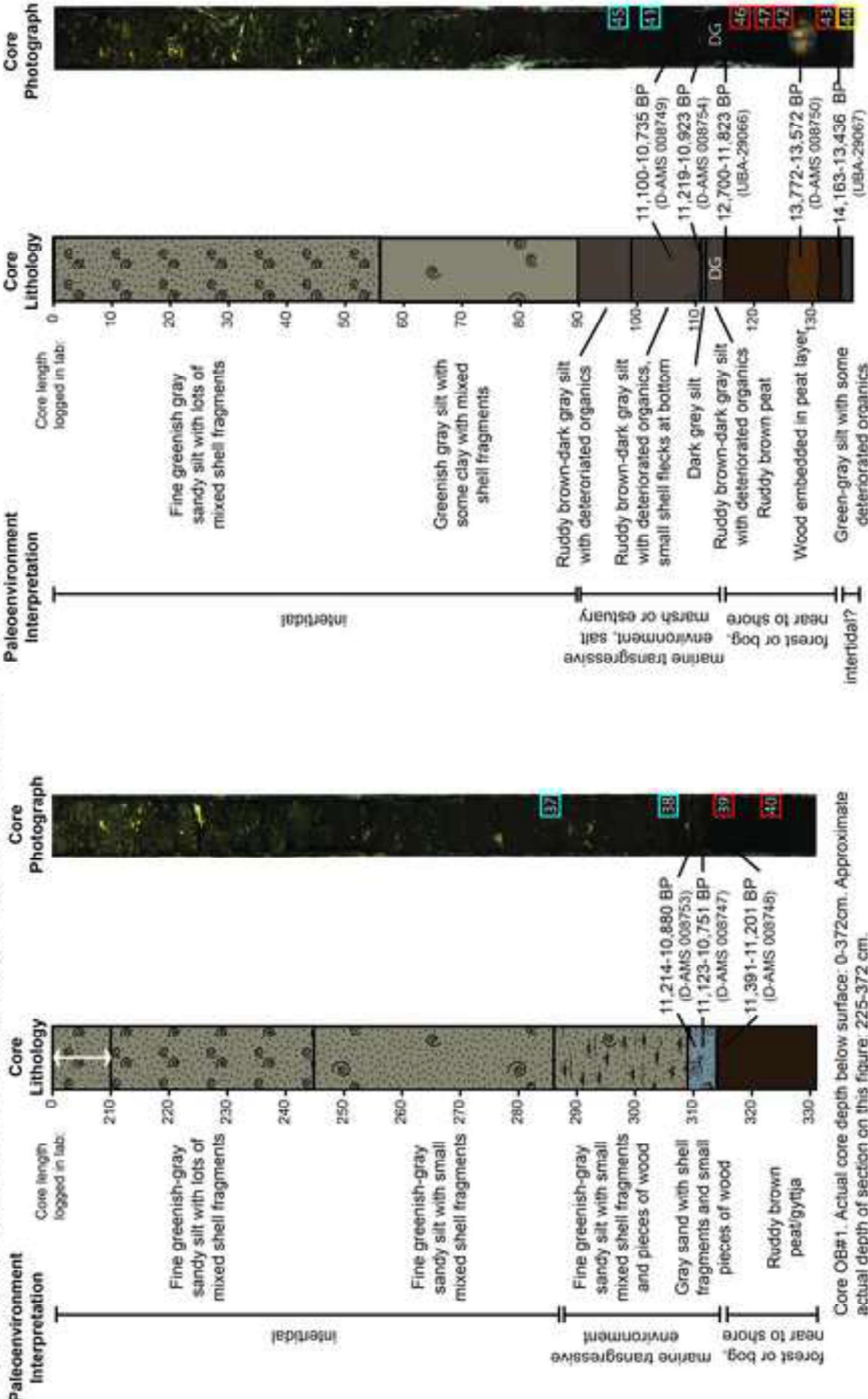


Figure 10 Optimism Bay Cores

[Click here to download high resolution image](#)

Core OB#1 (left) and OB#2 (right), Optimism Bay, Surface Elevation=-1.36 m asl



Core OB#1. Actual core depth below surface: 0-372cm. Approximate actual depth of section on this figure: 225-372 cm.

Core OB#2. Actual core depth below surface: 0-500 cm. Approximate actual depth of section on this figure: 320-500 cm.

Core Lithology Legend

- (solid colour) Fine-grain sized sediment (silt, clay, gyttja)
- Sand
- Coarse sand or gravel
- Marine mollusc shells, frequent
- Marine mollusc shells, infrequent
- Plant macrofossils

DG *Didymosphenia geminata* specimen location

Stable isotope sample, blue box = known brackish/marine context, red box = freshwater/terrestrial context inferred through C/N results, yellow box = unknown salinity. Number in the box equals the last two digits of the unique SUBC numbers in Supplemental Table 1.

Figure 11 Tea Bay Creek
[Click here to download high resolution image](#)

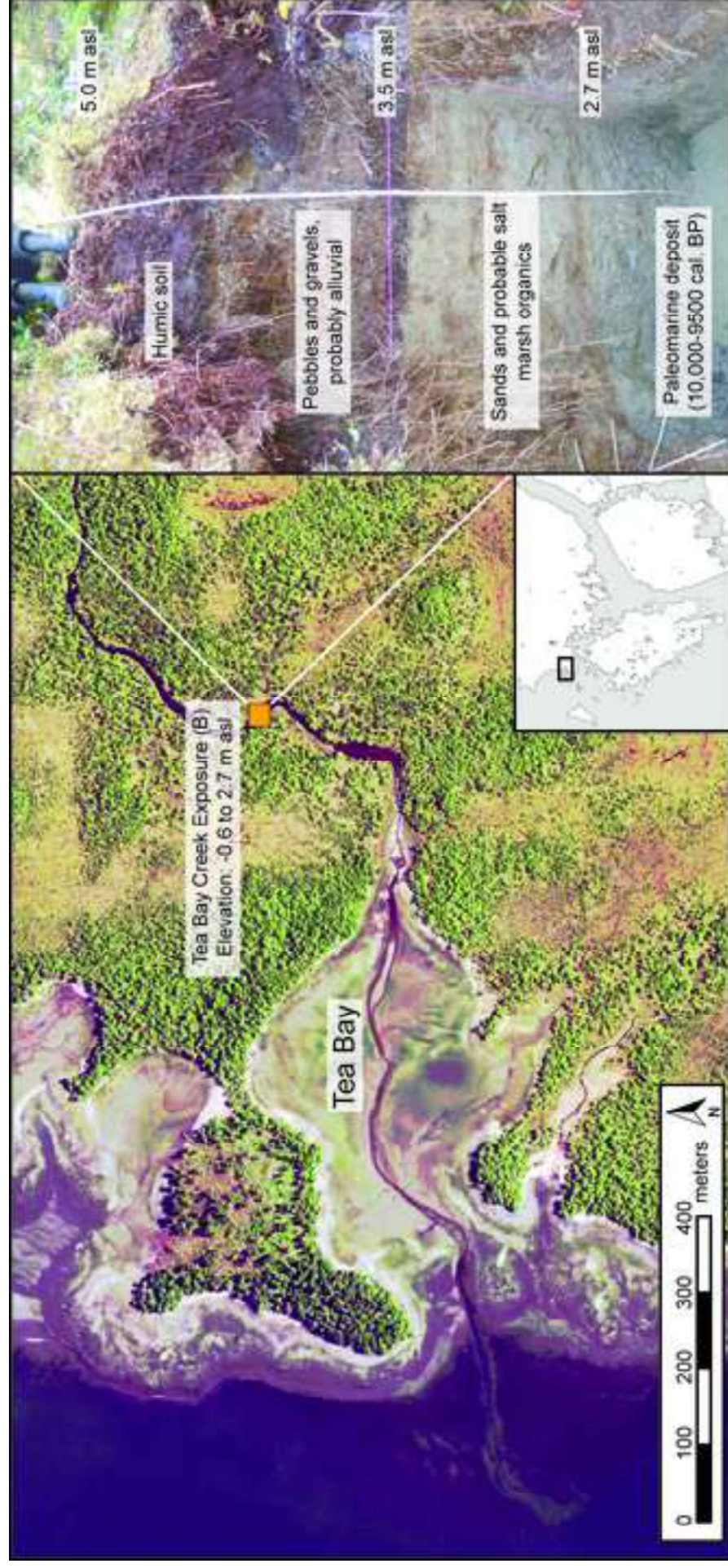


Figure 12 Paleoshoreline Features
[Click here to download high resolution image](#)

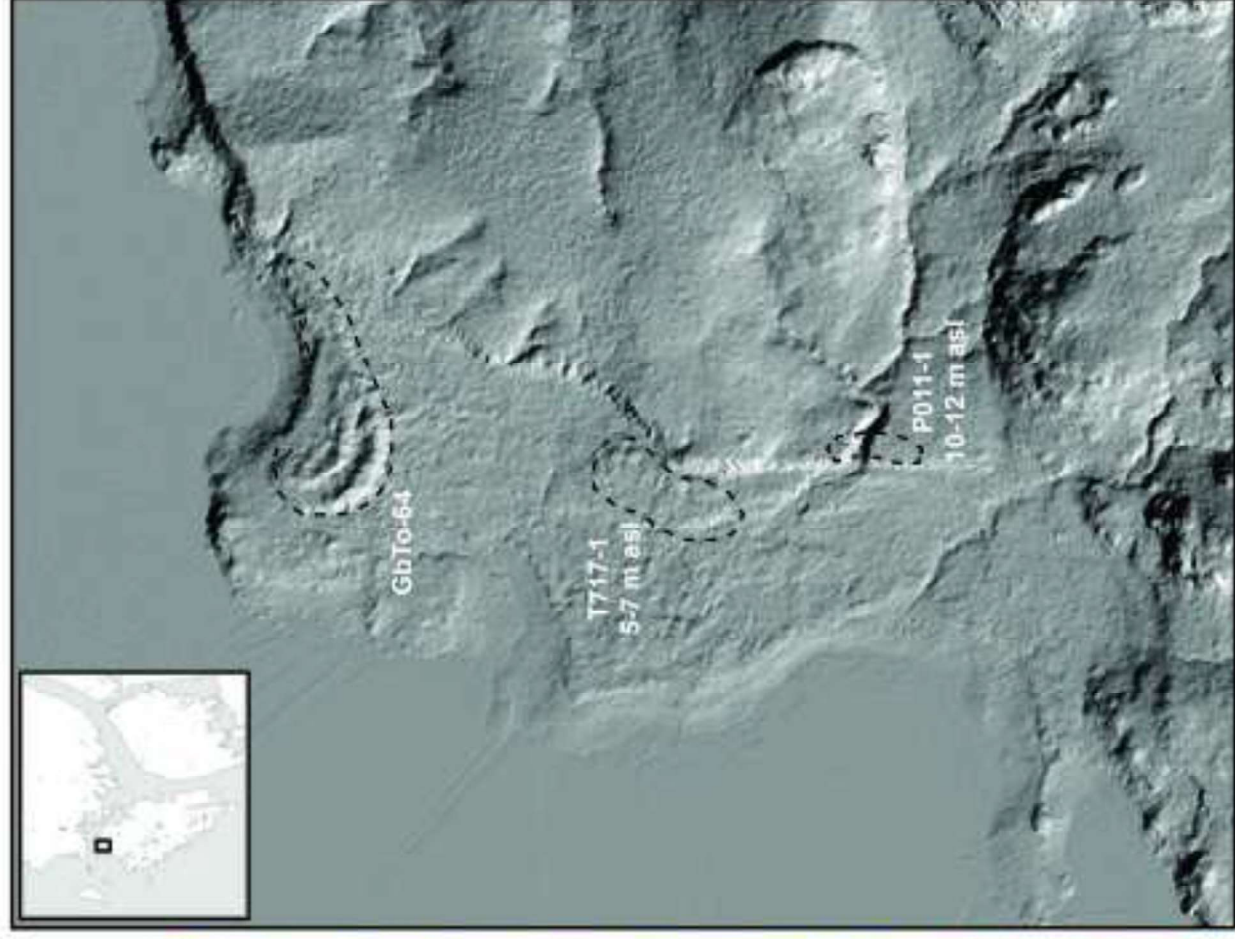
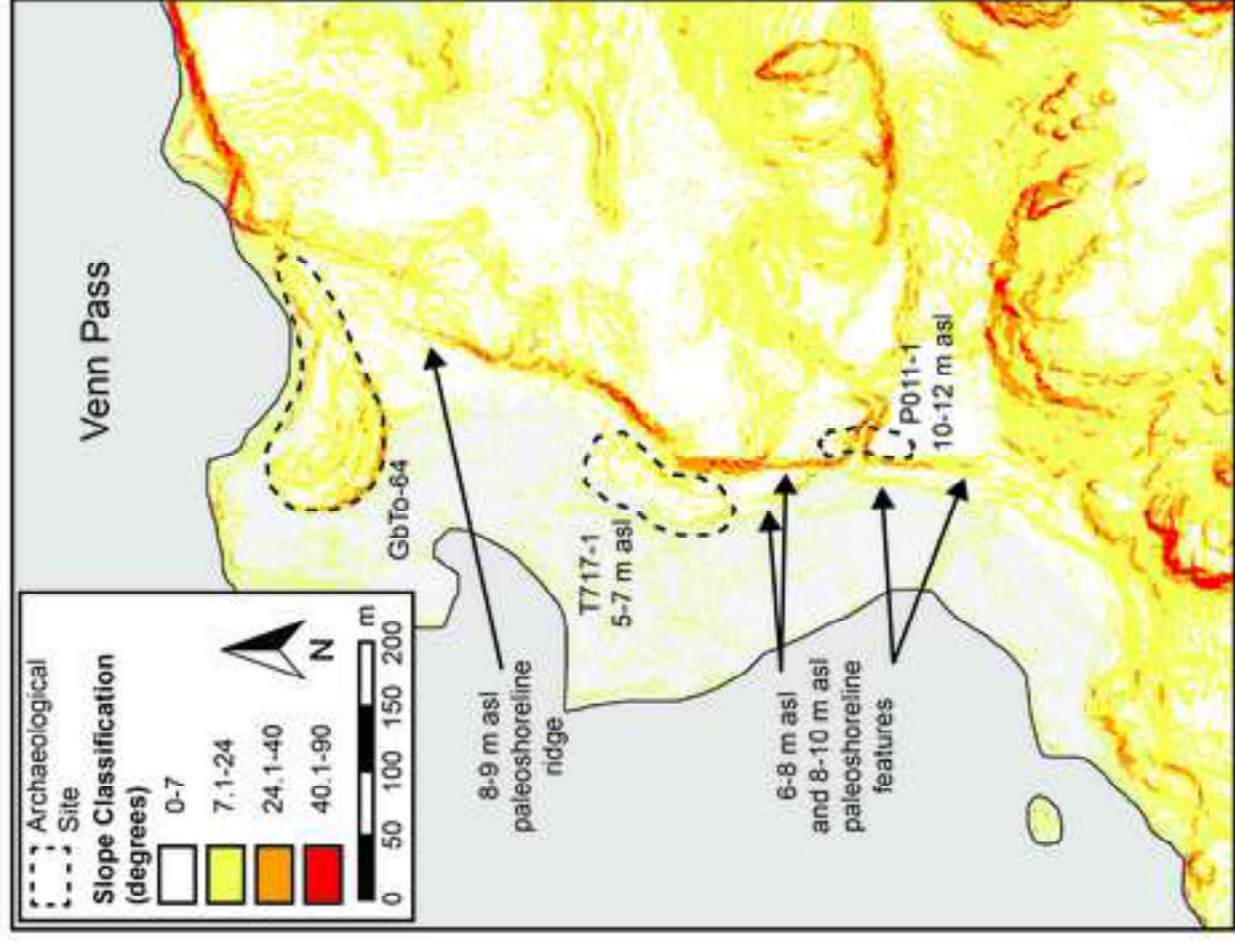


Figure 13 RSL Curve

[Click here to download high resolution image](#)

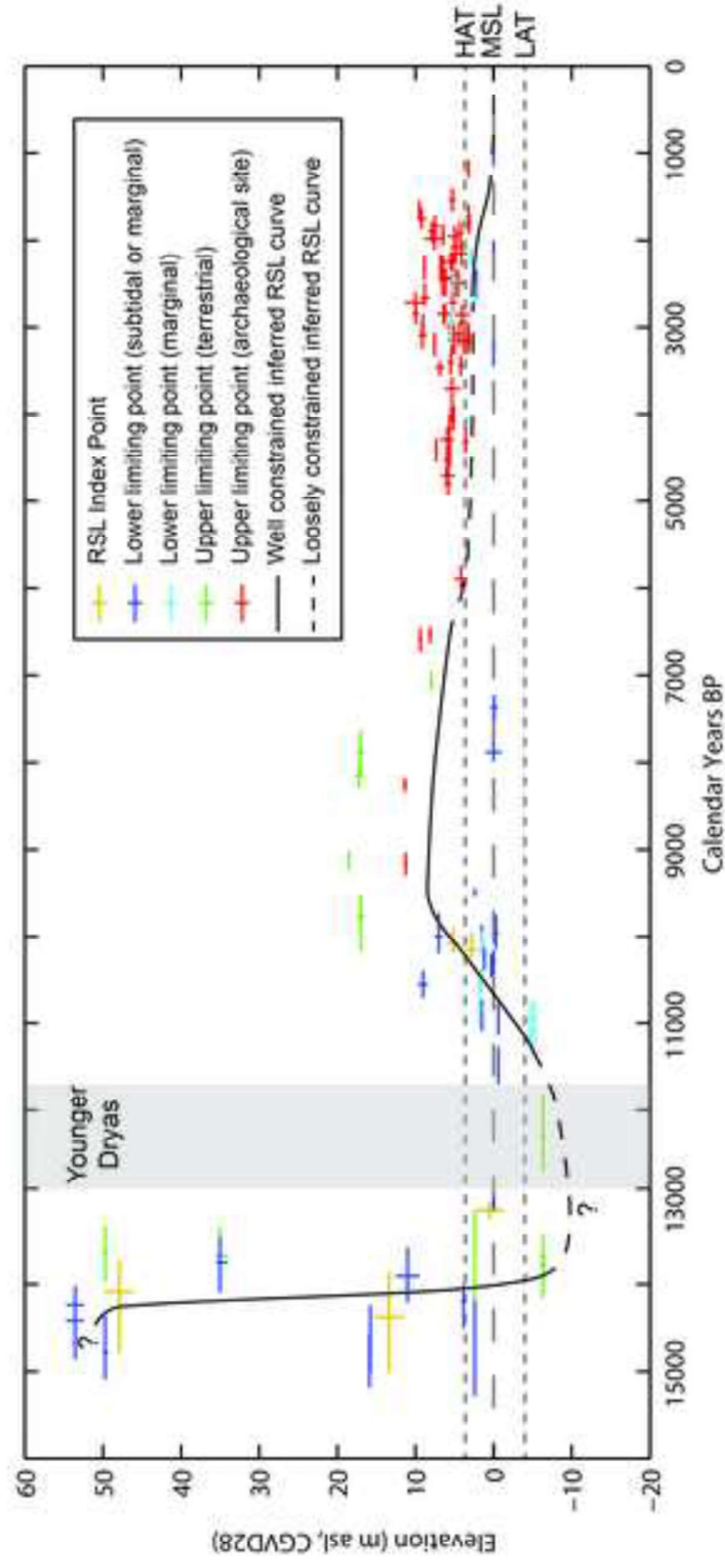


Figure 14 Late Holocene Data Points

[Click here to download high resolution image](#)

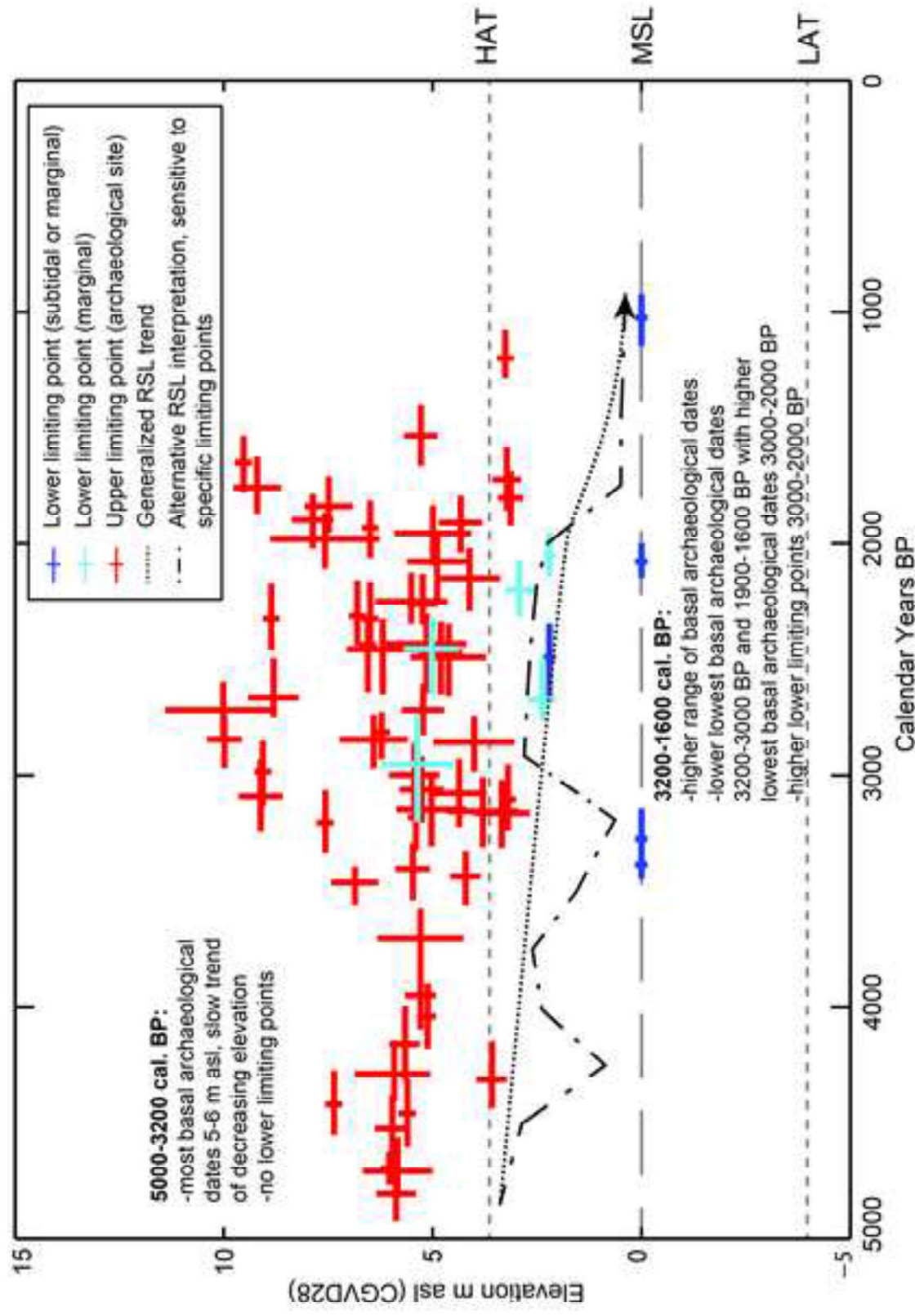


Table Captions:

Table 1: RSL data point types used in the present study and descriptions of indicative meanings.

Table 2: Tidal Parameters and their definitions for Canadian Hydrographic Survey Benchmark Station 9354, predicted over 19 years, start year 2010 (Canadian Hydrographic Survey, personal communication, September 28, 2015). Note that MWL and MTL are essentially the same and are equal to 0 m asl. Note that in Canada, tidal parameters are calculated based on predicted tides, whereas in the USA tidal parameters are calculated based on observed data.

Table 3. Stable carbon ($\delta^{13}\text{C}$) and nitrogen ($\delta^{15}\text{N}$) isotope compositions and elemental carbon-to-nitrogen (C/N) ratios of known marine sediments and known freshwater sediments from the study area. Bencke Lagoon sample and Optimism Bay samples were of unknown environmental salinity origin and tested against the knowns. Bencke Lagoon is intermediate between fresh and marine values (though closer to freshwater) and suggests a mixture of inputs. Optimism Bay samples fall within the range of known freshwater samples.

Table 4: Radiocarbon dates for RSL Index and Limiting Points used to constrain the Prince Rupert Harbour area RSL curve. Map ID letters and numbers refer to locations on Figure 2.

Table 5. Detailed list of most common or key diatoms observed in Livingstone Core Samples. Salinity Class (1=halophobic, 2=oligohalobous indifferent, 3=oligohalobous halophilic, 4=mesohalobous, 5=polyhalobous) and percent of total sample assemblage given in parentheses after each species name.

Figure Captions:

Figure 1: Northern coast of British Columbia with study area highlighted. RSL curves for locations across a west-east transect are shown (modified from Shugar et al. 2014), including the previously hypothesized curve for the Prince Rupert Harbour area. Modern communities are indicated by black dots.

Figure 2: Study area and location of data points used to reconstruct the Prince Rupert Harbour area RSL history. Letter and number codes correspond to data points in Table 4 and Figure 3. For Livingstone Sediment Cores, TL=Tsook Lake, OB=Optimism Bay, BL=Bencke Lagoon, NDB=North Digby Bog 1, DL=Digby Island Lake 1, DIB=Digby Island Bog 1, GLP=Auriol Point Lagoon, PL=Philip's Lagoon, SL=Salt Lake, RA=Russell Arm, RR=Rifle Range Lake 1. For Geological Exposures, A=Swamp Creek, B=Tea Bay Creek, C=estuary north of Optimism Bay, D=shell exposure in creek north of Bencke Lagoon #2, E=shell exposure in creek north of Bencke Lagoon #1, F=Russell Arm/Philip's Lagoon Isthmus, G=Melville Arm, H=McNichol Creek, I=Northwest Digby Island near GbTo-82, J=Pillsbury Cove Lagoon, K=West Kaien Island. For numbered archaeological sites, Borden Numbers or other identifying numbers are in Table 4.

Figure 3: Age-Altitude Plot of all limiting and index points used in this study. Letter and number labels correspond with data point site locations in Figure 2 and data point details in Table 4. Time ranges for data points indicate 2-sigma calibrated ranges, the elevation of these ranges is set at paleo-mean sea level for Index Points, and actual measured elevations for limiting points. Vertical lines indicate 95% confidence ranges for vertical error, and they cross the age range at the median age of each data point.

Figure 4: Tsook Lake Core TL#1 log, photo, and diatom analysis results. Diatom species comprising 7% or greater of the total assemblage of any given sample are shown on the expanded bar graph.

Figure 5: Rifle Range Lake core RR1#1 log, photo, and diatom analysis results. Diatom species comprising 8% or greater of the total assemblage of any given sample are shown on the expanded bar graph.

Figure 6: Digby Island Lake 1 core DL1#1 log, photo, and diatom analysis results. Diatom species comprising 10% or greater of the total assemblage of any given sample are shown on the expanded bar graph.

Figure 7: Orthophoto of a section of northern Venn Pass, showing Bencke Lagoon, Scott Inlet, and Optimism Bay. Note the extensive sand and mudflats exposed at low tide. Livingstone core locations are indicated by yellow circles, paleomarine sediment exposures indicated by yellow squares. Letters in parentheses correspond with test locations in Figure 2.

Figure 8: Upper section of Bencke Lagoon core BL#1 log, photo, and diatom analysis results. Diatom species comprising 5% or greater of the total assemblage of any given sample are shown on the expanded bar graph.

Figure 9A: Plot of $\delta^{13}\text{C}$ vs $\text{C}_{\text{ORG}}/\text{N}_{\text{TOTAL}}$ for known marine sediment samples (blue diamonds), known terrestrial samples (green diamonds), a sample of organic-rich sediment from the upper layer in core BL#1 (yellow triangle), and samples from the organic-rich layer at the bottom of cores OB#1 and OB#2 (red triangles). 9B: Plot of $\delta^{13}\text{C}$ vs $\delta^{15}\text{N}$ values for the same samples. There are slightly fewer marine samples represented because not all of these samples yielded reliable $\delta^{15}\text{N}$ values.

Figure 10: Optimism Bay Cores OB#1 and OB#2 logs, photos, and stable isotope analysis sample locations (coloured squares).

Figure 11: Orthophoto of the location of Tea Bay Creek paleomarine exposure and photograph the profile, showing sequence from marine conditions to high intertidal/salt marsh to alluvial/estuarine conditions to the current forest soil buildup.

Figure 12: Left: LiDAR-derived slope-classified map of a portion of northwest Digby Island showing inland linear ridges that likely represent stranded paleoshorelines. GbTo-64 is an archaeological site located on the modern shoreline. T717-1 is an archaeological site on a 5-7 m asl terrace dating with dates from ~3500 cal. BP to ~2000 cal. BP, associated with slightly higher RSL in the latter half of the Holocene. P011-1 is an archaeological site on a 10-12 m asl terrace from the early Holocene RSL high stand. Solid black line is the modern shoreline; light gray shading indicates 'flooding' to 7 m asl for reference. Intensifying colours indicate increasing slope. Right: LiDAR-derived hillshaded DEM of the same area.

Figure 13. Plot of all data points and the preferred RSL curve for the Prince Rupert Harbour region. Time ranges for data points indicate 2-sigma calibrated ranges, the elevation of these ranges is set at paleo-mean sea level for Index Points, and actual measured elevations for limiting points. Vertical lines indicate 95% confidence ranges for vertical error, and they cross the age range at the median age of each data point. Our preferred inferred RSL curve is indicated by the solid (well constrained sections) and dashed (loosely constrained sections) line.

Figure 14: Plot of all data points from the last 5000 years, and two potential RSL interpretations. The dotted line is a conservative general trend of regressing RSL that smooths out potential noise in the data while keeping most of the lowest basal archaeological data points above HHWMT (2.32 m above RSL). The dashed line attempts to fit all the data at 250 year intervals in a way that the lowest basal archaeological dates are close to or above a 2.32 m HHWMT and all lower limiting dates above RSL are at least within the relative tidal range. Time ranges for data points indicate 2-sigma calibrated ranges. Vertical lines indicate 95% confidence ranges for vertical error, and they cross the age range at the median age of each data point.

Highlights

1. 123 data points constrain 15,000 year sea level history around Prince Rupert.
2. Sea level position varies from >50 m asl to <-6.3 m asl after deglaciation.
3. Variation in relative sea level change exists over relatively short distances.
4. Sea level history helps identify early Holocene archaeological sites.
5. The oldest archaeological site recorded in area (9000 cal. BP) is identified.

